

1-1-1997

## Synthesis and characterization of poly (3,3,3-trifluorolactic acid).

Derrick Bernard McKie  
*University of Massachusetts Amherst*

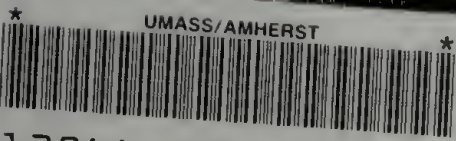
Follow this and additional works at: [https://scholarworks.umass.edu/dissertations\\_1](https://scholarworks.umass.edu/dissertations_1)

---

### Recommended Citation

McKie, Derrick Bernard, "Synthesis and characterization of poly (3,3,3-trifluorolactic acid)." (1997).  
*Doctoral Dissertations 1896 - February 2014*. 960.  
<https://doi.org/10.7275/7v8c-re64> [https://scholarworks.umass.edu/dissertations\\_1/960](https://scholarworks.umass.edu/dissertations_1/960)

This Open Access Dissertation is brought to you for free and open access by ScholarWorks@UMass Amherst. It has been accepted for inclusion in Doctoral Dissertations 1896 - February 2014 by an authorized administrator of ScholarWorks@UMass Amherst. For more information, please contact [scholarworks@library.umass.edu](mailto:scholarworks@library.umass.edu).



312066 0264 0707 7



DATE DUE

APR 01 1999

JUN 02 2000

il: 9920657

UNIVERSITY LIBRARY  
UNIVERSITY MASSACHUSETTS

AMHERST

PHYS  
SCI  
LD  
3234  
M267  
1997  
M1585

SYNTHESIS AND CHARACTERIZATION OF  
POLY(3,3,3-TRIFLUOROLACTIC ACID)

A Dissertation Presented  
by  
DERRICK BERNARD M<sup>c</sup>KIE

Submitted to the Graduate School of the  
University of Massachusetts Amherst in partial fulfillment  
of the requirements for the degree of

DOCTOR OF PHILOSOPHY

September 1997

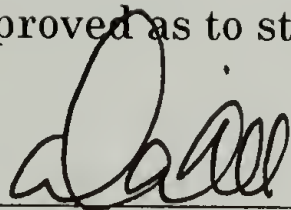
Polymer Science and Engineering

© Copyright by Derrick Bernard M<sup>c</sup>Kie 1997  
All Rights Reserved

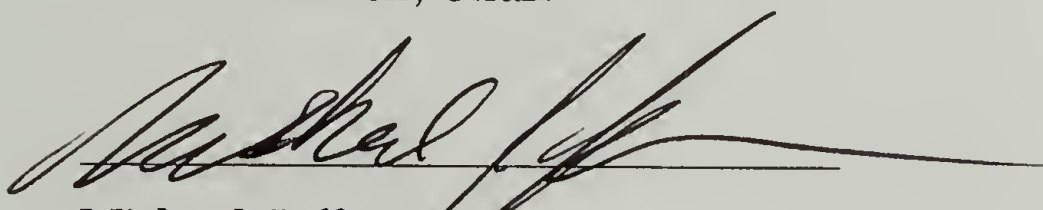
SYNTHESIS AND CHARACTERIZATION OF  
POLY(3,3,3-TRIFLUOROLACTIC ACID)

A Dissertation Presented  
by  
DERRICK BERNARD MCKIE

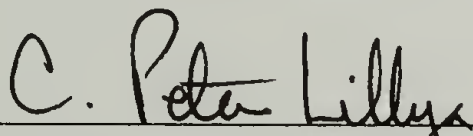
Approved as to style and content by:



David A. Tirrell, Chair



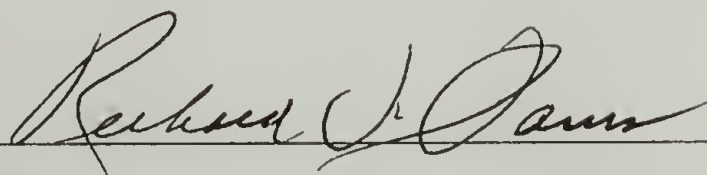
Michael Jaffe, Member



C. Peter Lillya, Member



Murugappan Muthukumar, Member



Richard J. Farris, Department Head  
Polymer Science and Engineering

TO MY MOTHER AND FATHER

## ACKNOWLEDGMENTS

It is a distinct pleasure to have Professor Dave Tirrell as an advisor. He is an outstanding teacher, scientist, and manager. I've learned much from him explicitly and implicitly. Through trust, support and good dialogue, an atmosphere of positive motivation and creativity prevails in his laboratory.

I am thankful to my committee member and supervisor at Hoechst Celanese, Dr. Mike Jaffe, for his faith, commitment, encouragement, and support from the very beginning. Also, I thank the Hoechst Celanese Corporation. for the financial support throughout this endeavor. The helpful dialog and understanding provided by my other committee members and teachers, Professor P. Lillya and Professor M. Muthukumar is also appreciated. I also thank the faculty of the Polymer Science and Engineering Department for challenging me to develop a better understanding of polymer science. In the process, I've learned much about the disciplines and myself.

In Amherst, I had the good fortune of developing many good friendships. In particular, I thank Geni Dessipri, Susan Dawson and Ajay Parkhe from our research group for providing an orientation to the polymer synthesis research laboratory. I thank Dr. Greg Dabkoski for providing timely elemental analysis results. The total UMass experience has been exciting, rewarding, and, positive.

I conducted most of this research at the Hoechst Celanese R.L. Mitchell Technical Center. I am thankful to many of the staff for their advice, support, and generosity with their assistance. In particular, Dr. Tony East, Dr. Robert Imes, and Dr. Mark Sebastian have been most helpful in discussions on synthetic organic chemistry. Professor Hank Hall has also been supportive and most helpful in discussions on synthetic polymer chemistry and characterization. I thank Dr. Josh Gurman for his positive attitude, encouragement and various technical discussions. I appreciate Dr. Joe Rafalko and Mr. Tom Davidson for sharing their experience with infrared spectroscopy and allowing me to use the instruments in their laboratory. I thank Dr. George Collins and Ms. Barbara Long for their discussions on polymer thermal analysis, conducting experiments, and the use their equipment. Dr. Marie Borzo and Mr. Chris Cook provided much assistance and discussions on NMR experiments and analysis of spectra. I thank Mr. John Letinski and Ms. Gerry Hogue for moisture analysis and pH measurements. I appreciate the persistence of Dr. Ho-Nan Sung and Ms. Rosemarie Petersen that enabled us to obtain light scattering data. The collaborations with Dr. Sol Jacobson on molecular modeling, Mr. Stefanos Lepeniotis on statistical optimization of the polymer synthesis and, Dr. Chen Xu on surface characterization by contact angle measurement, XPS and dynamic SIMS experiments were all rewarding experiences. Wide angle x-ray scattering experiments were conducted with Ms. Theresa Aversa and Dr. Cheng Saw with whom I had many useful discussions on x-ray

diffractogram analysis. Drs. Rong-Tsang Chen and Douglas Karim provided much useful advice on scanning figures into computer files and Mr. Andrzej Vorbrodt scanned many of the figures for me.

Thanks to all my friends, especially Mr. John Ross and Dr. Wes Henderson for their affirmation and support through the years. Finally, I thank my parents, Marion and Bernard McKie for their enduring love, faith, friendship and, encouragement and providing me with a great start in life.

# ABSTRACT

## SYNTHESIS AND CHARACTERIZATION OF POLY(3,3,3-TRIFLUOROLACTIC ACID)

SEPTEMBER 1997

DERRICK BERNARD M<sup>c</sup>KIE

S.B., MASSACHUSETTS INSTITUTE OF TECHNOLOGY

M.S., POLYTECHNIC INSTITUTE OF NEW YORK

Ph.D., UNIVERSITY OF MASSACHUSETTS AMHERST

Directed by: Professor David A. Tirrell

A long-standing goal in polymer research is to predictably relate the primary molecular structural features of polymeric materials with ultimate macroscopic physical characteristics. This continues to be a challenging undertaking in polymer science, considering the statistical nature of synthetic macromolecules. The science and technology of naturally occurring polymers in the form of proteins offer an opportunity from which potentially substantial advances can be made in synthetic polymer science. Application of what is understood about the molecular structures of natural macromolecules and processes by which they are formed can be applied in synthetic polymer science. The investigation of polymers of  $\alpha$ -hydroxyacids

represents a reasonable starting point for application of what is known about proteins and applying it to wholly synthetic materials.

Lactic acid is the simplest asymmetric  $\alpha$ -hydroxyacid. A model monomer, trifluorolactic acid, is formed when the methyl group is replaced by a trifluoromethyl group. Acidity of the methine hydrogen of an  $\alpha$ -hydroxyacid is expected to increase when the strongly electron withdrawing trifluoromethyl group is introduced to the stereogenic carbon. In this way, the hydrogen bonding capability of the polymer molecule would be enhanced. Polymerization of trifluorolactic acid represents a part of the effort toward the ultimate goal of the production of bio-inspired synthetic polymers with predictable and enhanced physical characteristics.

Racemic 3,3,3-trifluorolactic acid ((RS)-3,3,3-trifluorolactic acid) was characterized and contrasted with lactic acid. Unlike lactic acid, it does not form intermolecular esters in the presence of trace water.

Poly((RS)-3,3,3-trifluorolactic acid) was synthesized by esterification with 1,3-diisopropylcarbodiimide condensing agent and catalytic salts of 4-dimethylaminopyridine and protic acids. Infrared and NMR spectroscopy as well as molecular weight characterization by inherent viscosity, GPC, and light scattering showed that the target polymer was produced. The DSC thermal trace indicated a  $T_g$  of 36°C. TGA indicated that the fluoropolyester compared favorably with poly(D,L-lactide) in thermal stability. Surface properties of poly(D,L-lactide) blends with poly((RS)-3,3,3-trifluorolactic acid)

showed increased contact angle with the presence of the fluorinated polymer.

Wide angle x-ray diffraction patterns indicated the emergence of a band indicative of weak interchain correlation despite the lack of chain stereoregularity. The analogous poly(D,L-lactide) showed no such correlation.

# TABLE OF CONTENTS

	<u>Page</u>
ACKNOWLEDGMENTS.....	v
ABSTRACT.....	viii
LIST OF TABLES .....	xiv
LIST OF FIGURES .....	xvi
LIST OF SCHEMES.....	xx
Chapter	
1. INTRODUCTION.....	1
1.1 Motivation.....	1
1.2 Fluorine Modified Organic Compounds.....	3
1.3 Bio-inspired Aliphatic Polyesters .....	4
1.4 Lactic Acid - Lactide Preparation and Polymerization .....	8
1.5 Esters and Polyesters of Fluorinated Aliphatic Compounds.....	9
1.6 Overview of the Dissertation.....	10
1.7 References and Notes .....	12
2. 3,3,3-TRIFLUOROLACTIC ACID AND LACTIC ACID: A CONTRAST OF $\alpha$ -HYDROXYACIDS .....	22
2.1 Introduction .....	22
2.2 Experimental Section .....	23
2.2.1 Materials.....	23
2.2.2 Methods .....	23
2.3 Results and Discussion.....	24
2.3.1 Physical Properties.....	24
2.3.2 Biochemical Properties.....	26
2.3.3 Pharmaceutical Chemistry .....	28
2.3.4 Chemical Properties .....	29
2.3.5 Spectroscopic Characterization .....	30
2.4 Conclusions .....	31
2.5 References and Notes .....	32

3.	SYNTHESIS OF POLY((RS)-3,3,3-TRIFLUOROLACTIC ACID) AND COMPARISON WITH POLYLACTIDES .....	46
3.1	Introduction .....	46
3.2	Experimental Section .....	47
3.2.1	Materials.....	47
3.2.2	Methods .....	48
3.2.3	Preparations .....	50
3.3	Results and Discussion.....	53
3.3.1	Characterization of the white precipitate by-product .....	55
3.3.2	Characterization of Poly((RS)-3,3,3-trifluorolactic acid) .....	56
3.4	Conclusions .....	62
3.5	References and Notes .....	64
4.	STATISTICAL OPTIMIZATION TECHNIQUES IN THE SYNTHESIS OF POLY((RS)-3,3,3-TRIFLUOROLACTIC ACID).....	94
4.1	Introduction .....	94
4.2	Experimental Section .....	96
4.2.1	Materials.....	96
4.2.2	Methods .....	96
4.2.3	Preparations .....	97
4.2.4	Statistically Designed Experiments .....	97
4.3	Results and Discussion.....	99
4.3.1	Statistical Data Analysis .....	99
4.4	Conclusions .....	102
4.5	References and Notes .....	104
5.	CHARACTERIZATION OF POLY((RS)-3,3,3-TRIFLUOROLACTIC ACID).....	113
5.1	Introduction .....	113
5.2	Experimental Section .....	114

5.2.1 Materials.....	114
5.2.2 Methods .....	115
5.3 Results and Discussion.....	118
5.3.1 Polymer Molecular Weight as a Function of Polymerization Time.....	118
5.3.2 Fractionation of Poly((RS)-trifluorolactic acid).....	119
5.3.3 Blends of Poly((RS)-3,3,3-trifluorolactic acid) with poly(D,L-lactide) .....	123
5.4 Conclusions .....	126
BIBLIOGRAPHY.....	149

## LIST OF TABLES

Table	Page
1.1	The pKa's of aliphatic acids and alcohols..... 15
1.2	Summary of the calculations from molecular modeling..... 16
2.1	Melting points of (RS)-3,3,3-trifluorolactic acid and lactic acid.... 35
2.2	The pKa's of (RS)-3,3,3-trifluorolactic acid, lactic acid and model compounds. .... 36
2.3	Elemental analysis of (RS)-3,3,3-trifluorolactic acid..... 37
2.4	FTIR and FT-Raman assignments of (RS)-3,3,3-trifluorolactic acid..... 38
3.1	Yield and inherent viscosity of poly((RS)-3,3,3-trifluorolactic acid) with 0.2 equivalent (monomer to catalyst 5/1) of catalyst (solutions filtered through 0.25 $\mu$ glass membrane) prior to measurement)..... 66
3.2	Elemental analysis of the white precipitate by-product..... 67
3.3	Elemental analysis of crude and purified poly((RS)-3,3,3-trifluorolactic acid). .... 68
3.4	Inherent viscosities (unfiltered solutions) of poly((RS)-3,3,3-trifluorolactic acid) and poly(D,L-lactide)..... 69
3.5	Absolute molecular weight measurements by light scattering; polylactides in HFIP and poly((RS)-TFL) in THF. .... 70
3.6	The d spacings of poly(L-lactide). .... 71
4.1	Experimental design worksheet with response results..... 105
5.1	The effect of polymerization time on poly((RS)-TFL) molecular weight and yield. .... 130
5.2	A comparison of the molecular weight of the fractionated polymer, control and poly(D,L-lactide). .... 131

5.3	XPS and contact angle measurements of poly(D,L-lactide) / poly((RS)-TFL) blend films cast from HFIP....	132
5.4	Elemental analysis of poly(D,L-lactide) / poly((RS)-TFL) blend films cast from HFIP.....	133
5.5	XPS and contact angle measurements of poly(D,L-lactide) / poly((RS)-TFL) blend films cast from acetone. ....	134
5.6	XPS data of annealed test specimens cast from HFIP and acetone. ....	135

## LIST OF FIGURES

Figure	Page
2.1	Vibrational spectra of (RS)-3,3,3-trifluorolactic acid. A: FTIR and B: FT-Raman..... 39
2.2	FTIR spectra of A: (RS)-TFL and B: methyl (RS)-3,3,3-trifluorolactic acid..... 40
2.3	FT-Raman spectra of A: (RS)-3,3,3-trifluorolactic acid and B: D,L-lactic acid..... 41
2.4	FT-Raman spectra of A: D,L-lactic acid and B: D,L-lactide..... 42
2.5	300-MHz $^{19}\text{F}$ NMR spectrum of (RS)-3,3,3-trifluorolactic acid in $\text{CDCl}_3$ . .... 43
2.6	200-MHz $^1\text{H}$ NMR of (RS)-3,3,3-trifluorolactic acid in $\text{DMSO}-d_6$ ..... 44
3.1	200-MHz proton NMR of the white precipitate by-product in $\text{DMSO}-d_6$ . .... 72
3.2	FTIR spectra of A: (RS)-TFL and B: crude poly((RS)-TFL)..... 73
3.3	FTIR spectra of A: poly(D,L-lactide) and B: crude poly((RS)-TFL)..... 74
3.4	FTIR spectrum of the white precipitate by-product ..... 75
3.5	FTIR spectra of (A): purified poly((RS)-TFL) and (B): crude poly((RS)-TFL)..... 76
3.6	200-MHz proton NMR of crude poly((RS)-TFL) in $\text{DMSO}-d_6$ ..... 77
3.7	200-MHz proton NMR of crude poly((RS)-TFL) with TFA in $\text{DMSO}-d_6$ . .... 78
3.8	200-MHz proton NMR of poly((RS)-TFL) in $\text{DMSO}-d_6$ after chloroform extraction. .... 79
3.9	50-MHz carbon 13 NMR (A) and APT (B) spectra of poly((RS)-TFL) in $\text{DMSO}-d_6$ ..... 80

3.10	200-MHz proton NMR spectra of (A): poly((RS)-TFL), (B): poly(D,L-lactide), both in DMSO-d <sub>6</sub> and (C): poly(L-lactide) in HFIP-d <sub>2</sub> . The signals at 2.49 and 3.3 ppm in spectra (A) and (B) are DMSO and water, respectively.....	81
3.11	GPC chromatograms (RI detector) of A: poly(D,L-lactide ), B: poly(L-lactide) and C: poly((RS)-TFL).....	82
3.12	GPC viscosity chromatograms of A: poly(D,L-lactide), B: poly(L-lactide) and C: poly((RS)-TFL) with HFIP solvent. ....	83
3.13	TGA curves of A: poly(RS)-TFL and B: poly(D,L-lactide) under N <sub>2</sub> at 10C° /min.....	84
3.14	Overview of the TGA curves of A: poly(RS)-TFL and B: poly(D,L-lactide) under N <sub>2</sub> at 10C° /min. ....	85
3.15	TGA curves of A: fractionated poly(RS)-TFL) and B: poly(D,L-lactide) under N <sub>2</sub> at 10C°/min. ....	86
3.16	Glass transition temperatures (T <sub>g</sub> ) of A: poly(RS)-TFL and B: poly(D,L-lactide) under N <sub>2</sub> at 20C°/min. ....	87
3.17	Peak melting temperature (T <sub>m</sub> ) of poly(L-lactide) under N <sub>2</sub> at 10C°/min.....	88
3.18	Glass transition temperature (T <sub>g</sub> ) of poly(L-lactide) under N <sub>2</sub> at 10C°/min.....	89
3.19	Wide angle X-ray scattering patterns of A: poly((RS)-TFL) and B: poly(D,L-lactide). Neat polymer is fixed to the X-ray sample mount with a small amount of silicone grease. ....	90
3.20	Wide angle X-ray scattering pattern of poly(L-lactide). Neat polymer is fixed to the X-ray sample mount with a small amount of silicone grease.....	91
4.1	Comparison of yield model coefficients. ....	106
4.2	Comparison of solution viscosity model coefficients. ....	107

4.3	Optimization surface of the yield with DPTS. ....	108
4.4	Optimization surface of the yield with DPTL. ....	109
4.5	Optimization surface of the solution viscosity with DPTS. ....	110
4.6	Optimization surface of the solution viscosity with DPTL. ....	111
5.1	GPC of A: poly((RS)-TFL) fractionated, B: poly((RS)-TFL) control and C: poly(D,L-lactide). ....	136
5.2	Differential weight fraction vs. molecular weight of A: poly((RS)-TFL) fractionated, B: poly((RS)-TFL) control and C: poly(D,L-lactide). ....	137
5.3	Cumulative weight fraction curves of A: poly((RS)-TFL) fractionated, B: poly((RS)-TFL) control and C: poly(D,L-lactide). ....	138
5.4	200-MHz proton NMR spectra of A: control poly((RS)-TFL) and B: fractionated poly((RS)-TFL) in DMSO- <i>d</i> <sub>6</sub> . ....	139
5.5	Integration of the isopropyl methine hydrogen and the amide hydrogen of Figure 5.4A. ....	140
5.6	TGA curves of A: control and B: fractionated poly((RS)-TFL) under N <sub>2</sub> at 10C°/min. ....	141
5.7	TGA curves of A: fractionated poly((RS)-TFL) and B: poly(D,L-lactide) under N <sub>2</sub> at 10C°/min. ....	142
5.8	DSC thermal traces of A: fractionated poly((RS)-TFL) and B: the control under N <sub>2</sub> at 10C°/min. ....	143
5.9	DSC of fractionated poly((RS)-TFL) under N <sub>2</sub> at 10C°/min. ....	144
5.10	WAXS of the A: control poly((RS)-TFL) and B: fractionated poly((RS)-TFL). ....	145
5.11	2θ vs. intensity of the A: the control and B: fractionated poly((RS)-TFL). ....	146

5.12	Dynamic SIMS of poly((RS)-TFL) cast from HFIP. ....	147
5.13	Dynamic SIMS of sample #3 (75/25, wt., poly(D,L-lactide) / poly((RS)-TFL) cast from HFIP.....	148

# LIST OF SCHEMES

Scheme		Page
1.1	The Peptide hydrogen bonds in an antiparallel $\beta$ pleated sheet.....	17
1.2	Molecular structures of lactic acid and 3,3,3-trifluorolactic acid. ....	18
1.3	The dimer conformation of methyl (R)-2-methoxy-3,3,3-trifluoromethylpropionate (R-MMFP). The carbonyl oxygen to methine hydrogen interatomic distances are 2.70 and 2.52 Å. ....	19
1.4	Ring opening polymerization of lactide.....	20
1.5	General polymerization reaction of trifluorolactic acid with carbodiimide condensing agent and 4-(dimethylamino)pyridinium 4-toluenesulfonate (DPTS) catalysis. ....	21
2.1	Fischer projections of the stereoisomers of lactic acid (LA) and 3,3,3-trifluorolactic acid (TFL). ....	45
3.1	Reaction pathways in the polymerization of (RS)-3,3,3-trifluorolactic acid). ....	92
4.1	Synthesis of Poly((RS)-3,3,3-trifluorolactic acid).....	112

## INTRODUCTION

### 1.1 Motivation

A long-standing goal in polymer research is to predictably relate the primary molecular structural features of polymeric materials with ultimate macroscopic physical characteristics. This continues to be a challenging undertaking in polymer science, considering the statistical nature of synthetic macromolecules. Dependent upon the monomer constituents, regiospecificity, stereoregularity, mer unit distribution and molecular weight will vary in the resultant polymer product. The semicrystalline and amorphous nature of these materials is such that macromolecular chain dynamics can result in gradual physical property changes over the useful life of the material.

The science and technology of naturally occurring polymers in the form of proteins offer a tremendous opportunity from which potentially substantial advances can be made in synthetic polymer science. Contemporary recombinant DNA technology, with utilization of the biosynthetic machinery, is used to produce precise macromolecular polypeptides that are regiospecific and stereoregular, and uniform in molecular weight, for the study of

structure/property relationships and materials application.<sup>1,2</sup> Also, application of what is understood about the molecular structures of these macromolecules and the processes by which they are formed can be applied in synthetic polymer science.<sup>3</sup>

In this regard, the investigation of polymers of  $\alpha$ -hydroxyacids represents a reasonable starting point for application of what is known about proteins and applying it to wholly synthetic materials. Polymers of  $\alpha$ -hydroxyacids are necessarily regiospecific due to the chemistry of the functional groups. However, as esters, they lack the acidic amide hydrogen; a key feature of proteins that enhances strong molecular interactions and provides the key to secondary structure.<sup>4</sup> The acidity of the methine hydrogen of an  $\alpha$ -hydroxyacid would be expected to increase if strongly electron withdrawing fluorine is introduced to the stereogenic carbon. In this way, the hydrogen bonding capability of the polymer molecule would be enhanced.

Lactic acid is the simplest asymmetric  $\alpha$ -hydroxyacid. A model monomer, trifluorolactic acid, is formed when the methyl group is replaced by a trifluoromethyl group. So, the polymerization of trifluorolactic acid represents a part of the effort toward the ultimate goal of the production of bio-inspired synthetic polymers with predictable and enhanced physical characteristics.

## 1.2 Fluorine Modified Organic Compounds

Fluorine can be used to modify the reactivity of organic compounds. In biologically important molecules, fluorine may be used to improve or modify molecular selectivity. This can be accomplished by substitution of hydrogen and hydroxyl groups with fluorine. This substitution can affect the molecular reactivity in two ways: through changes in the  $pK_a$  of adjacent functional groups, and through differences in the properties of the C-F and C-H bonds. The altered chemical function of fluorine substituted compounds arises from the high electronegativity of fluorine. This can affect the  $pK_a$  of adjacent ionizable functional groups and dipole moments thus influencing chemical reactivity/stability and biological function.<sup>5</sup> The lipophilicity of a molecule and thus its distribution throughout an organism can be modified through fluorine in the structure. This is generally true for aromatics and compounds with fluorine adjacent to atoms or groups with  $\pi$ -electrons. In aliphatic molecules, monofluorination and trifluoromethylation generally reduce lipophilic character when the fluorination site is separated from any heteroatoms or  $\pi$ -bonds by at least 3 C-C bonds.<sup>6</sup> Also, the carbon-fluorine bond (107-121 kcal) is stronger than the carbon-hydrogen bond (98.7 kcal),<sup>7</sup> so covalently bonded fluorine is less labile than hydrogen.

The fluoroalkyl group has a strong inductive effect that can be clearly seen when comparing the  $pK_a$  of hydrocarbon and fluoroalkyl acids and

alcohols.<sup>8</sup> This is shown in Table 1.1. These data indicate that the active hydrogens can become more labile presumably by reducing electron density at the hydroxy oxygens due to the presence of the trifluoromethyl group. This has a significant effect on the esterification chemistry of fluorinated aliphatic alcohols that is mentioned (vide infra) in a subsequent section of this chapter.

### 1.3 Bio-inspired Aliphatic Polyesters

Proteins and polypeptides form inter- and intramolecular hydrogen bonds through the peptide linkage. Tendons, hair and muscles are natural materials with properties dictated through their primary structure or  $\alpha$ -amino acid sequence. As stereoregular, monodisperse derivatives of nylon 2, with a high frequency of aliphatic amide links, proteins have the potential to form high packing density with hydrogen bonding. The central stereogenic carbon of each residue is bonded to an amino group, hydrogen, carboxy group and an R side group as shown in Scheme 1.1.

This secondary structural feature is considered to be a significant contributor to the remarkable strength and stiffness characteristics of natural protein fibers such as spider dragline silk which contains repetitive sequences of the amino acid L-alanine ( $R = CH_3$  in Scheme 1.1).<sup>9</sup>

It is hypothesized here that increased attractive intra- and intermolecular electronic interactions may be induced in polyesters through the appropriate placement of fluorine in an aliphatic polyester repeat unit.

Aliphatic  $\alpha$ -hydroxy acids form polymers that can be considered polyester analogs of polypeptides. Lactic acid is the  $\alpha$ -hydroxy acid that is an analog of alanine. It is considered that if the methyl group of lactic acid is converted to a trifluoromethyl group that the acidity of the  $\alpha$ -hydrogen would be significantly increased. Trifluorolactic acid (TFL) is a fluorocarbon analog of lactic acid. The structures of lactic acid and 3,3,3-trifluorolactic acid are displayed in Scheme 1.2. A PM3<sup>10</sup> computation indicates that the partial positive charges of the  $\alpha$ -hydrogens of lactic acid and trifluorolactic acid are  $\delta = +0.067$  and  $\delta = +0.095$ , respectively. With increased partial positive charge, the  $\alpha$ -hydrogen may then serve to enhance inter- and intramolecular electronic interactions among the macromolecular chains. Schultz and coworkers<sup>11</sup> have used E-coli biosynthetic machinery (in vitro) to synthesize mutant T4 lysozyme (T4L) with lactic acid substituted for a specific alanine residue, (Ala<sup>82</sup>). They report that the thermodynamic stability indicated by  $T_m$  determined by circular dichroism decreases by 3.7°C from that for the wild type T4L. It would be of interest to synthesize a mutant T4L with trifluorolactic acid to assess the affect of this  $\alpha$ -hydroxy acid on the protein thermodynamic stability.

Molecular modeling studies were completed in collaboration with Dr. S. Jacobson of the Materials, Models and Characterization Department of Hoechst Corporate Research and Technology. In these studies, the interactions of fluorine-containing ester model compounds were compared with the corresponding hydrogen-containing molecules as well as an aliphatic amide model compound. Dimer formation energies<sup>12</sup> were calculated along with the methine hydrogen-to-carbonyl oxygen distance; in the case of the amide, the amide hydrogen-to-carbonyl oxygen distance was calculated.

Molecular structures were created with the Insight<sup>®</sup> II<sup>13</sup> molecular modeling system. Insight<sup>®</sup> II is a graphic molecular modeling program used to build, display, manipulate and print molecular structures. The initial pair geometries were selected by sampling random pair conformations followed by molecular mechanics energy minimization using Discover<sup>®</sup> 14 forcefield simulations. The lowest energy conformation from molecular mechanics minimization was then further minimized with DMol<sup>®</sup> 15 computations. DMol<sup>®</sup> is a software package that performs first principles (*ab initio*) quantum chemistry calculations. This was done by calculating solutions to the local density functional equations expressed in a double numerical atomic orbital basis. The basis set is two atomic orbitals for each occupied orbital and the diffuse unoccupied atomic orbitals.

The resultant dimer formation energies and the hydrogen-to-carbonyl oxygen interatomic distances are reported in Table 1.2. *N*-methylacetamide and ethyl acetate were used as model compounds for the peptide and ester linkages, respectively. Methyl 2-methoxypropionate (MMP) and methyl 2-methoxy-3,3,3-trifluoromethylpropionate (MMFP) (in both cases *R* and *S* absolute configurations) were used as model compounds for polylactide and poly(trifluorolactic acid), respectively. The *R*-MMFP dimer is displayed in Scheme 1.3. The calculation results in Table 1.2 show, as expected that the amide model dimer is quite stable with a relatively close approach of the amide hydrogen and the carbonyl oxygen. The ethyl acetate dimer has the smallest interaction energy. The stereoregular model of polylactide (*R*-MMP) is also predicted to form a stable dimer. The dimer of the stereoregular model of poly((*R*)-3,3,3-trifluorolactic acid) (*R*-MMFP) is not as stable as the dimer of *R*-MMP but is more stable than the dimer of ethyl acetate. The model for the polylactide stereocomplex, *R*-MMP/*S*-MMP has a larger interaction energy than *R*-MMP dimer. This correlates with literature data for stereoregular polylactides and polylactide stereocomplexes.<sup>16,17</sup> Interestingly, the stereocomplex of *R*-MMFP and *S*-MMP has the largest interaction energy of the group at -12.59 kcal/mol. This result suggests that blends of stereoregular polylactide and poly(3,3,3-trifluorolactic acid) may exhibit remarkably good physical property profiles compared to ordinary polylactides. It also implies that the strongly electron withdrawing species

fluorine can be used to enhance the strength of intermolecular interactions. This is consistent with the empirical results described by Lavallée et al. with stereoregular polymers of  $\beta$ -trichloromethylpropiolactone (poly(CCl<sub>3</sub>-PL)).<sup>18</sup> They found that  $T_m$  measured by differential scanning calorimetry ranged from 238 to 268°C dependent upon enantiomeric excess. This was contrasted with polymers of  $\beta$ -(trifluoromethyl,methyl)- $\beta$ -propiolactone (poly(CF<sub>3</sub>,Me-PL)) with  $T_m$  from 78 to 100°C. They indicate that higher melting point could be due to intermolecular hydrogen bonds. The electron withdrawing trichloromethyl group provides an acidic  $\beta$ -hydrogen. In poly(CF<sub>3</sub>,Me-PL), there is no  $\beta$ -hydrogen available for hydrogen bonding.

#### 1.4 Lactic Acid - Lactide Preparation and Polymerization

Polymers from the  $\alpha$ -hydroxy acids glycolic acid and lactic acid are used commercially to produce biodegradable fibers and plastics for medical applications.<sup>19</sup> Glycolic acid and lactic acid form six membered dimer rings (dilactones), termed glycolide and lactide, respectively. Synthesis of the dilactones is accomplished by thermal dehydration of the hydroxy acid in the presence of the catalyst titanium(IV) isopropoxide (TIP).<sup>20,21</sup> A polymerization/depolymerization equilibrium is established by transesterification backbiting. The dilactone is removed from the system thus driving the equilibrium toward further formation of the ring compound.

Dilactones (such as lactides) can be polymerized by ring opening polymerization methods<sup>22-24</sup> to produce high molecular weight polymer; poly(lactide) in the case of lactic acid. This is shown in Scheme 1.4. Stannous octoate is used to catalyze the ring opening polymerization of lactide in many commercial applications.<sup>25</sup>

### 1.5 Esters and Polyesters of Fluorinated Aliphatic Compounds

The preparation of trifluoromethyl trifluoroacetate in 1934 was the earliest report on the esterification of fluorinated aliphatic compounds.<sup>26</sup> Hauptschien et al.<sup>27</sup> reported the preparation of a series of fluorinated esters and diesters from mono and dibasic acids as well as mono- and dialcohols. In order to obtain good yields within reasonable reaction times, they prepared activated carboxylic acid compounds (anhydrides or acid chlorides) to react with the weakly nucleophilic fluorinated alcohols. In 1957, Schweiker and Robitschek prepared condensation polymers of aliphatic fluorinated diols and fluorinated acid chlorides.<sup>28</sup> The polymers they prepared ranged from tan viscous liquids to waxy solids with melting points ranging from 35° to 75°C and  $M_n$  from ~5,000 to 8,000 g/mole. Even with activated carboxylic acid groups, long reaction times and elevated temperature are required to obtain good yields.

## 1.6 Overview of the Dissertation

The initial plan in this research was to use trifluorolactic acid (TFL) in the chemistry analogous to that of lactic acid. Specifically, efforts were undertaken to synthesize hexafluorolactide; the dilactone analog of lactide. The catalyst titanium(IV) isopropoxide was used but it proved ineffective. Also attempted was dehydration with phosphorous pentoxide of the hydroxyacid in ether adapted from work by I.L. Knunyants.<sup>29</sup> A complex mixture of products was formed. The preparation of alkyl trifluorolactates was also undertaken from 1-*n*-butanol and methanol with sulfuric acid catalysis and molecular sieves to drive the equilibrium toward ester formation as described in a patent.<sup>30</sup> This would then be used in transesterification chemistry to form hexafluorolactide. Yields, however, were low.

Direct polymerization of trifluorolactic acid by the use of the condensing agent diisopropyl carbodiimide and catalysis proved successful. The procedure was adapted from that described by Moore and Stupp.<sup>31</sup> The overall reaction is shown in Scheme 1.5.

This dissertation comprises four topics. The synthesis and basic characterization of this poly(trifluorolactic acid) are herein described. In Chapter 2, the physical and chemical characteristics of lactic acid and trifluorolactic acid are described and compared. Details of the synthetic

chemistry used to prepare poly(trifluorolactic acid) are discussed in Chapter 3 and the new polymer is contrasted with the polylactide analog. Statistical experimental design was used to optimize the polyesterification and the results of this effort are documented in Chapter 4. Finally, in Chapter 5, further characterization of the fluoropolyester is discussed, including studies of the fractionated polymer and surface characterization.

## 1.7 References and Notes

- (1) Tirrell, D. A.; Fournier, M. J.; Mason, T. L. *Curr Opin Struct Biol* **1991**, *1*, 638.
- (2) Cappello, J.; Crissman, J.; Dorman, M.; Mikolajczak, M.; Textor, G.; Marquet, M.; Ferrari, F. *Biotechnol Prog* **1990**, *6*, 198.
- (3) Dessipri, E., Ph.D. Dissertation, University of Massachusetts Amherst, 1995.
- (4) Stryer, L. *Biochemistry*; 3rd ed.; W. H. Freeman: New York, 1988, p 28.
- (5) Imperiali, B. *Biotechnol Processes* **1988**, *10*, 97.
- (6) Smart, B. E. In *Organofluorine Chemistry*; R. E. Banks, B. E. Smart, and J. C. Tatlow, Eds.; Plenum Press: New York, 1994, p 66.
- (7) Sheppard, W. A.; Sharts, C. M. *Organic Fluorine Chemistry*; W.A. Benjamin: New York, 1969, p 27.
- (8) Chambers, R. D. *Fluorine in Organic Chemistry*; R D Chambers: Durham UK, p 65.
- (9) Hinman, M. B.; Stauffer, S. L.; Lewis, R. V. In *Silk Polymers*; D. Kaplan, W. W. Adams, B. Farmer, and C. Viney, Eds.; American Chemical Society: Washington DC, 1994, p 226.
- (10) PM3 is a semi-empirical quantum chemistry program, supplied as part of Mopac, Version 6 from the Quantum Chemistry Program Exchange, Indiana University, Bloomington, IN.
- (11) Ellman, J. A.; Mendel, D.; Schultz, P. G. *Science* **1992**, *255*, 197.

- (12) Dimer formation energy was determined by calculating the difference between the energy of the dimer and the sum of the individual molecular energies of the isolated dimer components.
- (13) Insight II software, Version 3.0.0, Biosym Molecular Simulations Technologies, San Diego CA, 1995.
- (14) Discover software, Version 95.0/3.00, Biosym Molecular Simulations Technologies, San Diego CA, 1995.
- (15) Dmol software, Version 2.1, Biosym Molecular Simulations Technologies, San Diego CA, 1991.
- (16) Murdoch, J. R.; Loomis, G. L. *U.S. Pat.* (assigned to E I Du Pont de Nemours Inc) 4,766,182 1988.
- (17) Brochu, S., Ph.D. Dissertation, Laval University, 1993.
- (18) Lavallée, C.; Leborgne, A.; Spassky, N.; Prudhomme, R. E. *J Polym Sci Polym Chem* 1987, 25, 1315.
- (19) Shalaby, S. W.; Johnson, R. A. In *Biomedical Polymers*; S. W. Shalaby, Ed.; Hanser: Munich Ger, 1994, p 1.
- (20) E.I. DuPont Co. *U.K. Pat.* (assigned to 1,007,347 1965.
- (21) Sinclair, R. G.; Gynn, G. M. "U.S. Tech Inform Serv report no. AD748411", 1972.
- (22) Kricheldorf, H. R.; Sumbel, M. *Eur Polym J* 1989, 25, 585.
- (23) Kricheldorf, H. R.; Boettcher, C.; Tonnes, K. *Polymer* 1992, 33, 2817.
- (24) Nijenhuis, A. J., Ph.D. Dissertation, University of Groningen, 1995.
- (25) Jacobson, H. W. *U.S. Pat.* (assigned to Ethicon Inc) 3,498,957 1970.

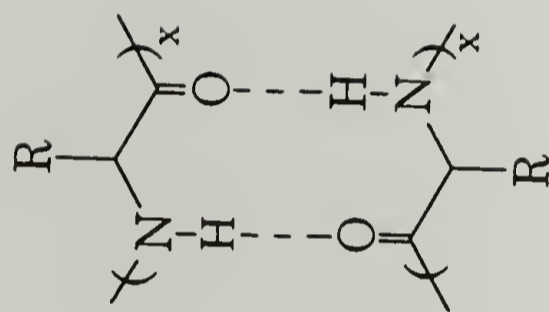
- (26) Swarts, F. *Bull. Soc. Chim. Belg.* **1934**, 43, 476.
- (27) Hauptschien, M.; O'Brien, J. F.; Stokes, C. S.; Filler, R. *J Am Chem Soc* **1953**, 75, 87.
- (28) Schweiker, G. C.; Robitschek, P. *J Polym Sci* **1957**, XXIV, 33.
- (29) Knunyants, I. L.; et al. *Izv Akad Nauk SSSR Otdele Khim* **1961**, 808.
- (30) Katagiri, Y.; Sata, I.; Ohara, I. *Japan Pat.* (assigned to Nikko Kyoseki Co Ltd) Public Patent Disclosure Bulletin no 5- 70406 **1993**.
- (31) Moore, J. S.; Stupp, S. I. *Macromolecules* **1990**, 23, 65.

Table 1.1 The pK<sub>a</sub>'s of aliphatic acids and alcohols.

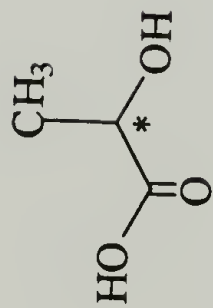
	pK <sub>a</sub> <sup>8</sup>
CH <sub>3</sub> COOH	4.8
CF <sub>3</sub> COOH	- 0.2
CH <sub>3</sub> CH <sub>2</sub> OH	17
CF <sub>3</sub> CH <sub>2</sub> OH	12.8

Table 1.2 Summary of the calculations from molecular modeling.

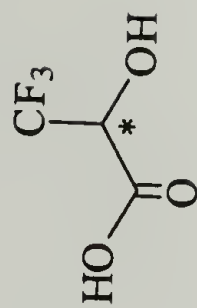
Model compound	Dimer Formation <sup>12</sup> Energy [kcal/mol]	H-----O distance [Å]
<i>N</i> -methylacetamide dimer	-12.04	2.13
ethyl acetate dimer	-4.02	2.19
R-MMP dimer	-10.85	2.71
R-MMFP dimer	-8.01	2.70
R-MMP/S-MMP	-11.27	3.85
R-MMFP/S-MMP	-12.59	3.88



Scheme 1.1 The Peptide hydrogen bonds in an antiparallel  $\beta$  pleated sheet.

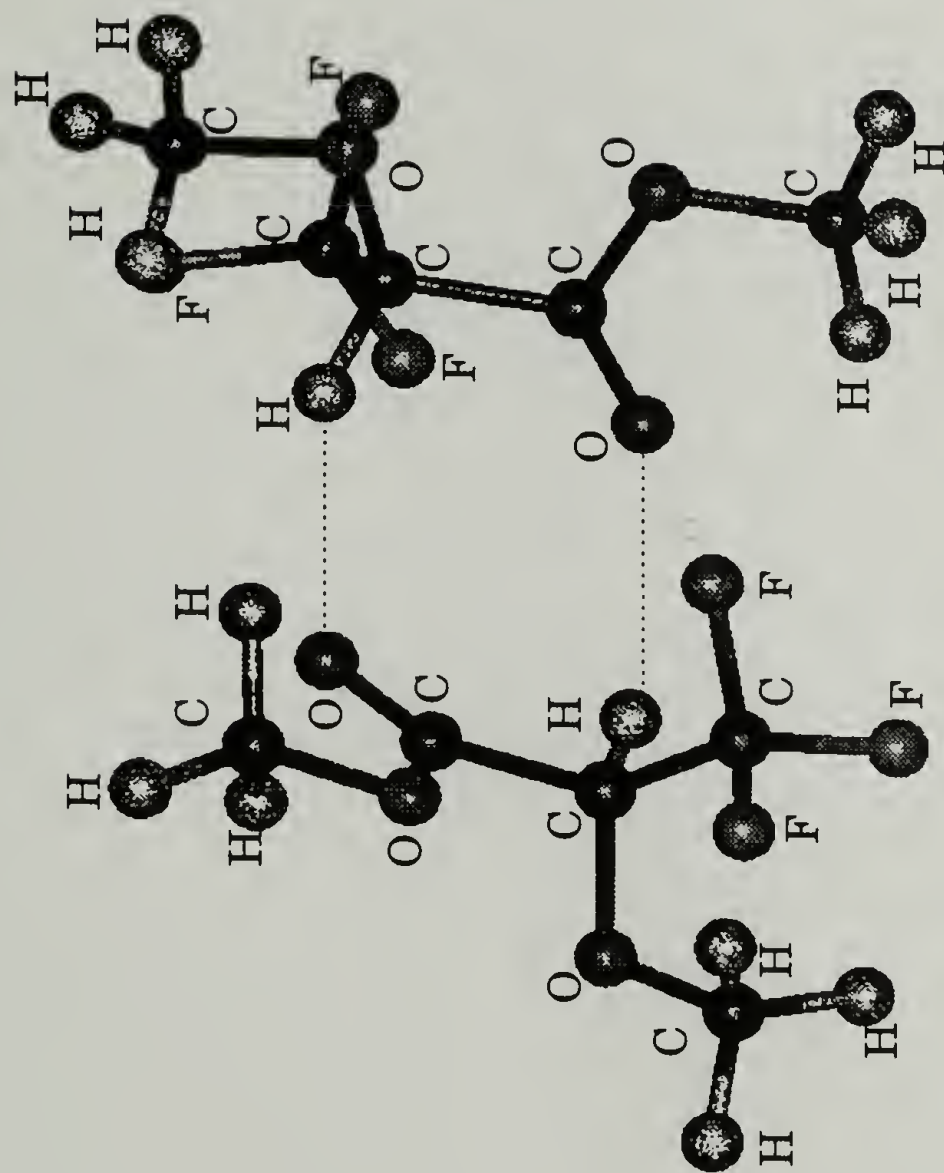


Lactic acid



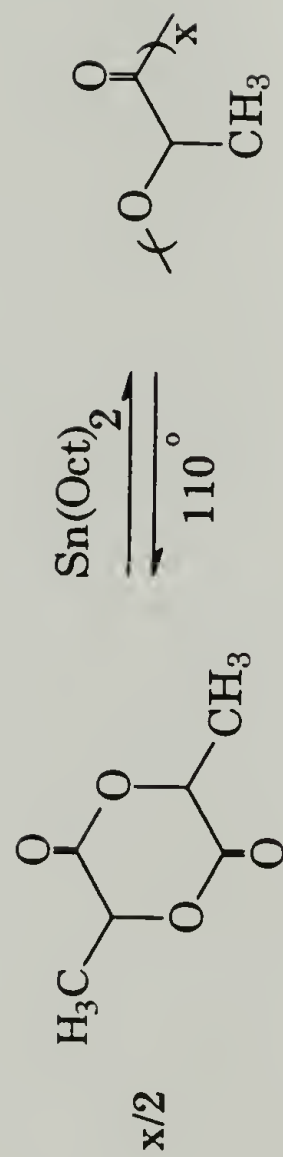
Trifluorolactic acid

Scheme 1.2 Molecular structures of lactic acid and 3,3,3-trifluorolactic acid.



Scheme 1.3 The dimer conformation of methyl (R)-2-methoxy-3,3,3-trifluoromethylpropionate (R-MMFP).

The carbonyl oxygen to methine hydrogen interatomic distances are 2.70 and 2.52 Å.



Scheme 1.4 Ring opening polymerization of lactide.



Scheme 1.5 General polymerization reaction of trifluorolactic acid with carbodiimide condensing agent and 4-(dimethylamino)pyridinium 4-toluenesulfonate (DPTS) catalysis.

## CHAPTER 2

### 3,3,3-TRIFLUOROLACTIC ACID AND LACTIC ACID: A CONTRAST OF $\alpha$ -HYDROXYACIDS

#### 2.1 Introduction

Trifluorolactic and lactic acid are both  $\alpha$ -hydroxy acids that differ in atomic composition. The naturally occurring lactic acid is the simplest hydroxy acid with a stereogenic center.<sup>1</sup> With a trifluoromethyl group instead of a methyl group, 3,3,3-trifluorolactic acid has a formula mass of 144 g/mol whereas lactic acid has a formula mass of 90 g/mol. The earliest record of the synthesis of this fluorohydroxyacid was due to Burstein and Ringold<sup>2</sup> in 1961. The molecular structures are displayed in Scheme 1.2.

The presence of the very strongly electron withdrawing fluorine imparts significantly different physical and chemical properties. As will be described (*vide infra*), 3,3,3-trifluorolactic acid is a crystalline solid at ambient conditions while lactic acid is liquid. Trifluorolactic acid is a rather deliquescent material forming an oily hydrate upon exposure to atmospheric moisture.<sup>3</sup> Also, the trifluoromethyl group causes increased acidity of the trifluorolactic acid compared to lactic acid and apparently reduces the nucleophilicity of the  $\alpha$ -hydroxy group.

Stereoregular trifluorolactic acid (TFL) and lactic acid (LA), in the Fischer projections, are illustrated in Scheme 2.1.<sup>4</sup> It is interesting to note that (S)-lactic acid is synonymous with L-lactic acid while (S)-3,3,3-trifluorolactic acid is equivalent to D-3,3,3-trifluorolactic acid. In this work, the Cahn-Ingold-Prelog (CIP) system of stereochemical notation was used to identify trifluorolactic acid to minimize ambiguity<sup>5,6</sup> and was consistent with nomenclature in the literature used to describe trifluorolactic acid.<sup>7,8</sup> So racemic trifluorolactic acid was described as (RS)-3,3,3-trifluorolactic acid. Lactic acid and derivatives are most often described in the literature with the D, L system of nomenclature. This is maintained here.

The physical, biochemical, chemical characteristics of lactic acid and trifluorolactic acid are discussed and compared in this chapter.

## 2.2 Experimental Section

### 2.2.1 Materials

D,L-lactic acid, (RS)-3,3,3-trifluorolactic acid and D,L-lactide were obtained from Aldrich Chemical Co. and used without further purification.

### 2.2.2 Methods

Capillary melting point data were obtained in a Electrothermal IA9200 digital melting point apparatus. Elemental analyses were performed

at the microanalysis laboratory at the University of Massachusetts Amherst. pK<sub>a</sub> measurements were obtained in the Hoechst Celanese analytical laboratory.

FTIR spectra were obtained with a Mattson Instruments Cignus 100 with a deuterated triglycine sulfate (DGTS) detector; 100 scans were recorded per spectrum with a resolution of 4 cm<sup>-1</sup>. FT-Raman spectra were recorded with a Bruker IFS-66 spectrometer with a FRA 106 Raman attachment; a 1.06 μ Nd-YAG laser; at 0.2 to 0.6 W laser power. Spectra were recorded on samples in glass vials. The <sup>1</sup>H NMR spectrum was recorded on a Varian XL-200 (200 MHz <sup>1</sup>H) spectrometer. The <sup>19</sup>F NMR spectrum was recorded on a Varian VXR 300, at PCR, Inc., with fluorotrichloromethane as a reference. Deuterated dimethyl sulfoxide (DMSO) and chloroform were used as solvents.

## 2.3 Results and Discussion

### 2.3.1 Physical Properties

(RS)-3,3,3-trifluorolactic acid (TFL, Racemic TFL or RS-TFL) was prepared by Aldrich Chemical Co. following the procedure of S.H. Burstein and H.J. Ringold<sup>2</sup> reported in 1961. Trifluoroacetaldehyde hydrate was reacted with KCN in the presence of sulfuric acid to produce the trifluoroacetaldehyde cyanohydrin. The cyanohydrin was then acid

hydrolyzed to TFL. The crude product was vacuum distilled and subsequently purified by sublimation.

M. Hauptschein et al. reported<sup>3,9</sup> and patented<sup>10</sup> in 1965 a commercial route to trifluorolactic acid from 2*H*-pentafluoropropene and dinitrogen tetroxide.

Racemic TFL is a deliquescent white crystalline solid that melts from 71-72°C. It was stored in a desiccator at atmospheric pressure with phosphorous pentoxide at -20°C as suggested by O'Neal.<sup>11</sup> It readily forms trifluorolactic acid hydrate upon exposure to moisture. This is in contrast to the behavior of lactic acid; racemic lactic acid absorbs moisture but does not form hydrates. Unlike racemic TFL, lactic acid is reactive enough to form intermolecular esters (lactoyllactic acid) at ambient conditions.<sup>12</sup> The melting points of these  $\alpha$ -hydroxy acids are compared in Table 2.1.

Lactic acid is completely miscible with numerous solvents including water, ethanol, ethyl ether and 2-furaldehyde. It has limited solubility in benzene, hydrocarbons and thiophene. It is practically insoluble in chloroform.<sup>13</sup> Racemic TFL is readily soluble in ethyl ether, methanol, dimethylformamide, dimethylsulfoxide, tetrahydrofuran, and methylene chloride and chloroform. It is insoluble in cyclohexane and probably other hydrocarbon solvents as well. Also, it is insoluble in perfluorinated ethers

and fluorohydrocarbons. Apparently, solvents with electron donor capability are good solvents for RS-TFL.

### 2.3.2 Biochemical Properties

The earliest reported work with racemic trifluorolactic acid was by Burstein and Ringold<sup>2</sup> in 1961. Their purpose for synthesis of this previously unknown compound was to prepare an inhibitor of the enzyme lactate dehydrogenase (LDH). LDH mediates the interconversion of L-lactate and pyruvate<sup>14</sup> with nicotinamide adenine dinucleotide (NAD<sup>+</sup>) as cofactor.

In experiments with rabbit muscle LDH, Burstein and Ringold determined that TFL or sodium trifluorolactate was not oxidized to pyruvate over a 30 minute period. Sodium D,L-lactate, under the same conditions, was oxidized as indicated by the appearance of NADH. Sodium pyruvate was reduced to lactate without inhibition by sodium trifluorolactate.

In 1973, A. Pogolotti and J.A. Rupley<sup>14</sup> reported that trifluorolactate was neither a substrate nor an inhibitor of rabbit muscle LDH. On the other hand, they indicated that trifluorolactate was not a substrate for pig heart enzyme but suggested that it was a competitive inhibitor of lactate oxidation. Also, they found that lactate and trifluorolactate were noncompetitive inhibitors of pyruvate reduction to lactate. They went on to state that "The failure of earlier experiments to demonstrate inhibition by trifluorolactate may be due to different sources of enzyme or to the reaction conditions."

In his 1980 dissertation,<sup>11</sup> C.C. O'Neil used trifluorolactate to study the structure of the ternary complex of the enzyme, cofactor and substrate. This was in the absence of the rapid interconversion upon hydride transfer since trifluorolactate is nonreactive; i.e., it is a competitive inhibitor of lactate oxidation. O'Neil also found that trifluorolactate was not a simple dead-end inhibitor and that it was connected to the productive pathway at more than one point. He concluded that this was consistent with the existence of two conformational states of LDH•NAD.

Sheppard and Sharts<sup>15</sup> have discussed the toxicity of  $\omega$ -fluoroaliphatic carboxylic acids. If the total number of carbons was odd, the acid was relatively innocuous. However, if the number of carbons was even, the molecule was highly toxic. In vivo, higher even numbered  $\omega$ -fluoroaliphatic carboxylic acids are broken down to fluoroacetic acid which is converted to fluorocitric acid. The citric acid cycle is blocked when certain enzymes necessary for hydrogen transfer are irreversibly complexed to fluorocitric acid. This was described well by Pattison in a monograph on toxic fluorine compounds.<sup>16</sup> Pattison also described the results of a toxicity investigation of ethyl  $\omega$ -fluorolactate which was found to be non-toxic.<sup>17</sup> RS-TFL has an odd number of carbons but it is an  $\omega$ -trifluoroaliphatic carboxylic acid.

A toxicity investigation of trifluorolactic acid conducted by Hoechst Celanese Corporate toxicology showed that there was no information in the open literature on the toxicity of RS-TFL. It was recommended that for laboratory

handling purposes, it be considered a severe skin and eye irritant and highly toxic by inhalation, oral or dermal administration.

### 2.3.3 Pharmaceutical Chemistry

TFL has also been used as an intermediate in the development of pharmaceutical drugs.<sup>18,19</sup> In 1984,  $\alpha$ -aryloxy methyl trifluorolactate and a series of similar compounds were reported by ICI Pharmaceuticals Division as fluoro analogs of the chlorinated compounds that are hypocholesterolaemic. The researchers found that these fluoro compounds lowered the plasma level of cholesterol in rats.

Recently (1991-1994), a series of Japanese public patent disclosure bulletins and a paper described the synthesis of optically active TFL and derivative esters.<sup>20-24</sup> Trifluoropropene was converted to optically active (-)-1,2-epoxy-3,3,3-trifluoropropane by microorganisms. The epoxide was oxidized to TFL by action of nitric acid in the presence of copper catalyst. The trifluorolactic acid isolated after recrystallization was reported to be of 98% enantiomeric excess. Also, a series of alkyl (3 through 6 carbons) and benzyl esters of optically active trifluorolactic acid was reported. The esters were prepared in an excess of the alcohol with sulfuric acid catalysis and molecular sieves to adsorb water and drive the equilibrium toward ester formation. The patent bulletins state that these compounds were useful as intermediate raw materials in the synthesis of drugs, agricultural chemicals,

functional polymers and organic compounds (liquid crystals, dyes and surface active agents).

#### 2.3.4 Chemical Properties

The inductive effect of the trifluoromethyl group increased the acidity of TFL by an order of magnitude over lactic acid. This is shown in Table 2.2. The  $pK_a$  of TFL is equivalent to that of monochloroacetic acid,<sup>25</sup> a relatively strong organic acid.

2,2,2-trifluoroethanol and 3,3,3-trifluoropropionic acid are model compounds for the hydroxy and carboxy functional groups of trifluorolactic acid, respectively. The  $pK_a$ 's of these molecules were determined by pH measurement at the one-half equivalence point.<sup>26</sup>

Elemental analysis of TFL is shown in Table 2.4. The elemental analysis results are in excellent agreement with the calculated values.

The  $pK_a$  of ethanol is 17<sup>25</sup> so the hydroxy group hydrogen of the fluorocarbon analog of ethanol (trifluoroethanol) is more acidic (Table 2.2). It is reasonable to assume that this is the case for the hydroxy group of TFL vis-a'-vis lactic acid. This property suggests that the hydroxy group of TFL is a poorer nucleophile than that of lactic acid.

### 2.3.5 Spectroscopic Characterization

The FTIR and FT-Raman spectra of TFL verified the presence of hydroxy groups, the carbonyl and the  $\alpha$ -hydrogen. The CH stretch is prominent in the Raman spectrum where hydroxy groups, which absorb near the same frequency in IR, are not Raman active. The infrared and the Raman spectra are directly compared in Figure 2.1. The band assignments are shown in Table 2.3.

Although the CH stretch is also IR active it is convoluted with a broad hydroxy absorption. The infrared band at  $1141\text{ cm}^{-1}$  is tentatively assigned to the  $\text{CF}_3$  group.<sup>27</sup> A comparison of RS-TFL and methyl trifluorolactate in Figure 2.2 allowed identification the OH band at  $3014\text{ cm}^{-1}$  as that of the carboxy group and therefore the band at  $3419\text{ cm}^{-1}$  was assigned to the  $\alpha$ -hydroxy group.

The Raman spectra of D,L-lactic acid and RS-TFL are displayed in Figure 2.3. D,L-lactic acid has the carbonyl peak at  $1734\text{ cm}^{-1}$ . The corresponding peak in TFL is at a higher frequency;  $+1746\text{ cm}^{-1}$ . This is apparently due to the strongly electron withdrawing  $\text{CF}_3$  group which reduces single bond character of the carbonyl achieved through electronic charge delocalization from the carbonyl carbon and oxygen bond to the carbonyl oxygen. The cyclic diester, D,L-lactide, has a higher carbonyl frequency compared to D,L-lactic acid (Figure 2.4) as expected.<sup>28</sup>

The  $^{19}\text{F}$  (prepared by PCR, Inc.) and  $^1\text{H}$  NMR spectra of RS-TFL are shown as Figures 2.5 and 2.6, respectively. The fluorine NMR spectrum (in  $\text{CDCl}_3$  with fluorotrichloromethane as the 0 ppm reference) indicates a signal for the three equivalent fluorines split into a doublet by the  $\alpha$ -hydrogen and centered near -76 ppm. The proton NMR spectrum (in deuterated DMSO) shows the  $\alpha$ -hydrogen signal split by the trifluoromethyl group into a quartet centered near 4.6 ppm. Water and the two exchangeable hydroxy protons appear as broad peaks centered near 3.3, 6.7 and 13.5, respectively. In the  $^1\text{H}$  NMR spectrum of L-lactic acid ((S)-lactic acid), in  $\text{D}_2\text{O}$  or  $\text{CH}_3\text{OD}$ , the  $\alpha$ -hydrogen quartet is centered at 4.4 ppm.<sup>29</sup>

## 2.4 Conclusions

(RS)-3,3,3-trifluorolactic acid has been characterized and shown to be significantly different from D,L-lactic acid in physical and chemical properties.

## 2.5 References and Notes

- (1) Holten, C. H. *Lactic Acid*; Verlag Chemie: Weinheim Germany, 1971, p 3.
- (2) Burstein, S. H.; Ringold, H. J. *Can J Chem* **1961**, *39*, 1848.
- (3) Hauptschein, M.; Oesterling, R. E. *J Org Chem* **1963**, *28*, 1279.
- (4) Eliel, E. L. *Stereochemistry of Carbon Compounds*; McGraw-Hill: New York, 1962, p 88.
- (5) Carey, F. A. *Organic Chemistry*; 2nd ed.; McGraw-Hill: New York, 1992, p 258.
- (6) Juaristi, E. *Introduction to Stereochemistry and Conformational Analysis*; Wiley-Interscience: New York, 1991, p 23.
- (7) von dem Bussche-Hunnefeld, C.; Cescato, C.; Seebach, D. *Chem Ber* **1992**, *125*, 2795.
- (8) Bravo, P.; Frigerio, M.; Resnati, G. *J Org Chem* **1990**, *55*, 4216.
- (9) Hauptschein, M.; Oesterling, R. E.; Braid, M.; Tyczkowski, E. A.; Gardener, D. M. *J Org Chem* **1963**, *28*, 1281.
- (10) Hauptschein, M.; Oesterling, R. E. *U.S. Pat.* (assigned to Pennsalt Chem Corp) 3,202,706 **1965**.
- (11) O' Neal, C. C., Jr., Ph.D. Dissertation, University of Arizona, 1980.
- (12) Holten, C. H. *Lactic Acid*; Verlag Chemie: Weinheim Germany, 1971, p 192.

- (13) Holten, C. H. *Lactic Acid*; Verlag Chemie: Weinheim Germany, 1971, p 53.
- (14) Pogolotti, A., Jr.; Rupley, J. A. *Biochem Biophys Res Comm* **1973**, *55*, 1214.
- (15) Sheppard, W. A.; Sharts, C. M. *Organic Fluorine Chemistry*; W A Benjamin: New York, 1969, p 462.
- (16) Pattison, F. L. M. *Toxic Aliphatic Fluorine Compounds*; Elsevier: Amsterdam, 1959, p 90.
- (17) Pattison, F. L. M. *Toxic Aliphatic Fluorine Compounds*; Elsevier: Amsterdam, 1959, p 100.
- (18) Haydock, D. B.; Mulholland, T. P. C.; Telford, B.; Thorp, J. M.; Wain, J. *S. Eur J Med Chem- Chim Ther* **1984**, *19*, 205.
- (19) Haydock, D. B. *France Pat.* (assigned to Imp Chem Ind) 2,293,196 **1976**.
- (20) Kubota, T. *Japan Pat.* (assigned to Nikko Kyoseki Co Ltd) Public Patent Disclosure Bulletin no 3-148249 **1991**.
- (21) Nikko Kyoseki Co. Ltd *Japan Pat.* (assigned to Public Patent Disclosure Bulletin no.: 5-78277 **1993**.
- (22) Katagiri, Y.; Sata, I.; Ohara, I. *Japan Pat.* (assigned to Nikko Kyoseki Co Ltd) Public Patent Disclosure Bulletin no 5- 70406 **1993**.
- (23) Katagiri, Y. *Japan Pat.* (assigned to Nikko Kyoseki Co Ltd) Public Patent Disclosure Bulletin no 5-78278 **1993**.
- (24) Katagiri, T.; Obara, F.; Toda, S.; Furuhashi, K. *Synlett Letters* **1994**, 507.

- (25) Hendrickson, J. B.; Cram, D. J.; Hammond, G. S. *Organic Chemistry*; 3rd edition ed.; McGraw-Hill: New York, 1970, p 306.
- (26) Letinski, J. "Analytical Services Report ref. no. R95-679-680", Hoechst Celanese Advanced Technology Group, 1995.
- (27) Silverstein, R. M.; Bassier, G. C.; Morrill, T. C. *Spectrometric Identification of Organic Compounds*; 5th ed.; J Wiley & Sons: New York, 1991, p 162.
- (28) Colthup, N. B.; Daly, L. H.; Wiberley, S. E. *Introduction to Infrared and Raman Spectroscopy*; 3rd ed.; Academic Press Inc: Boston, 1990, p 290.
- (29) Holten, C. H. *Lactic Acid*; Verlag Chemie: Weinheim Germany, 1971, p 518.
- (30) Holten, C. H. *Lactic Acid*; Verlag Chemie: Weinheim Germany, 1971, p 20.
- (31) Henne, A. L.; Pelley, R. L. *J Am Chem Soc* **1952**, *74*, 1426.
- (32) Kortum, G.; Vogel, W.; Andrussov, K. *Dissociation Constants of Organic Acids in Aqueous Solution*; Butterworths: London, 1961

Table 2.1 Melting points of (RS)-3,3,3-trifluorolactic acid and lactic acid.

	[°C]
RS-TFL (capillary tube)	71-72
RS-TFL <sup>2</sup>	68-69
Racemic lactic acid <sup>30</sup>	18

Table 2.2 The pK<sub>a</sub>'s of (R,S)-3,3,3-trifluorolactic acid, lactic acid and model compounds.

	pK <sub>a</sub> (found)	pK <sub>a</sub> (literature)
Racemic TFL	—	2.75 <sup>7</sup>
Lactic acid	—	3.8 <sup>7</sup>
2,2,2-trifluoroethanol	11.6	11.4 <sup>31</sup>
3,3,3-trifluoropropionic acid	2.9	3.0 <sup>32</sup>

Table 2.3 Elemental analysis of (RS)-3,3,3-trifluorolactic acid.

	Carbon [wt. %]	Hydrogen [wt. %]	Fluorine [wt. %]
TFL - Calculated	25.01	2.08	39.57
TFL - Found	24.96	1.96	39.6

Table 2.4 FTIR and FT-Raman assignments of (RS)-3,3,3-trifluorolactic acid.

Absorption bands $\nu$ [ $\text{cm}^{-1}$ ]		Assignment
FTIR	FT-Raman	
3419		OH ( $\alpha$ hydroxy)
3014		OH (carboxy)
	2980	CH
1738	1745	C=O
1141		CF <sub>3</sub> 27

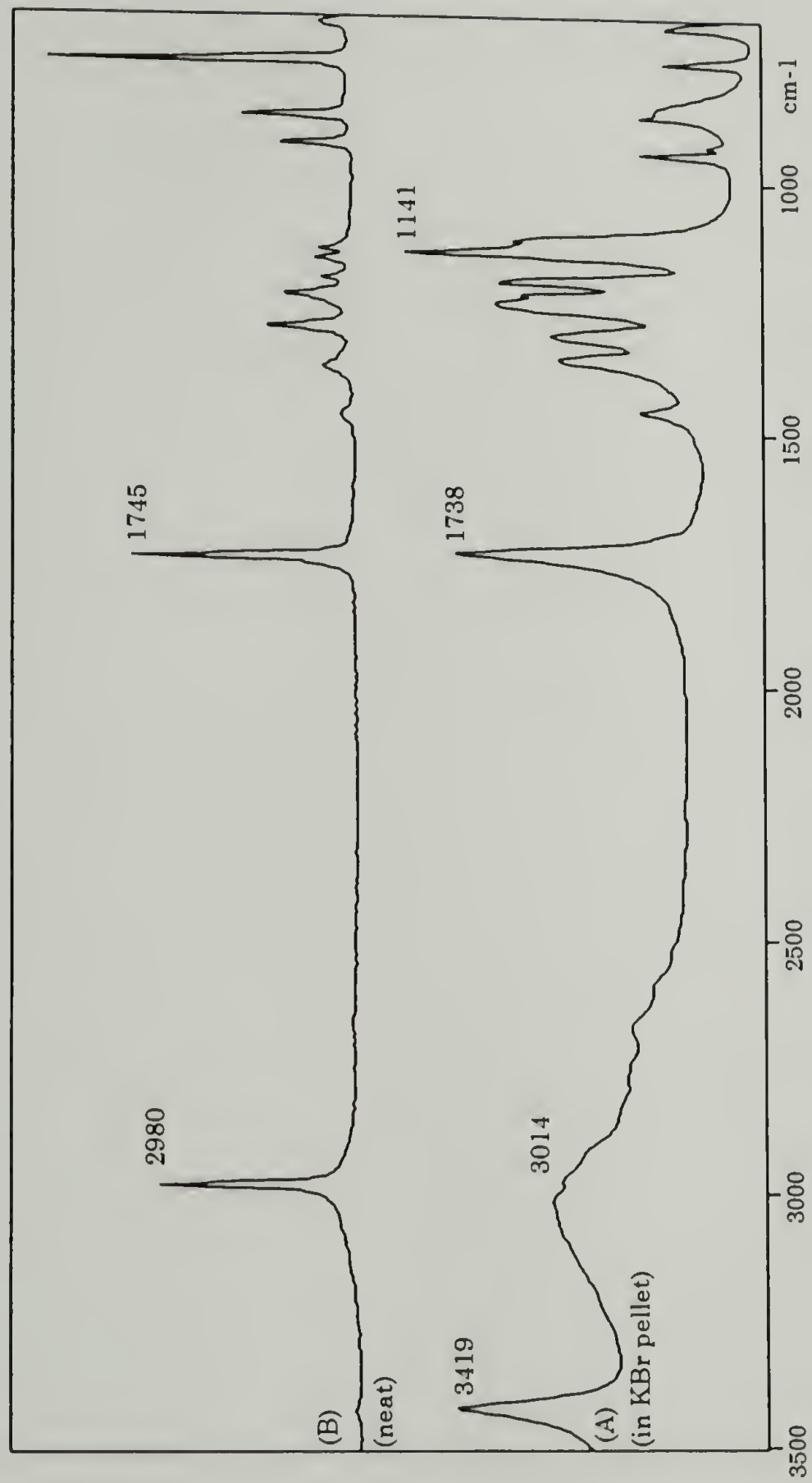


Figure 2.1 Vibrational spectra of (RS)-3,3,3-trifluorolactic acid. A: FTIR and B: FT-Raman.

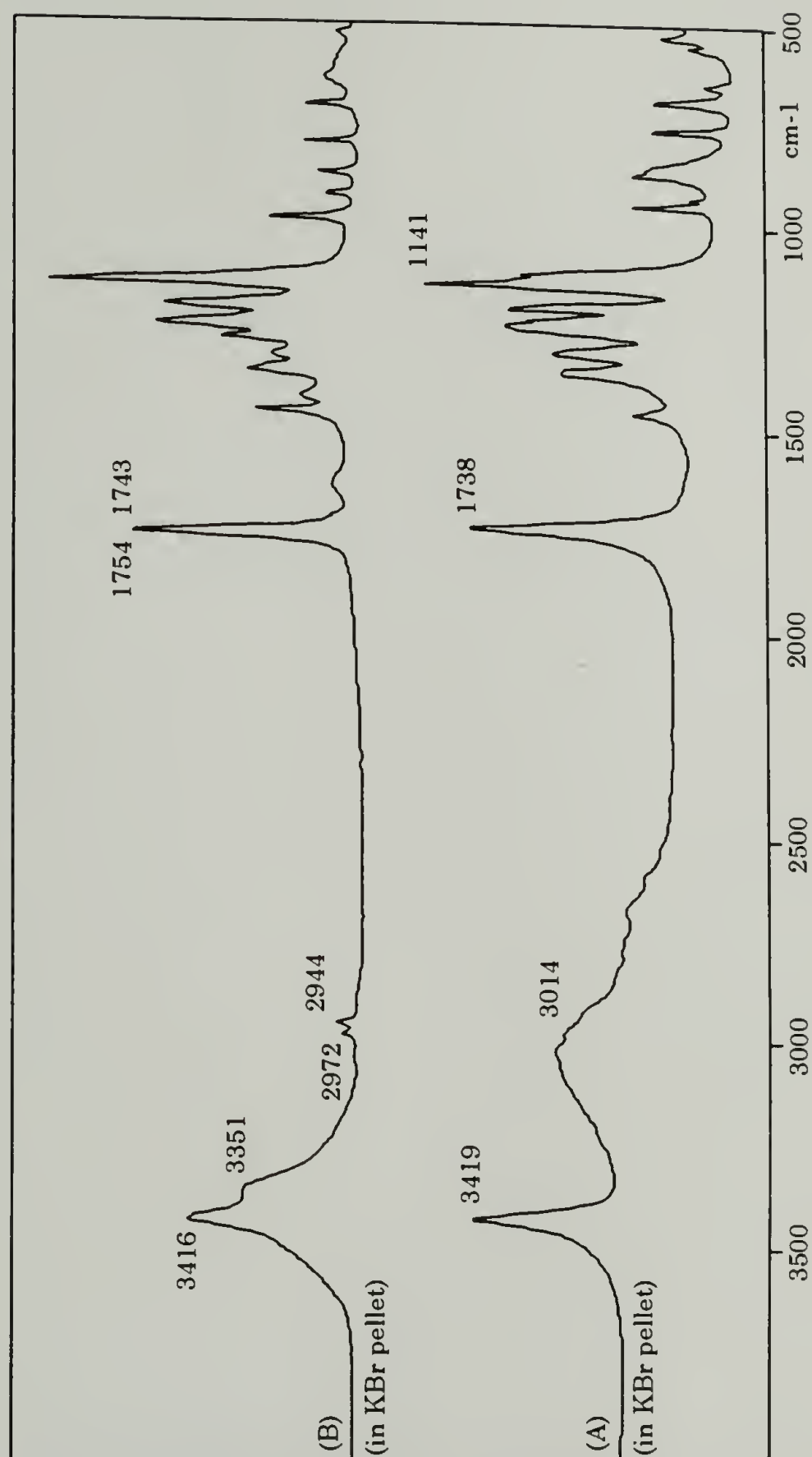


Figure 2.2 FTIR spectra of A: (RS)-TFL and B: methyl (RS)-3,3,3-trifluorolactic acid.

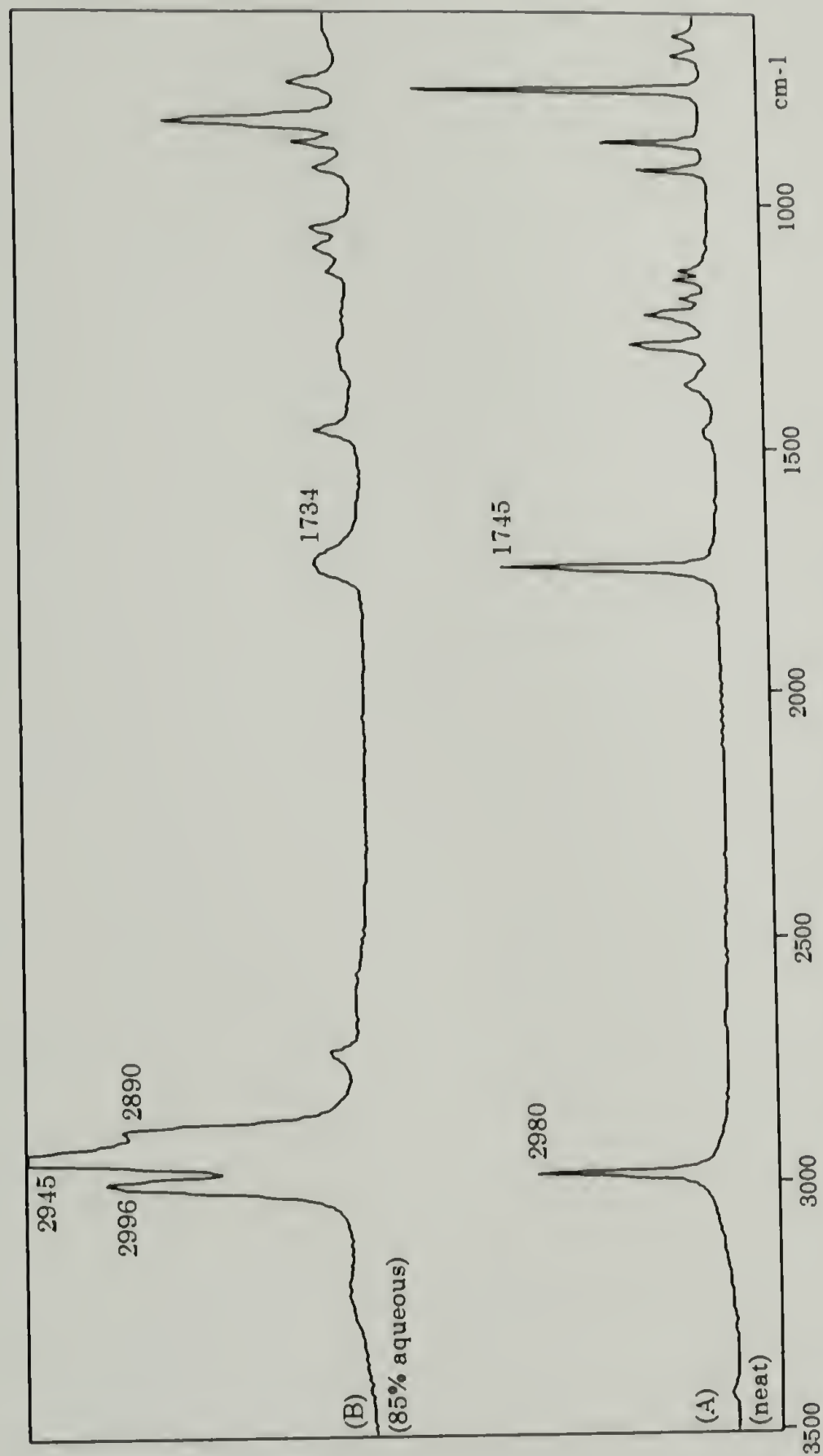


Figure 2.3 FT-Raman spectra of A: (RS)-3,3,3,3-tetrafluorolactic acid and B: D,L-lactic acid.

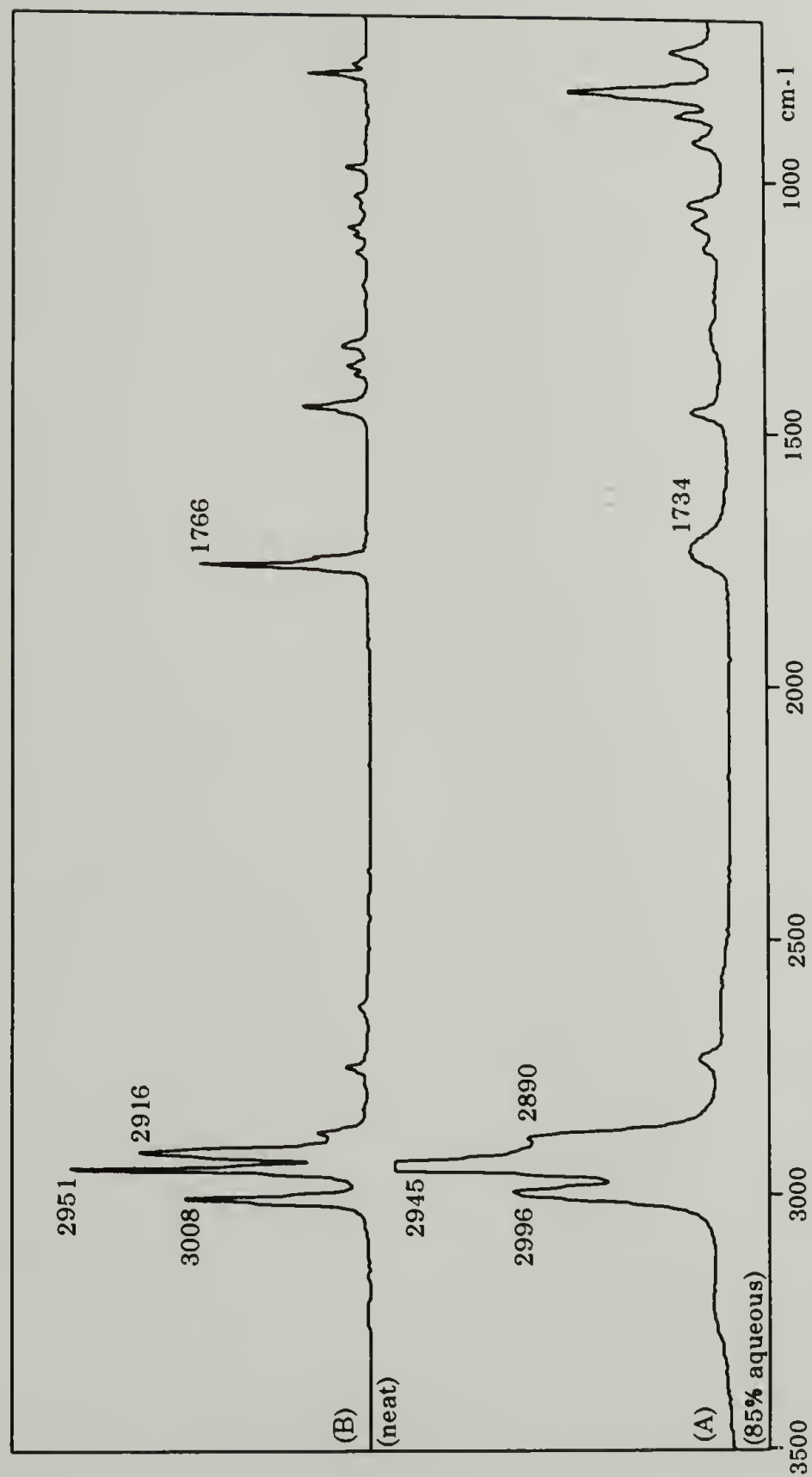


Figure 2.4 FT-Raman spectra of A: D,L-lactic acid and B: D,L-lactide.

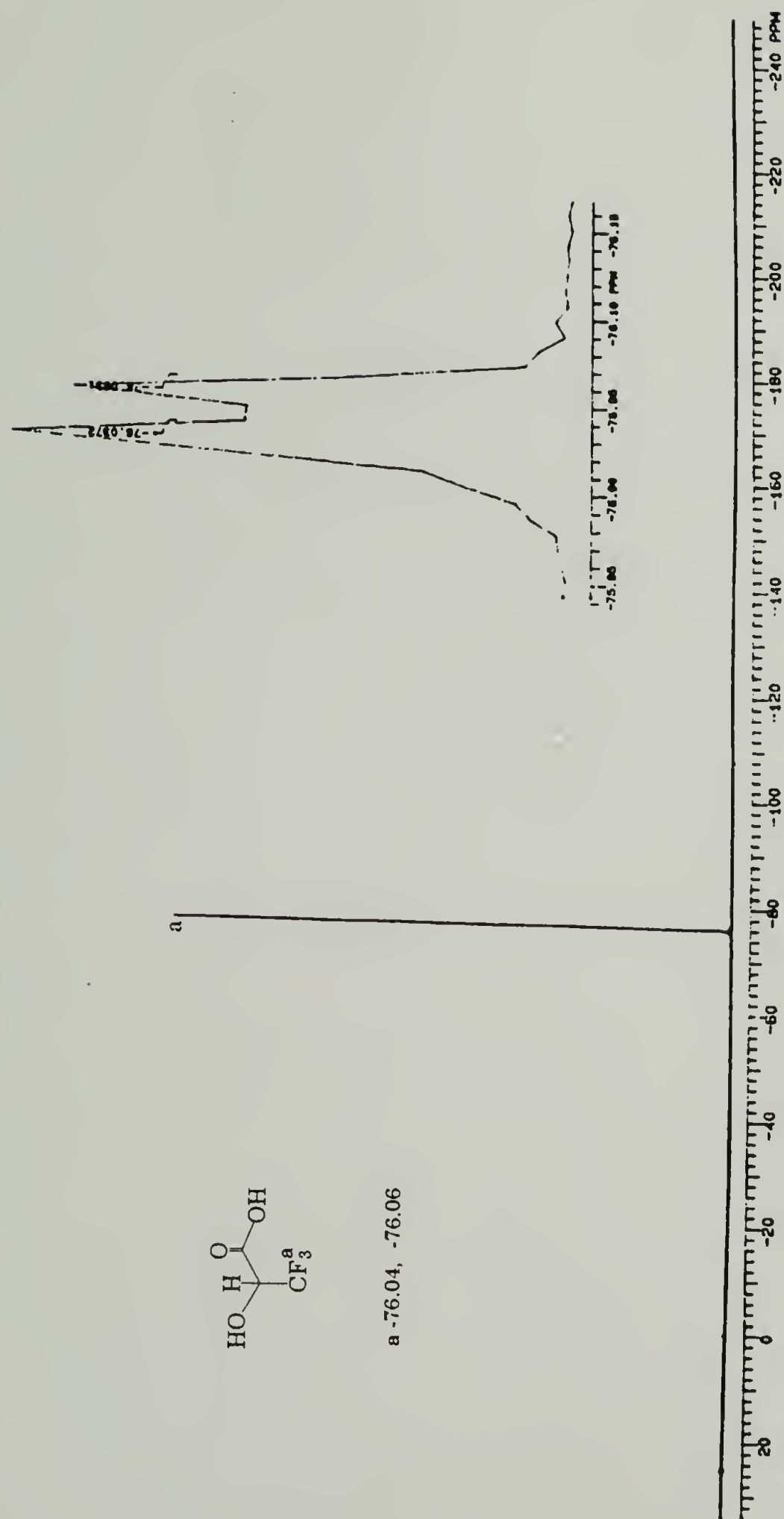
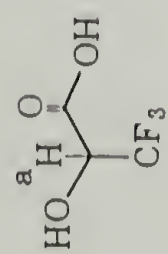


Figure 2.5 300-MHz  $^{19}\text{F}$  NMR spectrum of (RS)-3,3,3-trifluorolactic acid in  $\text{CDCl}_3$ .



a 4.65  
b 2.49 DMSO

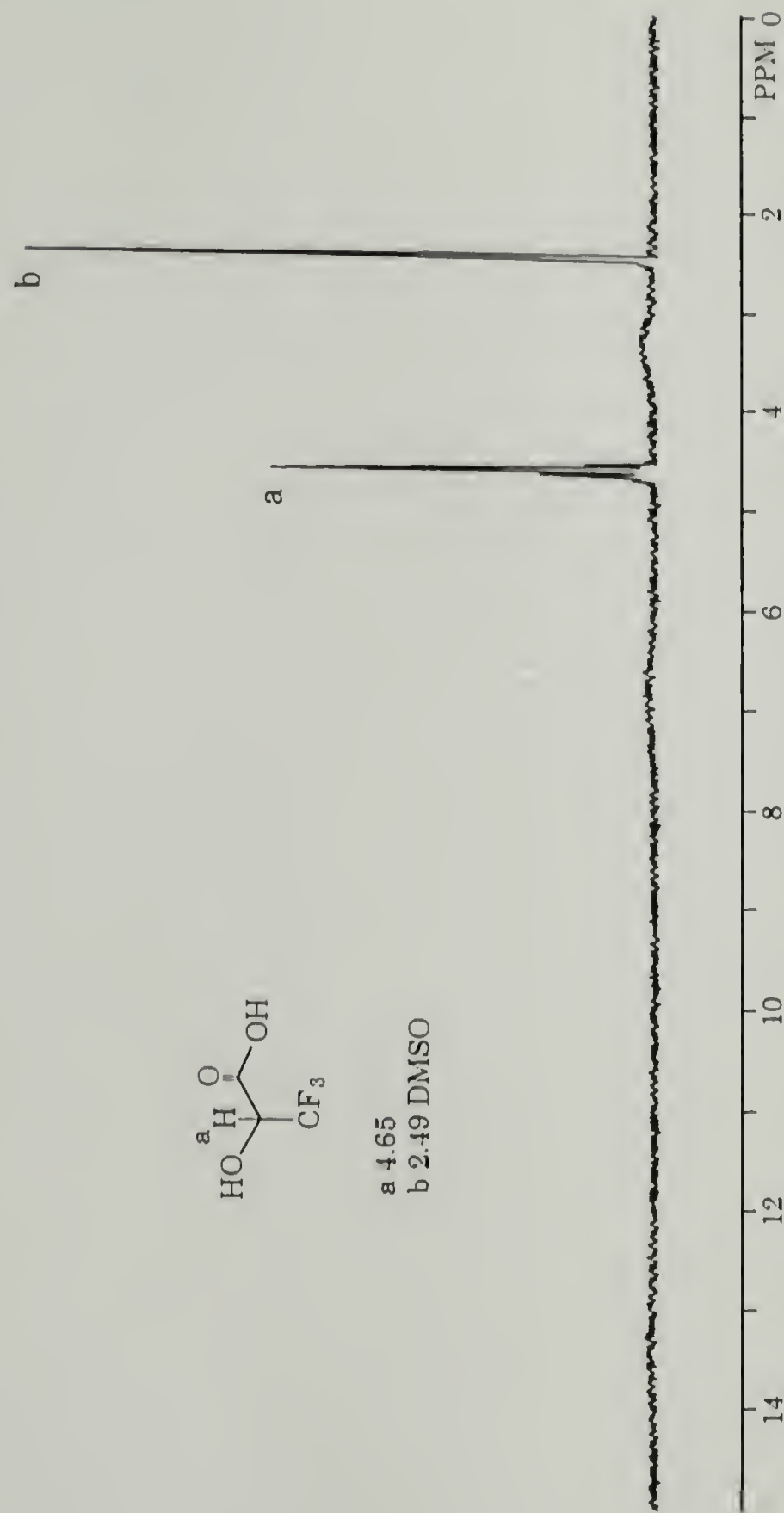
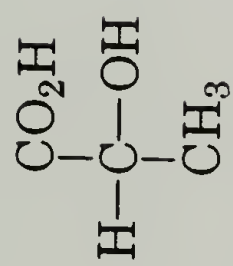
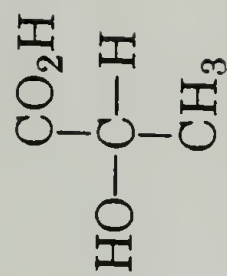


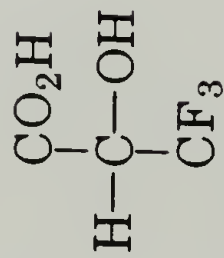
Figure 2.6 200-MHz <sup>1</sup>H NMR of (RS)-3,3,3-trifluorolactic acid in DMSO-*d*<sub>6</sub>.



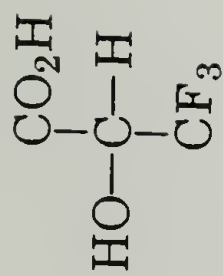
R-LA or D-LA



S-LA or L-LA



S-TFL or D-TFL



R-TFL or L-TFL

Scheme 2.1 Fischer projections of the stereoisomers of lactic acid (LA) and 3,3,3-trifluorolactic acid (TFL).

## CHAPTER 3

### SYNTHESIS OF POLY((RS)-3,3,3-TRIFLUOROLACTIC ACID) AND COMPARISON WITH POLYLACTIDES

#### 3.1 Introduction

Proteins and polypeptides form strong inter- and intramolecular hydrogen bonds through the peptide linkage. As derivatives of nylon 2, with a high frequency of aliphatic amide links, proteins have the potential for high packing density with hydrogen bonding. To the extent that increased attractive intra- and intermolecular interactions may be induced in polyesters through appropriate placement of fluorine, fluoroaliphatic  $\alpha$ -hydroxyacids form polymers that can be considered analogs of polypeptides. Lactic acid is the  $\alpha$ -hydroxy acid analog of alanine. If the methyl group of lactic acid is converted to a trifluoromethyl group, it is reasonable to expect that the acidity of the  $\alpha$ -hydrogen would be significantly increased. With increased partial positive charge, the  $\alpha$ -hydrogen may then serve to enhance inter- and intramolecular electronic interactions. Polymers of fluorinated  $\alpha$ -hydroxyacids are thus a bio-inspired variation of lactide and glycolide polymers.

The synthesis of poly((RS)-3,3,3-trifluorolactic acid) (poly((RS)-TFL) was carried out as an initial attempt to explore this hypothesis. By applying

the synthetic techniques described by Moore and Stupp<sup>1</sup> (with some modifications), the transformation of the halo  $\alpha$ -hydroxyacid to polymer was carried out with 1,3-diisopropylcarbodiimide condensing agent in the presence of equimolar 4-(dimethylamino)pyridine (DMAP) and *p*-toluenesulfonic acid. The general polymerization reaction is shown in Scheme 1.5. The synthesis and basic characterization of this novel polymer are herein described. Poly((RS)-3,3,3-trifluorolactic acid) is contrasted with the lactide polymers, poly(D,L-lactide) and poly(L-lactide).

## 3.2 Experimental Section

### 3.2.1 Materials

Anhydrous toluene, 1,2-dichloroethane, methylene chloride, chloroform and tetrahydrofuran (THF) were obtained from Aldrich Chemical Co. and used without further purification. All other reagents and pyridinium triflate, dimethylformamide (DMF), dimethyl sulfoxide (DMSO), methyl ethyl ketone (MEK), acetone, ethyl acetate, methanol, 1,3-bis(trifluoromethyl)benzene, 1,4-bis(trifluoromethyl)benzene,  $\alpha,\alpha,\alpha$ -trifluorotoluene, petroleum ether, cyclohexane, ethyl ether and pyridine were also obtained from Aldrich Chemical Co. and used without further purification.

Poly(D,L-lactide) (Medisorb<sup>®</sup> 100DL) and poly(L-lactide) (Medisorb<sup>®</sup> 100L) were obtained from Medisorb Technologies International L.P..

### 3.2.2 Methods

All glassware was oven dried at 125°C for at least two hours and assembled in an argon atmosphere glove box with less than 0.5 PPM water vapor. Solid reagents were weighed out and introduced into the assembly in the glove box. The assembled reaction system was then placed in a fume hood for subsequent activities.

Capillary melting point data were obtained in a Electrothermal IA9200 digital melting point apparatus. Elemental analyses were performed at the microanalysis laboratory at the University of Massachusetts Amherst.

FTIR spectra were obtained with a Mattson Instruments Cignus 100 with a deuterated triglycine sulfate (DGTS) detector; 100 scans were recorded per spectrum with a resolution of 4 cm<sup>-1</sup>. FT-Raman spectra were recorded with a Bruker IFS-66 spectrometer with a FRA 106 Raman attachment; a 1.06 μ Nd-YAG laser; at 0.2 to 0.6 W laser power. Spectra were recorded on samples in glass vials.

<sup>1</sup>H NMR and <sup>13</sup>C NMR spectra were recorded on a Varian XL-200 (200 MHz <sup>1</sup>H) spectrometer. Deuterated DMSO, THF, chloroform and 1,1,1,3,3,3-hexafluoro-2-propanol (HFIP) were used as solvents. Inherent viscosity was measured with Cannon-Ubbelohde size 50 viscometers in a constant temperature water bath at 29.95°C ± 0.01°C. THF was used as solvent. Solution concentration was 0.2 g/dL. Data reported in Table 3.1 were

obtained from solutions filtered (0.25  $\mu$  glass membrane) prior to measurement. Inherent viscosities reported in Table 3.4 were obtained without filtration.

Gel permeation chromatography (GPC) traces were obtained at ambient temperature in a Waters 210 GPC with a WISP 712 sample autoinjector and a Waters 410 visible LED differential refractometer. In HFIP, shot size was 200  $\mu$ L at a concentration of 2 mg/mL for all polymer samples. Shot size was also 200  $\mu$ L but at a concentration of 12 mg/mL for the poly((RS)-TFL) sample in THF. Columns were from American Polymer Standards PL-Gel, 10  $\mu$ m particles, mixed-B (bed with nominal 500,  $10^3$ ,  $10^4$ ,  $10^5$ , and  $10^6$  Å particle porosity). THF or HFIP solvent was degassed and passed through a 5  $\mu$ m filter.

A Wyatt DAWN-FH 1992 flow through instrument with 18 simultaneously scattering angles of detection was used to obtain light scattering data. The incremental indices of refraction (dn/dc) for the polymer solutions were measured in a Wyatt optilab DSP interferometric refractometer. Solutions at 3 different concentrations were prepared for each type of polymer. Shot size was 200  $\mu$ L at a concentration of 12 mg/mL.

Differential scanning calorimeter (DSC) and thermogravimetric analysis (TGA) data were obtained in a Perkin-Elmer series 7 thermal analysis system. Thermal responses were measured with samples in a nitrogen atmosphere at a 10° C/min rate of temperature rise in the TGA

experiments. In the DSC experiments, a 20° C/min rate of temperature rise was used except for the poly(L-lactide) tested at 10°C/min. The second heat trace data of the DSC measurements are reported.

Wide angle X-ray scattering (WAXS) data were obtained with a Siemens instrument in a helium atmosphere with monochromated CuK $\alpha$  (1.542 Å) radiation via a Rigaku Ru-200 rotating anode generator. Data were processed by Siemens HI-STAR software.

### 3.2.3 Preparations

**4-(Dimethylamino)pyridinium 4-toluenesulfonate (DPTS):**<sup>1</sup> *p*-Toluenesulfonic acid monohydrate (PTSA, 19.5 g, 0.103 mol) was placed in a 3 L round bottom flask equipped with a stir bar. Anhydrous toluene (1.2 L) was cannulated into the flask. The flask was fitted with a condenser, Dean-Stark trap and mineral oil bubbler and heated to reflux to remove the PTSA water of hydration. The flask was then cooled to 80°C and a warm (60-90°) toluene solution of (4-dimethylamino)pyridine (DMAP, 12.6 g, 0.103 mol) was added to the anhydrous PTSA. DPTS immediately precipitated from solution and was collected on a fritted glass funnel. The crude product was washed with toluene and dried overnight in a vacuum oven at 35°. 1,2-Dichloroethane was used to recrystallize the crude product resulting in needle crystals (22.1 g, 0.08 mol, 77.7% yield) of DPTS, m.p. 175°C (literature m.p. 165°C.<sup>1</sup>) DPTS was found to be readily soluble in methylene chloride,

chloroform and pyridine, DMF and DMSO and methanol. It is only slightly soluble in THF, 1,2-dichloroethane and ether. Elemental analysis,  $C_{14}H_{18}O_3N_2S$ , calculated: C 57.15, H 6.12, O 16.31, N 9.52, S 10.90, found: C 56.99, H 6.10, O 16.06, N 9.38, S 11.02.

#### **4-(Dimethylamino)pyridinium triflate (DPTL):**

(4-Dimethylamino)pyridine (DMAP, 24.4 g, 0.20 mol) was added to a 1 L three neck round bottom flask in the glove box. The flask was equipped with a stir bar and fitted with gas and outlet adapters as well as a thermometer. Anhydrous toluene (400 mL) was cannulated into the flask in the fume hood. The flask was warmed to 70°C to completely dissolve the DMAP and then cooled to room temperature. A pressure equalizing dropping funnel was filled with trifluoromethanesulfonic acid (triflic acid) (TLA) (28 g, 0.19 mol) in the glove box, sealed and then placed on the flask. The flask was then fitted with argon inlet and outlet tubes. The gas outlet tube was attached to a 250 mL surge flask which was connected to a gas scrubber filled with saturated aqueous sodium carbonate. The reaction flask was then placed in an ice bath and stirred while TLA was added dropwise. A white precipitate formed immediately. The temperature rose to 40° during the addition of the acid. The crude product was collected on a fritted glass funnel washed with toluene and dried overnight (52.5 g) in a vacuum oven at 70° (52.5 g, 0.2 mol, >99 % yield). 1,2-Dichloroethane (500 mL) was used to recrystallize the crude product. The melting range of the purified DPTL, is 145-147°C. DPTL was

found to dissolve in the same solvents as DPTS but was less soluble.

Elemental analysis,  $C_8H_{11}O_3N_2F_3S$ , calculated: C 32.31, H 4.23, N 10.77, F 21.92, S 12.31, found: C 35.20, H 3.96, N 10.75, F 20.55, S 12.08.

**Poly((RS)-3,3,3-trifluorolactic acid) (Poly(RS-TFL)):**

(RS)-3,3,3-Trifluorolactic acid ((RS)-TFL, 3.39 g, 0.024 mol) was added to a jacketed 300 ml round bottom flask equipped with a stir bar in the glove box with an argon atmosphere. DPTS (3.38 g, 0.012 mol) or DPTL (1.4 g, 0.005 mol) was placed in a solids addition funnel. The flask was fitted with the funnel, a condenser, septum, and argon gas inlet adapter. The assembled apparatus was placed in a forced draft hood where the condenser, flask jacket and gas inlet were connected to cooling water, a constant temperature fluid system and dried, deoxygenated argon, respectively. A mineral oil bubbler was placed on the condenser. Anhydrous methylene chloride (100 mL) was cannulated into the flask. The system was stirred while fluid at 30°C was circulated through the flask jacket. After dissolution of (RS)-TFL, the DPTS was added to the flask and the temperature was reduced to -10°C. 1,3-Diisopropylcarbodiimide (5.43 mL, 0.035 mol) was syringed into the flask. The system was stirred at -10° for 30 min and then the temperature was raised to 15° for 24 h. A white precipitate by-product formed immediately and floated on top of the methylene chloride solution. The polymer also precipitated from solution and collected at the bottom of the flask. It was removed and purified by mixing in anhydrous chloroform at 50°. The polymer

was placed in a vacuum oven at 35° overnight (0.89 g, 30.1% yield).

Elemental analysis,  $C_3H_1O_2F_3$ , calculated: C 28.57, H 0.79, F 45.24, found: C 28.82, H 0.76, F 45.15.

### 3.3 Results and Discussion

Use of DPTS salt provides a convenient way of introducing equimolar DMAP and toluenesulfonic acid catalysts. Moore and Stupp showed the best yields of polyesters from hydroxyacids when DPTS was used with a carbodiimide condensing agent in the room temperature polyesterification of hydroxyacids.<sup>1</sup> Wagener et al.<sup>2</sup> showed that highest molecular weights and yield in the polyesterification of 3-hydroxy-2-phenylpropionic acid were achieved well below room temperature (-20°) applying chemistry similar to that described by Moore and Stupp. In this research, on the polymerization of (RS)-3,3,3-trifluorolactic acid, it was determined that yields and molecular weight can be enhanced by reduction of reaction temperature from ambient conditions (Table 3.1). With the use of DPTS as catalyst, yield and inherent viscosity are increased with temperature reduction. The use of DPTL however only shows an increase in yield with a decrease in inherent viscosity with temperature.

DPTL was introduced as a more acidic<sup>3,4</sup> catalyst than DPTS catalyst. Boden and Keck<sup>5</sup> showed the efficacy of increased proton concentration in macrolactonization with product yield significantly increased to quantitative

levels. In this dissertation research, pyridinium triflate was also investigated as a catalyst in this regard but without success.

As results in Table 3.1 show, poly((RS)-3,3,3-trifluorolactic acid) was successfully synthesized with DPTS and DPTL. DPTL can produce polymer with good solution viscosity and essentially the same physical characterization as polymer from DPTS but the yield is not as high.<sup>6</sup>

Possible reaction pathways are outlined in Scheme 3.1. In this procedure, the activated (RS)-3,3,3-trifluorolactic acid is formed (reaction A.) as an *O*-acylisourea (1); a rather reactive species.<sup>7</sup> Bimolecular reaction then occurs between (1) and a hydroxy group or a free acid group to form an ester linkage (reaction B.) or (RS)-3,3,3-trifluorolactic acid anhydride (3) (reaction C1.). The methylene chloride insoluble by-product *N,N'*-diisopropylurea (DIPU) (2) is formed in each case. The anhydride and RS-TFL can be converted (reaction C2.) to an ester linkage and RS-TFL, in a reaction mediated by the hyperacylation catalyst 4-(dimethylamino)pyridine (DMAP).

Also, in another pathway, (reaction D1.), DMAP/H<sup>+</sup> catalyzes the formation of a 4-(dimethylamino)-(RS)-3,3,3-trifluorolactoylpyridinium 4-toluenesulfonate intermediate and by-product DIPU. The pyridinium intermediate (4) and hydroxy group of TFL interact (reaction D2.) to form an ester linkage and regenerate the DMAP/H<sup>+</sup> catalyst system.

Finally, a significant side reaction E., is the formation of the *N*-acylurea (NAU) (5). This is an undesirable reaction that consumes monomer and consequently compromises molecular weight and yield.

The polyesterification preparation described here was adopted from previous work on esterification with carbodiimide condensing agents.<sup>1,2,8</sup> It was found that introduction of the carbodiimide at subzero temperature and polymerization below ambient temperature led to high yield and high molecular weight polymer<sup>6</sup> (vide supra).

Within seconds of the introduction of the 1,3-diisopropylcarbodiimide, a white precipitate formed that floated on the methylene chloride. After several hours and after a temperature increase to the plateau reaction temperature, another precipitate heavier than the solution was observed.

### 3.3.1 Characterization of the white precipitate by-product

The elemental analysis of the white precipitate is shown in Table 3.2. The data compare reasonably with the calculated values for *N,N'*-diisopropylurea. Trace sulfur, which can be associated with the catalyst, and fluorine and were identified in the sample. The <sup>1</sup>H NMR spectrum of the white precipitate (Figure 3.1) is consistent with that of *N,N'*-diisopropylurea similar to what has been reported in the literature.<sup>9</sup>

### 3.3.2 Characterization of Poly((RS)-3,3,3-trifluorolactic acid)

Infrared spectroscopy (FTIR), Raman (FT-Raman), elemental analysis,  $^1\text{H}$  and  $^{13}\text{C}$  NMR spectroscopy, solution viscosity, gel permeation chromatography (GPC), solution viscosity, thermogravimetric analysis (TGA) and differential scanning calorimetry (DSC) as well as wide angle X-ray diffraction (WAXS) were utilized to characterize the polymer precipitate.

The polymer was found to be soluble in DMSO and DMF, MEK, THF, acetone, ethyl acetate and methanol. Chloroform,  $\alpha,\alpha,\alpha$ -trifluorotoluene, 1,3- and 1,4-bis(trifluoromethyl)benzene appear to only wet and plasticize the polymer. Petroleum ether and cyclohexane are non-solvents.

The infrared spectrum is shown in Figure 3.2B. The key feature is the strong carbonyl absorption at  $1792\text{ cm}^{-1}$ . This is in contrast to the carbonyl band of the monomer  $\alpha$ -hydroxy acid, which appears at  $1738\text{ cm}^{-1}$  (Figure 3.2A). This is suggestive of ester formation. For comparison, Figure 3.3 shows the infrared spectrum of poly(D,L-lactide) (Medisorb<sup>®</sup> 100DL) and poly((RS)-TFL). The carbonyl vibration frequency increases from  $\sim 1725\text{ cm}^{-1}$  to  $1764\text{ cm}^{-1}$  upon polyesterification of lactic acid. Bands at  $3565\text{ cm}^{-1}$  and  $2968\text{ cm}^{-1}$  in the poly((RS)-TFL) spectra of Figures 3.2 and 3.3 are assigned to polymer as a carbonyl overtone<sup>10</sup> and C-H stretch,<sup>11</sup> respectively. The band at  $3340\text{ cm}^{-1}$  is addressed in a subsequent section.

The elemental analysis of the crude precipitate is shown in Table 3.3 where it is compared with the calculated values for poly((RS)-TFL). The low sulfur content suggests that essentially no catalyst is present. The presence of nitrogen is indicative of the presence of DIPU and/or NAU and NAU end groups on the polymer. These comments are in agreement with the relative solubilities of the by-products and catalyst and with the fact that the crude product was precipitated from methylene chloride. This along with a comparison of the infrared spectra of the white precipitate in Figure 3.4 and crude polymer in Figure 3.3B suggest an assignment for the band found at  $3340\text{ cm}^{-1}$  to the N-H stretch of DIPU.

This was indeed confirmed when the infrared spectrum of poly((RS)-TFL) purified by mixing with warm anhydrous chloroform was examined. In Figure 3.5, the spectra of crude and purified poly(TFL) are directly compared. The band at  $3340\text{ cm}^{-1}$  vanishes upon purification of the polymer. The elemental analysis of the purified polymer is shown in Table 3.3. The polymer has <1% nitrogen suggesting that chloroform extraction removes most of the nitrogen containing contaminants.

The  $^1\text{H}$  NMR spectrum of the crude polymer is displayed in Figure 3.6. The doublet at 0.99 ppm is due to the  $-\text{CH}_3$  groups of the isopropyl moiety (compare with Figure 3.1) that may be associated with NAU, DIPU and polymer end groups. The peak at 3.32 ppm is assigned to water. This peak shifts upon addition of  $\text{TFA-}d$  as it goes into exchange with acidic protons.

This is shown in Figure 3.7. The broad peak at 6.93 ppm is associated with the  $\alpha$ -hydrogen of poly(TFL). This is verified in the  $^1\text{H}$  NMR spectrum of minimally contaminated poly(TFL) in Figure 3.8. The polymer is purified by mixing with warm anhydrous chloroform followed by drying in a vacuum oven at 35°C for several days. The methyl hydrogens of DIPU are evident at 1.0 ppm. This signal consists of 12 hydrogens whereas there is only a single  $\alpha$ -hydrogen. The NMR signals are on a molar basis so that a trace quantity of a substance with relatively large molar representation may show up in the spectrum. On a normalized basis, the quantitative difference between the  $\alpha$ -hydrogen and the methyl hydrogens, in Figure 3.8, is 3 orders of magnitude. Apparently, chloroform was effectively removed as there is no signal near 8.3 ppm where chloroform appears when it is diluted in DMSO according to the literature<sup>12</sup>.

The  $^{13}\text{C}$  and  $^{13}\text{C}$  APT spectra of poly((RS)-3,3,3-trifluorolactic acid) are shown in Figures 3.9A and B, respectively. The trifluoromethyl carbon and the stereogenic carbon signals show splitting patterns consistent with carbon/fluorine coupling.<sup>13</sup> The stereogenic carbon signal centered at 70.3 ppm has  $^2J = 50$  Hz and the trifluoromethyl carbon signal at 120.4 ppm has  $^1J = 300$  Hz. In the  $^{13}\text{C}$  APT (Attached Proton Test) spectrum, the carbon signal directions in the spectrum will be different (by 180°) depending upon the number of attached protons. The convention is up for unaffected (i.e., not covalently bound to any hydrogens) carbons and also carbons bound to an

even number of hydrogens. The bands of carbons bonded to an odd number of protons point down. The APT spectrum (Figure 3.9B) corroborates the assignments in the  $^{13}\text{C}$  spectrum in Figure 3.9A. It confirms that the signal at 70 ppm is due to the stereogenic carbon attached to a single (odd number) hydrogen. The strong splitting (vide supra) of the trifluoromethyl carbon by fluorine is quite apparent. It should also be pointed out that this APT spectrum is of the poly((RS)-TFL) sample before chloroform extraction of DIPU so there are two downward peaks associated with the isopropyl  $-\text{CH}_3$  (near 23 ppm) and the isopropyl  $\equiv \text{CH}$  (near 40 ppm), respectively. The  $^{13}\text{C}$  spectrum is of polymer after chloroform extraction.

The  $^1\text{H}$  NMR spectrum of poly((RS)-TFL) is compared with those of poly(D,L-lactide) and poly(L-lactide) in Figure 3.10. In Figure 3.10A and B, signals at 2.49 and 3.3 ppm are due to DMSO and water, respectively. The methine hydrogen in the fluorinated polymer is much more deshielded with a signal at 6.9 ppm, than the comparable hydrogens of the lactide polymers which are approximately at 5 ppm. Of course, the lactide polymers clearly show the methyl hydrogen signals in the vicinity of 1.6 ppm<sup>14</sup>; a feature that is absent in the poly((RS)-TFL) with a trifluoromethyl group.

The inherent viscosity of the poly(TFL) (0.2g/dL, THF,  $29.95^\circ\text{C} \pm 0.01^\circ$ ) was determined before and after extraction with hot anhydrous chloroform. Viscosity data were assessed without filtration. The inherent viscosity of poly(D,L-lactide) was also measured. The data are presented in Table 3.4.

The measured value (0.42 dL/g) is indicative of the presence of high polymer particularly since it is comparable to that of the commercial poly(D,L-lactide) (0.53 dL/g,  $M_w = 41,800$  g/mol).

The GPC chromatograms (RI detection) of poly(D,L-lactide), poly(L-lactide) and poly((RS)-TFL) are displayed in Figure 3.11A, B and C, respectively. The corresponding viscosity chromatograms are shown in Figures 3.12A, B and C. These data were obtained with 1,1,1,3,3,3-hexafluoro-2-propanol (HFIP) as solvent. The poly(D,L-lactide) apparently has the greatest hydrodynamic volume with a peak centered near 13 mL retention while the poly((RS)-TFL) has the lowest with a peak centered 16 mL retention volume. All the peaks at greater retention volumes than 18 mL are solvent peak artifacts. The small peaks near 17 mL are low molecular weight species present in each sample. In the viscosity chromatograms (Figure 3.12), these peaks are insignificant. These GPC results indicate that the technique of carbodiimide activation with catalyst has resulted in the production of high polymer from trifluorolactic acid.

The absolute molecular weight data (see Table 3.5) by light scattering reported for poly((RS)-TFL) are based on measurements in THF. The lactide polymers were measured in HFIP. The light scattering from this fluoropolymer sample in HFIP was too weak for measurement. Subsequent light scattering evaluations with this polymer proved successful by increasing the concentration from 2 to 12 mg/mL.

Thermogravimetric analysis (TGA) of the poly((RS)-3,3,3-trifluorolactic acid) is compared with poly(D,L-lactide) in Figures 3.13 and 3.14. Significant weight loss (1.5 %) begins at 162°C for the crude poly((RS)-TFL) (Figure 3.13A). For poly(D,L-lactide), it begins at 242°C (also 1.5 % weight loss) as shown in Figure 3.13B. An overview in Figure 3.14 shows, however that while the poly((RS)-TFL) starts to lose weight before poly(D,L-lactide) it does not drop off in weight precipitously. Subsequent studies with purified, fractionated poly((RS)-TFL) did not show the large initial drop off in weight and had a profile similar to behavior of poly(D,L-lactide) except extending to a higher temperature by ~25°. <sup>15</sup> The TGA of fractionated poly((RS)-TFL) (10% weight loss at 325°, 50% weight loss at 360°) and poly(D,L-lactide) (10% weight loss at 280°, 50% weight loss at 325°) are shown in Figure 3.15. The comparison of this fluoropolymer with poly(L-lactide) shows essentially the same pattern as described above.

DSC characterization showed  $T_g$ 's of poly((RS)-3,3,3-trifluorolactic acid) and poly(D,L-lactide) are similar. The measured values of 36° and 46°C for poly((RS)-TFL) and poly(D,L-lactide), respectively are shown in Figure 3.16. The  $T_g$  range for poly(D,L-lactide) according to the supplier is 45-50°C. <sup>16</sup>

An overview of the thermal trace of semicrystalline poly(L-lactide) is shown in Figure 3.17 with the peak  $T_m$  of 178°C. The  $T_g$  presented in Figure 3.18 is 61°C. Kalb and Pennings report  $T_g$  and  $T_m$  of ~55° and

$\sim 215^\circ$ , respectively for samples crystallized from the melt.<sup>17</sup> The supplier of poly(L-lactide) indicates that the  $T_g$  and  $T_m$  ranges are:  $55-60^\circ$  and  $170-175^\circ$ , respectively.<sup>16</sup>

The wide angle X-ray scattering patterns of poly((RS)-TFL) (Figure 3.19A) and poly(D,L-lactide) (Figure 3.19B) both suggest that each polymer is substantially amorphous. However, the amorphous halo of poly(D,L-lactide) is much broader. Moreover, there are discrete spots in the diffraction pattern of poly((RS)-TFL) indicative of polycrystallinity probably from low molecular weight polymer and urea contaminant.<sup>15</sup> The WAXS of poly(L-lactide), shown in Figure 3.20 shows discrete reflections, as expected, indicative of crystallinity. The d spacings are comparable with values reported in the literature.<sup>18</sup> The data are shown in Table 3.6.

### 3.4 Conclusions

A high molecular weight fluorinated aliphatic polyester has been synthesized from (RS)-3,3,3-trifluorolactic acid. The condensing agent 1,3-diisopropylcarbodiimide and catalyst DPTS have been used to produce the product by solution polyesterification in methylene chloride at  $15^\circ\text{C}$ . Infrared and  $^1\text{H}$  NMR spectroscopy clearly confirm the structure of the polymer product. Solution viscosity and GPC data confirm the presence of high polymer. The polymer is substantially amorphous as indicated by DSC

and WAXS. The  $T_g$  is 36°C. TGA data suggest that the fluoropolyester has a higher decomposition temperature than the poly(D,L-lactide).

### 3.5 References and Notes

- (1) Moore, J. S.; Stupp, S. I. *Macromolecules* **1990**, *23*, 65.
- (2) Wagener, K. B.; Linert, J. G.; O'Gara, J. E. *J Macromol. Sci. - Pure Appl. Chem.* **1994**, *A31*, 775.
- (3) March, J. *Advanced Organic Chemistry*; Wiley Interscience: New York, 1992, p 250.
- (4) Olah, G. A.; Prakash, G. K. S.; Sommer, J. *Superacids*; Wiley Interscience: New York, 1985, p 33.
- (5) Boden, E. P.; Keck, G. E. *J. Org. Chem.* **1985**, *50*, 2394.
- (6) McKie, D. B.; Lepeniotis, S.; Tirrell, D. A. , manuscript in preparation.
- (7) Balcom, B. J.; Petersen, N. O. *J. Org. Chem.* **1988**, *54*, 1922.
- (8) Neises, B.; Steglich, W. *Angew Chem Int Ed* **1978**, *17*, 522.
- (9) Benoiton, L. N.; Chen, F. M. F. *J. Chem. Soc. Chem. Commun.* **1981**, *11*, 543.
- (10) Colthup, N. B.; Daly, L. H.; Wiberley, S. E. *Introduction to Infrared and Raman Spectroscopy*; 3rd ed.; Academic Press Inc: Boston, 1990, p 16.
- (11) Silverstein, R. M.; Bassier, G. C.; Morrill, T. C. *Spectrometric Identification of Organic Compounds*; 5th ed.; J Wiley & Sons: New York, 1991, p 103.
- (12) The (1)H chemical shift of chloroform in DMSO-d6 was obtained from technical literature supplied by Isotec, Inc., Miamisburg, OH, U.S.A..

- (13) Bovey, F. A.; Jelinski, L.; Mirau, P. A. *Nuclear Magnetic Resonance Spectroscopy*; 2nd ed.; Academic Press: San Diego, 1988, p 457.
- (14) Brochu, S., Ph.D. Dissertation, Laval University, 1993.
- (15) McKie, D. B.; Tirrell, D. A.; Lillya, C. P.; Muthukumar, M.; Jaffe, M. , manuscript in preparation.
- (16) These T<sub>g</sub> and T<sub>m</sub> data were obtained from technical literature supplied by the manufacturer, Medisorb Technologies International L.P., Cincinnati, OH, U.S.A..
- (17) Kalb, B.; Pennings, A. J. *Polymer* **1980**, *21*, 607.
- (18) Iannace, S.; Ambrosio, L.; Huang, S. J.; Nicolais, L. *J. Appl. Polym. Sci.* **1994**, *54*, 1525.

Table 3.1 Yield and inherent viscosity of poly((RS)-3,3,3-trifluorolactic acid) with 0.2 equivalent (monomer to catalyst 5/1) of catalyst (solutions filtered through 0.25  $\mu$  glass membrane) prior to measurement).

Temperature [°C]	Catalyst	Yield [wt.%]	Inherent viscosity in THF @ 29.95°C (conc. = 0.2g/dL) (dL/g)
5	DPTS	41.3	0.33
9.3	DPTS	35.4	0.22
5	DPTL	26.5	0.16
25	DPTL	16.5	0.32

Table 3.2 Elemental analysis of the white precipitate by-product.

Sample ID	% Carbon	% Hydrogen	% Nitrogen	% Fluorine	% Sulfur
DIPU, calculated	58.3	11.2	19.4	--	--
Precipitate, found	57.42	10.98	18.80	0.69	0.65%

Table 3.3 Elemental analysis of crude and purified poly((RS)-3,3,3-trifluorolactic acid).

Sample ID	% Carbon	% Hydrogen	% Nitrogen	% Fluorine	% Sulfur
poly(TFL), calculated	28.6	0.8	--	45.2	--
poly(TFL), crude	29.07	1.45	1.16	39.08	<0.40
poly(TFL) purified	28.82	0.76	0.17	45.2	--

Table 3.4 Inherent viscosities (unfiltered solutions) of poly((RS)-3,3,3-trifluorolactic acid) and poly(D,L-lactide).

	Inherent viscosity in THF @ 29.95°C (conc. = 0.2g/dL) (dL/g)
crude poly((RS)-3,3,3-trifluorolactic acid) (before CHCl <sub>3</sub> extraction)	0.46
purified poly((RS)-3,3,3-trifluorolactic acid) (after CHCl <sub>3</sub> extraction)	0.42
poly(D,L-lactide)	0.53

Table 3.5 Absolute molecular weight measurements by light scattering; polylactides in HFIP and poly((RS)-TFL) in THF.

Polymer Sample	M <sub>w</sub> [g/mol]	M <sub>w</sub> /M <sub>n</sub>
poly((RS)-TFL)	29,500	3.1
poly(D,L-lactide) (Medisorb® 100DL)	41,800	2.8
poly(L-lactide) (Medisorb® 100L)	52,200	1.8

Table 3. 6 The d spacings of poly(L-lactide).

Found		Literature <sup>18</sup>	
$2\theta$ [°]	d [Å]	$2\theta$ [°]	d [Å]
16.3	5.4	17.2	5.2
18.9	4.7	19.4	4.6

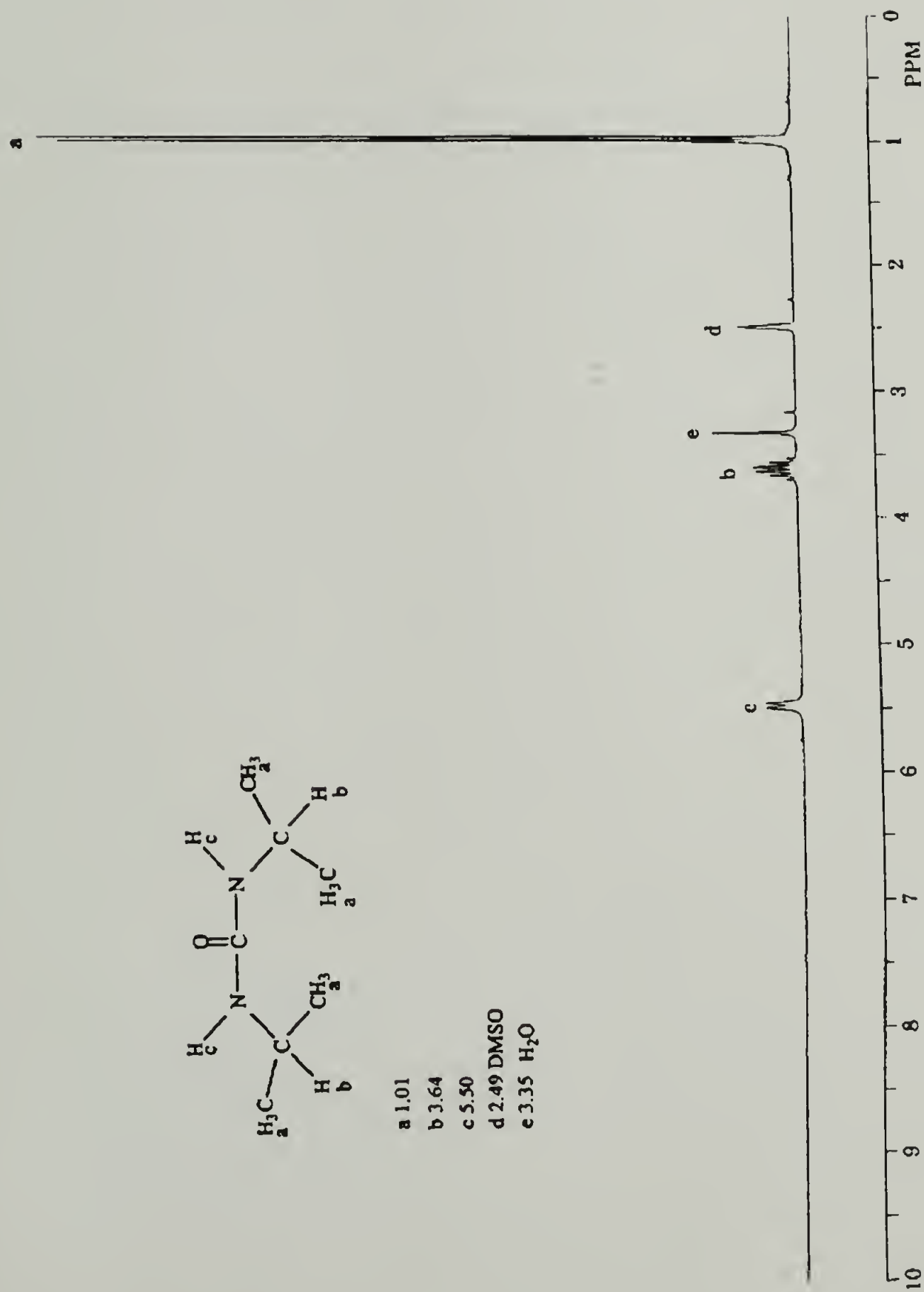


Figure 3.1 200-MHz proton NMR of the white precipitate by-product in DMSO-d<sub>6</sub>.

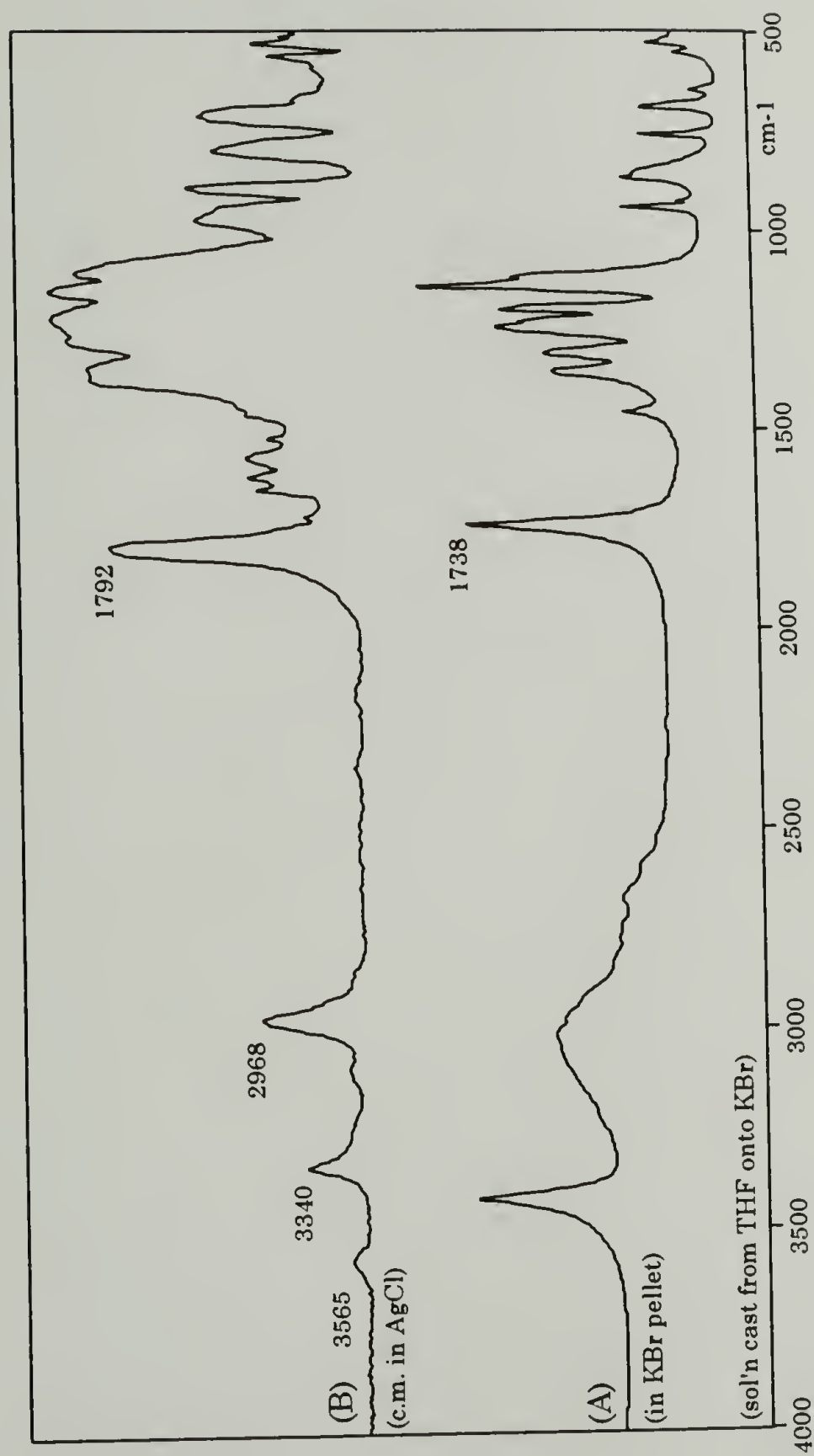


Figure 3.2 FTIR spectra of (A): (RS)-TFL and (B): crude poly((RS)-TFL).

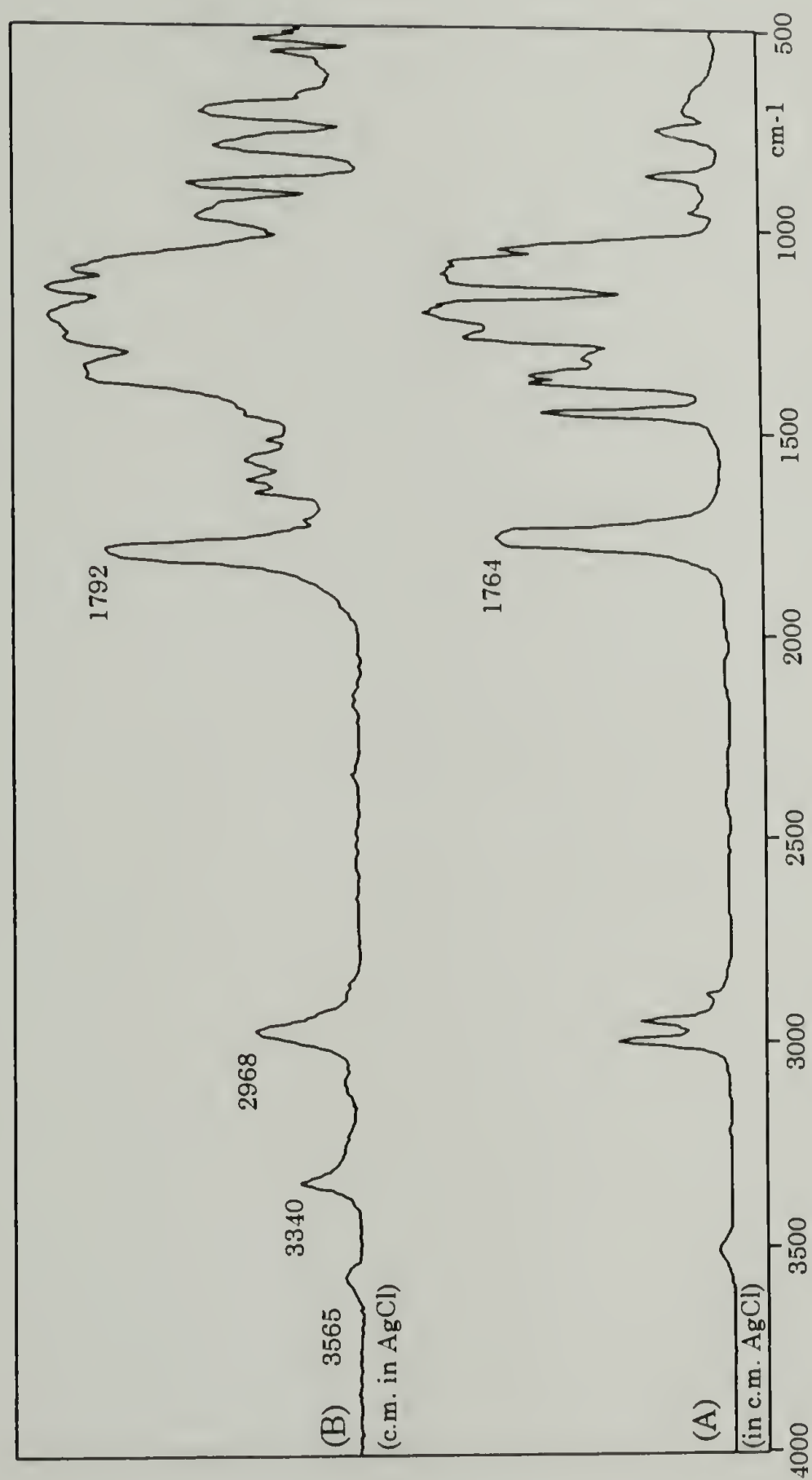


Figure 3.3 FTIR spectra of (A): poly(D,L-lactide) and (B): crude poly((RS)-TFL).

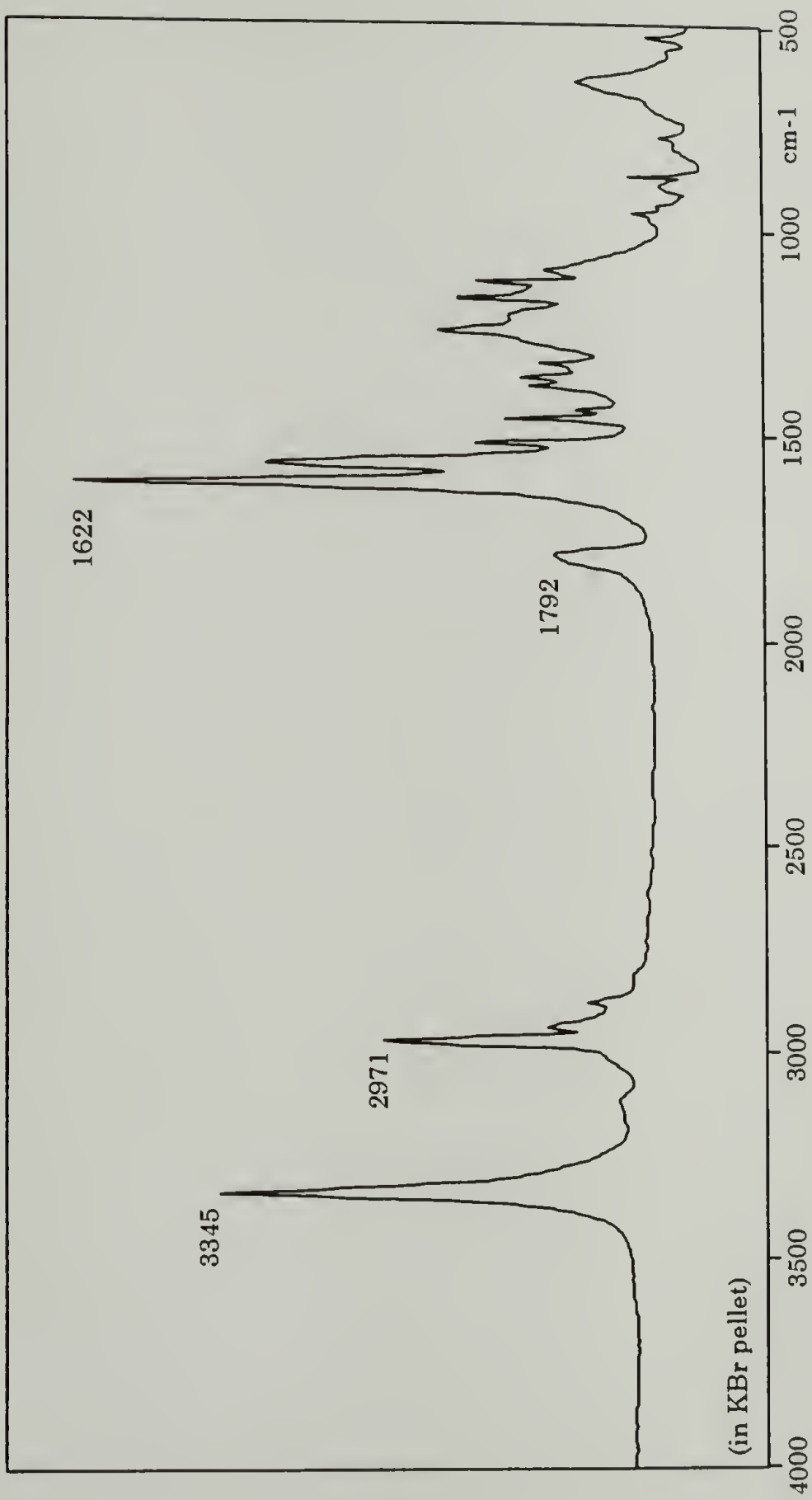


Figure 3.4 FTIR spectrum of the white precipitate by-product

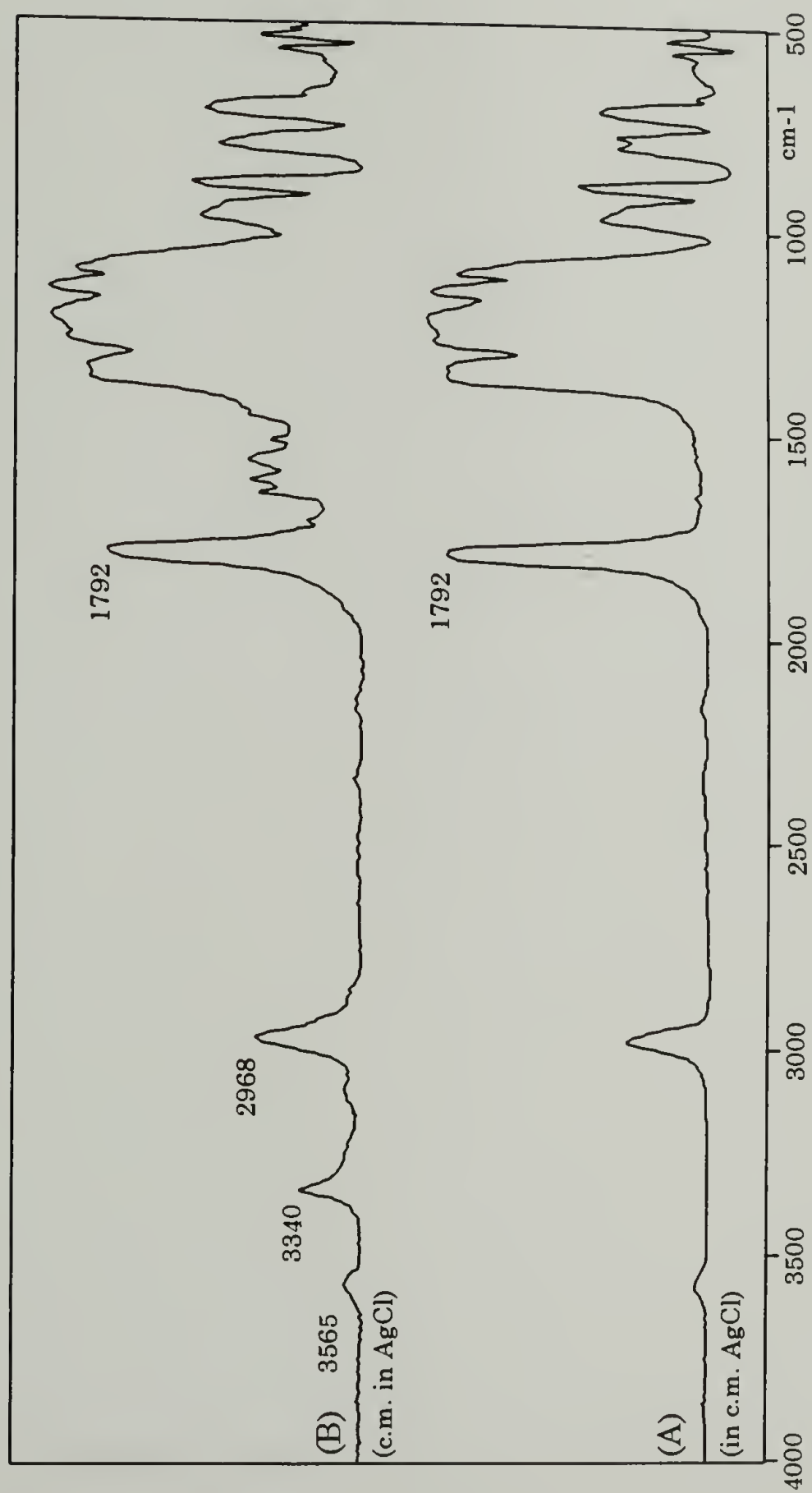


Figure 3.5 FTIR spectra of (A): purified poly((RS)-TFL) and (B): crude poly((RS)-TFL).

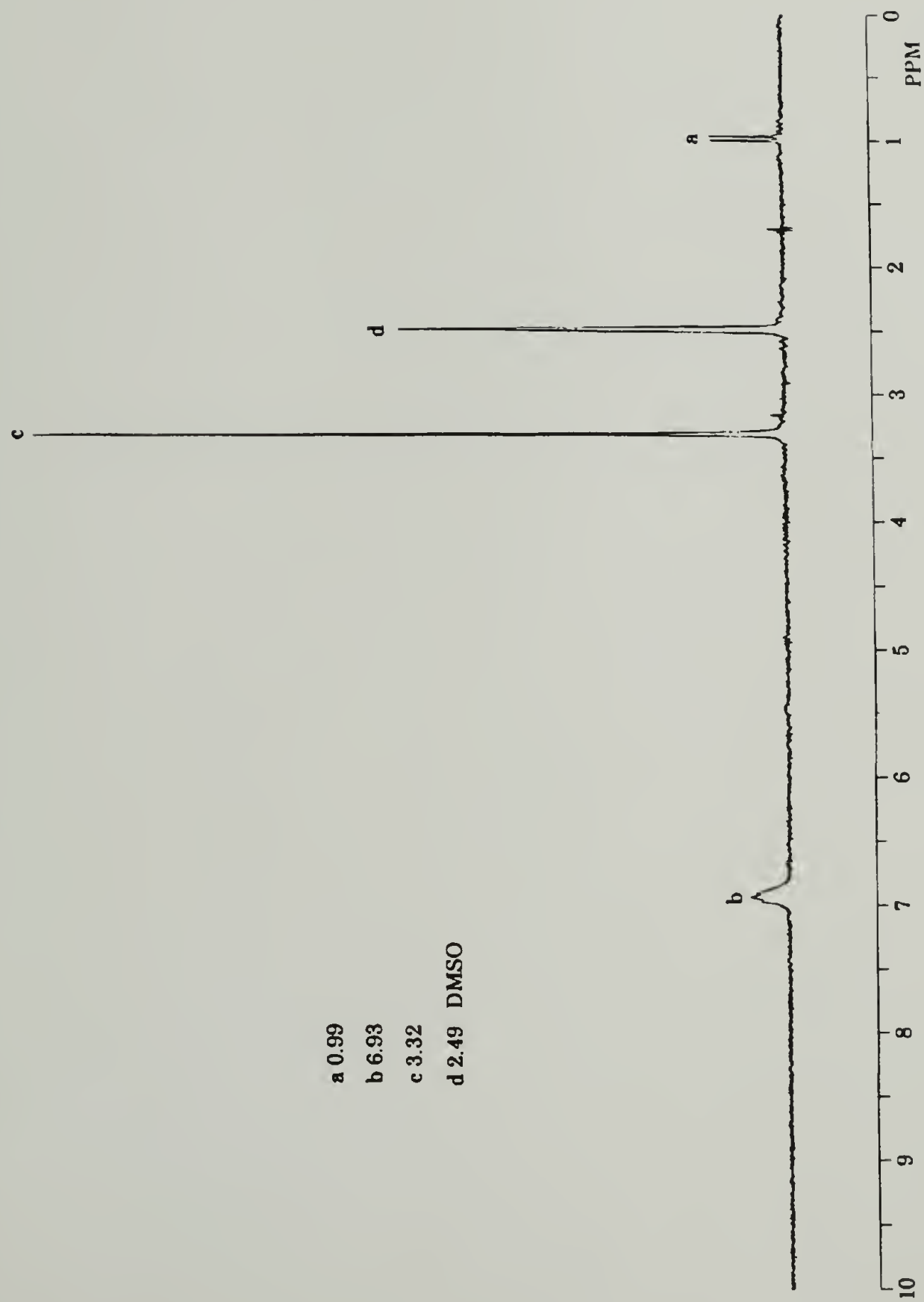


Figure 3.6 200-MHz proton NMR of crude poly((R,S)-TFL) in DMSO-d<sub>6</sub>.

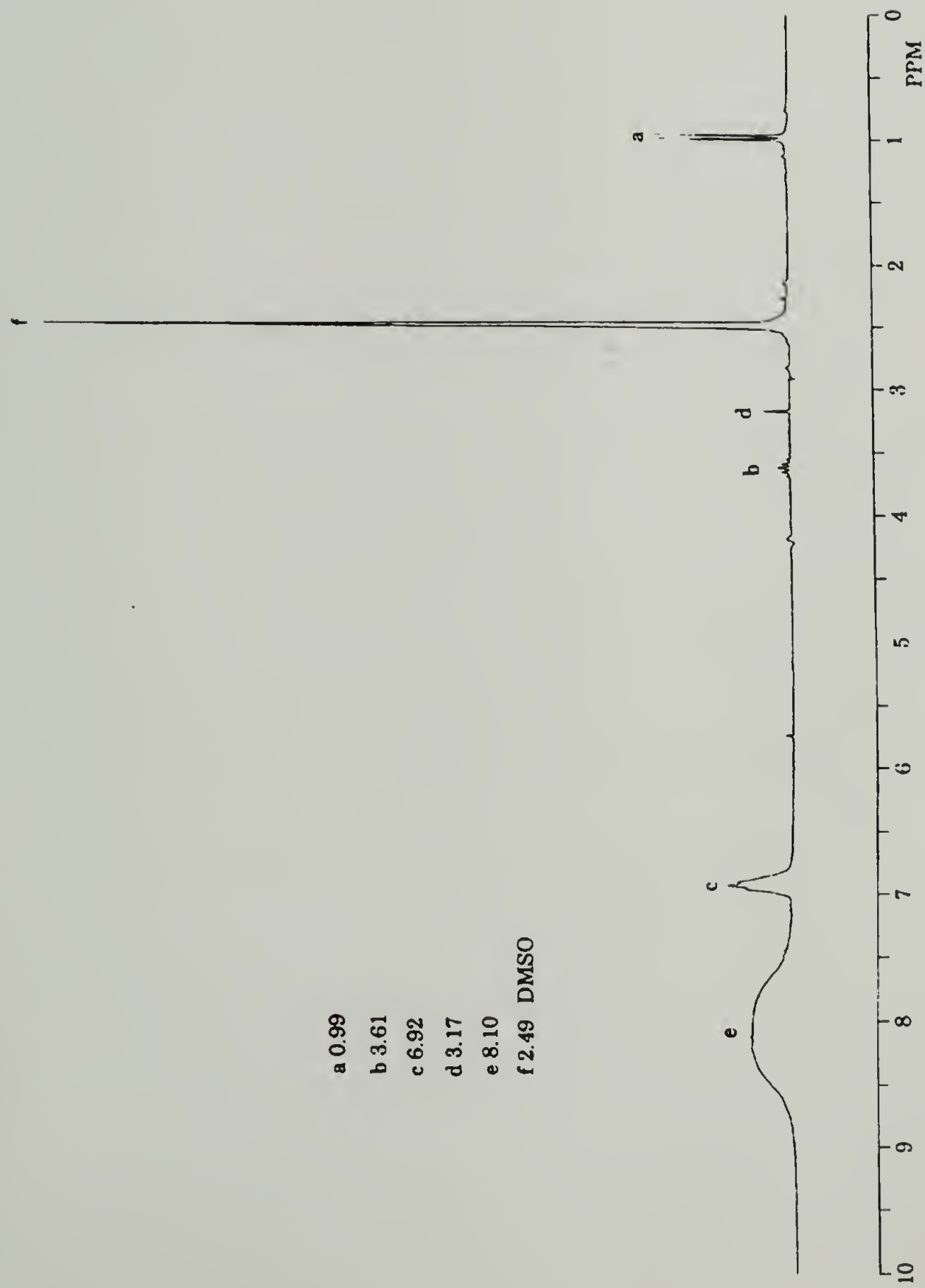


Figure 3.7 200-MHz proton NMR of crude poly((RS)-TFL) with TFA in DMSO-d<sub>6</sub>.

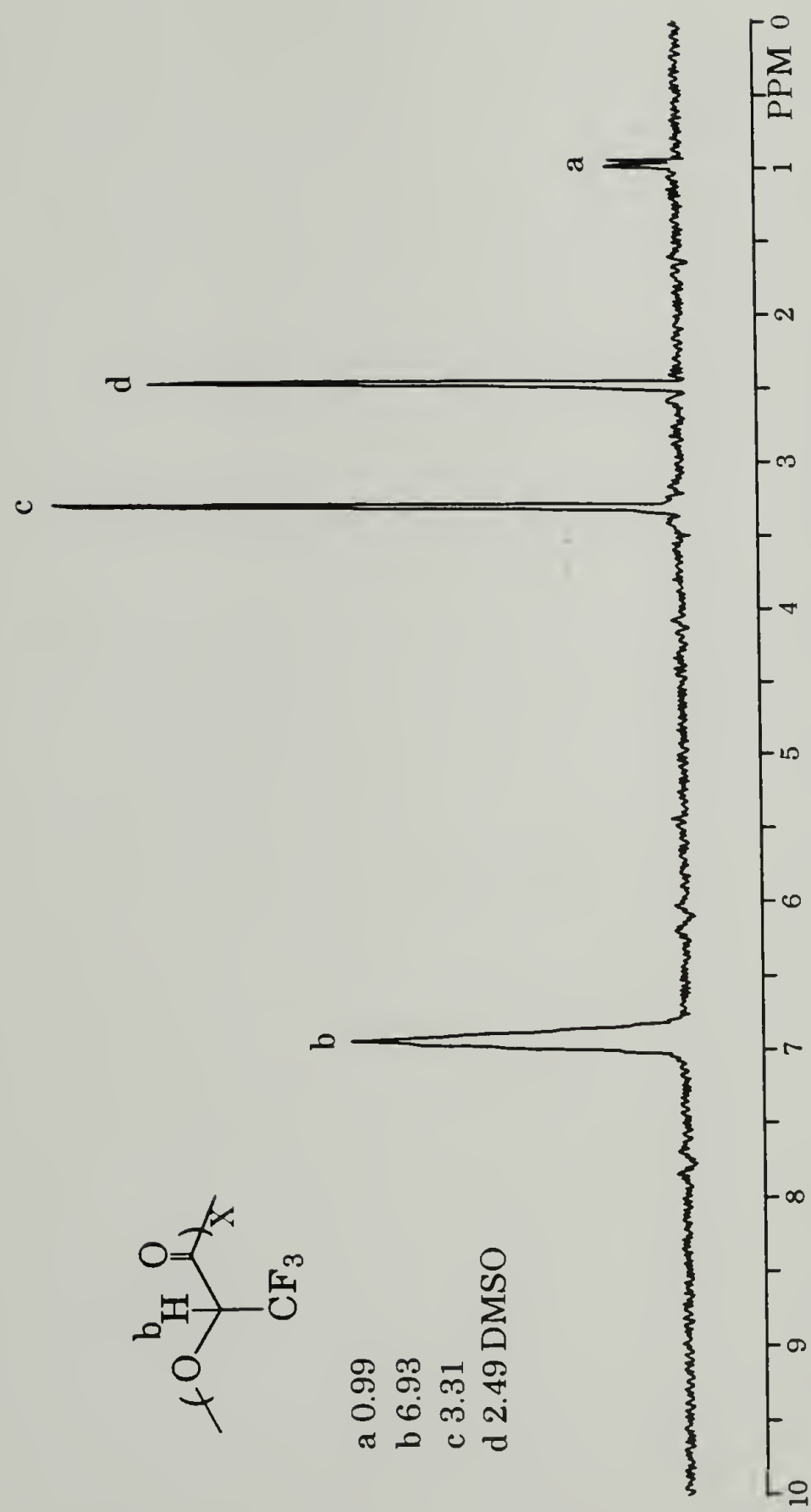


Figure 3.8 200-MHz proton NMR of poly((R,S)-TFL) in DMSO-*d*<sub>6</sub> after chloroform extraction.

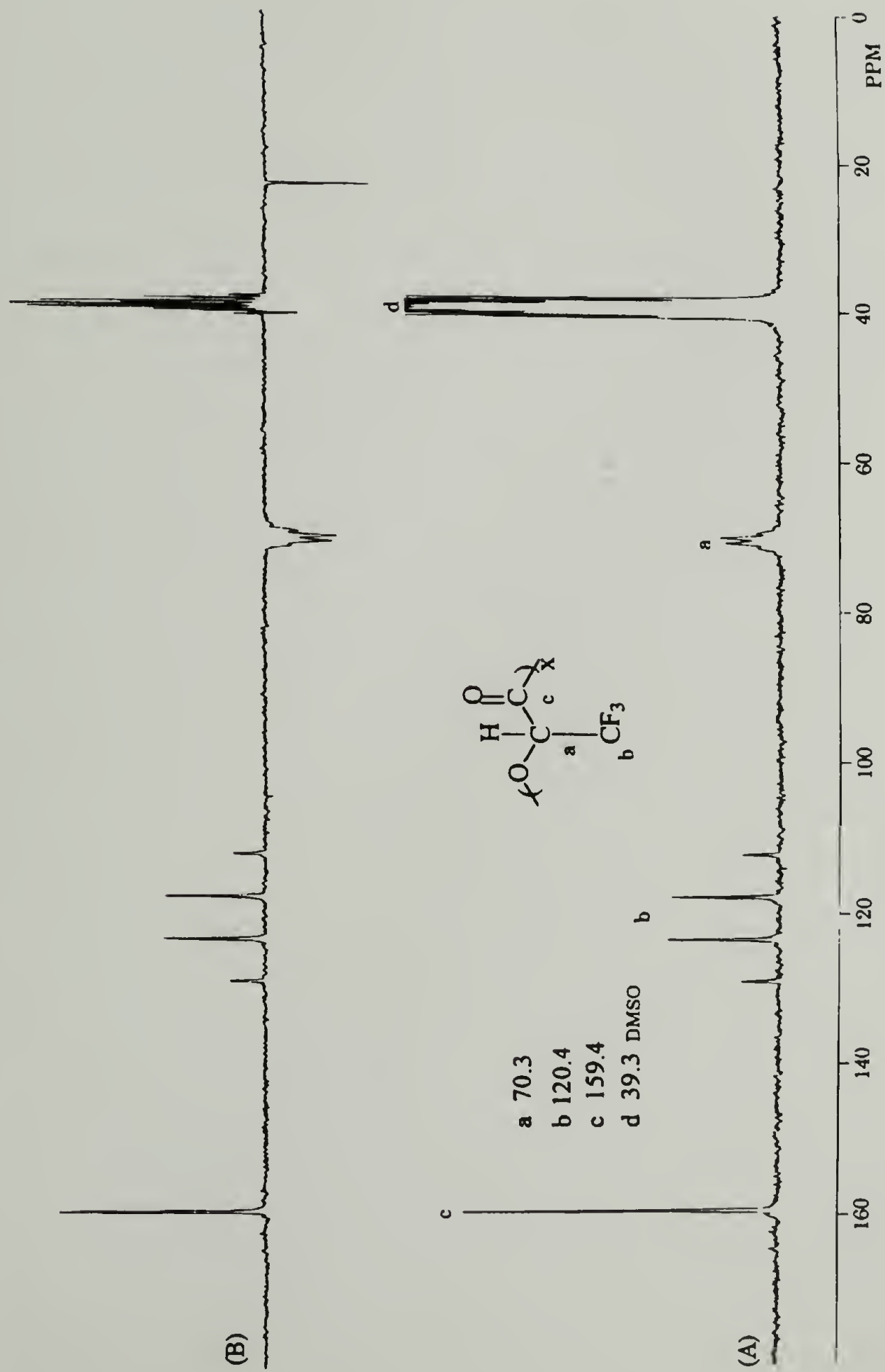


Figure 3.9 50-MHz carbon 13 NMR (A) and APT (B) spectra of poly((RS)-TFL) in DMSO-d6.



Figure 3.10 200-MHz proton NMR spectra of (A): poly((RS)-TFL), (B): poly(D,L-lactide), both in DMSO-d<sub>6</sub> and (C): poly(L-lactide) in HFIP-d<sub>2</sub>. The signals at 2.49 and 3.3 ppm in spectra (A) and (B) are DMSO and water, respectively.

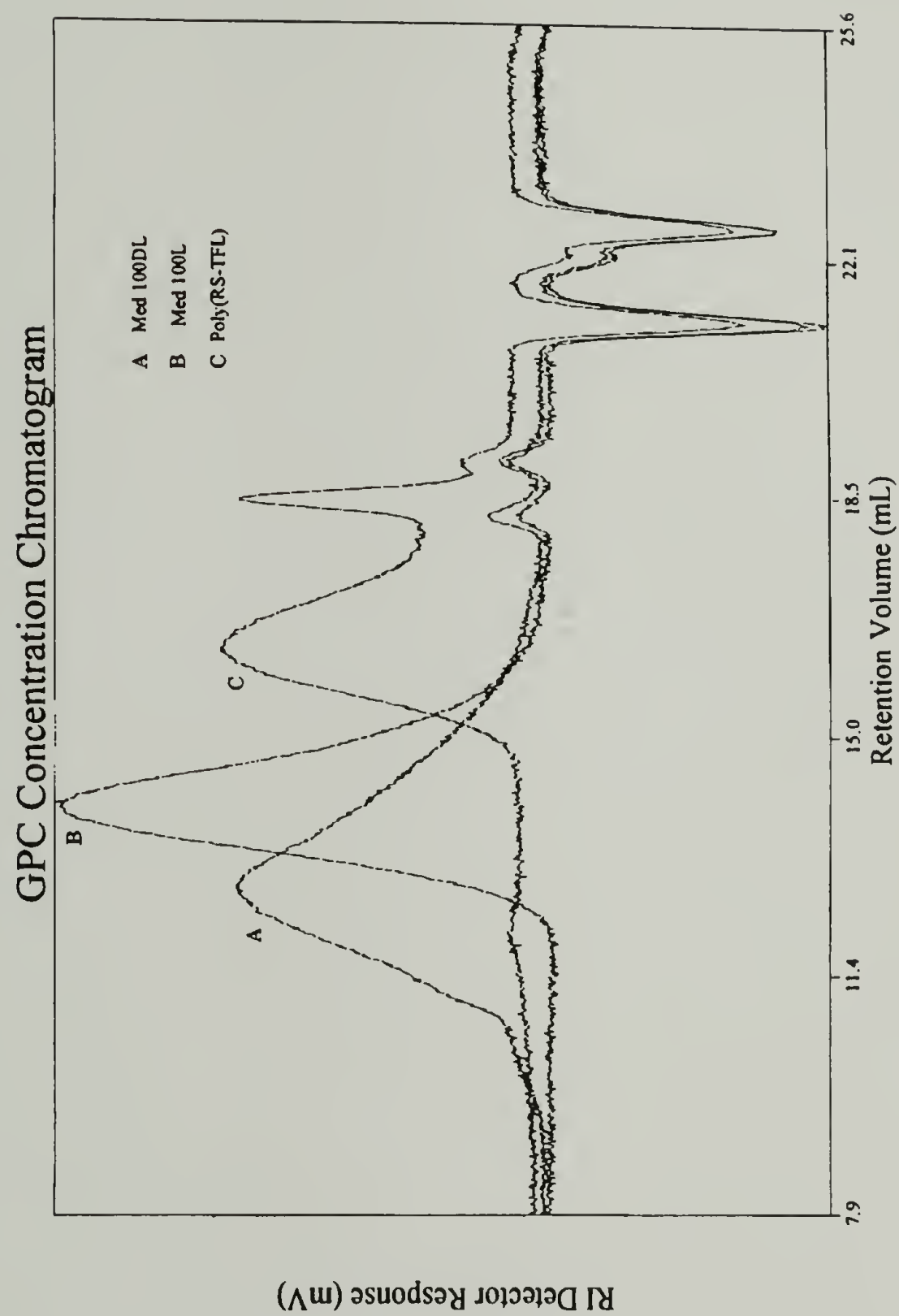


Figure 3.11 GPC chromatograms (RI detector) of A: poly(D,L-lactide), B: poly(L-lactide) and C: poly((RS)-TFL).

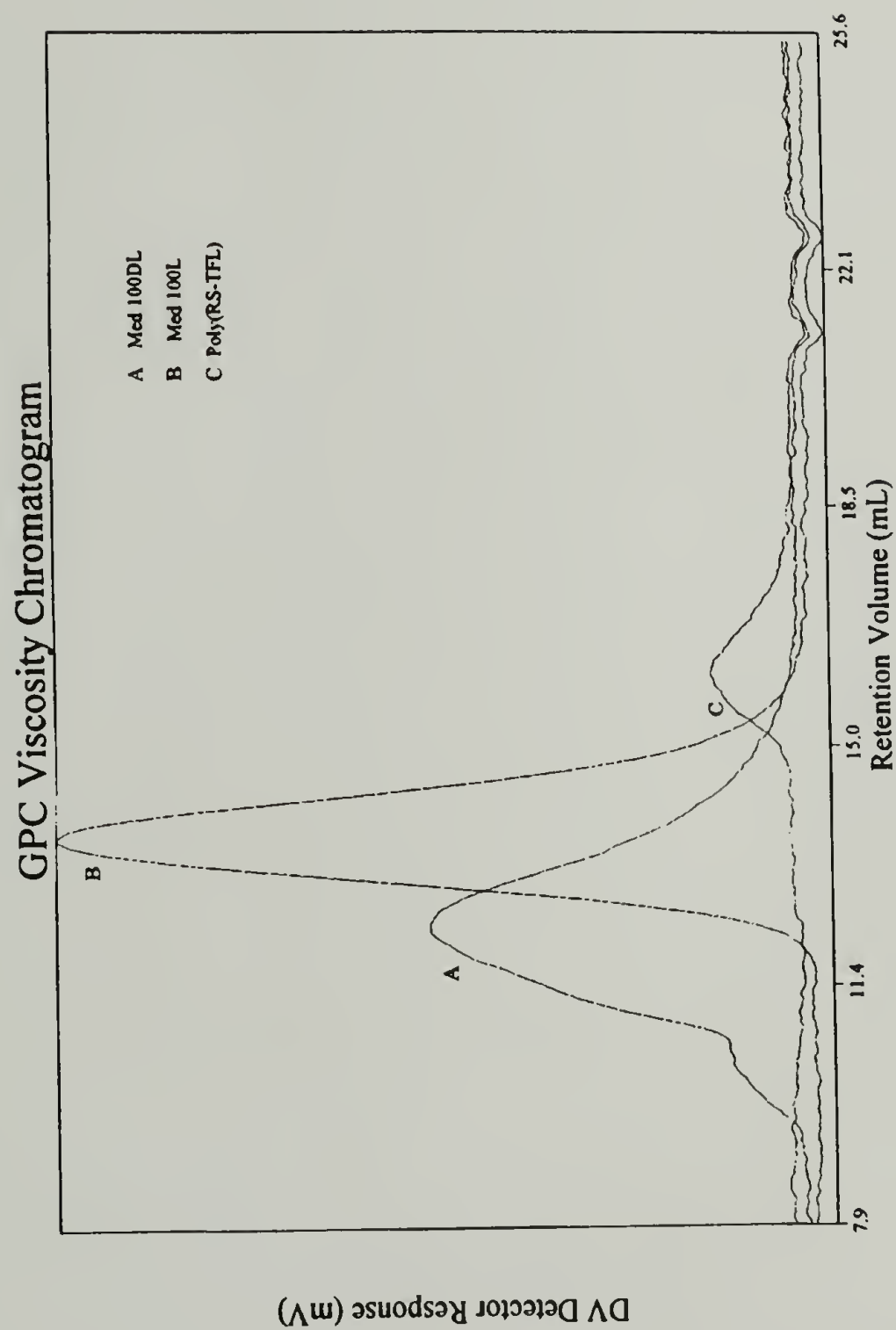


Figure 3.12 GPC viscosity chromatograms of A: poly(D,L-lactide), B: poly(L-lactide) and C: poly((RS)-TFL) with HFIP solvent.

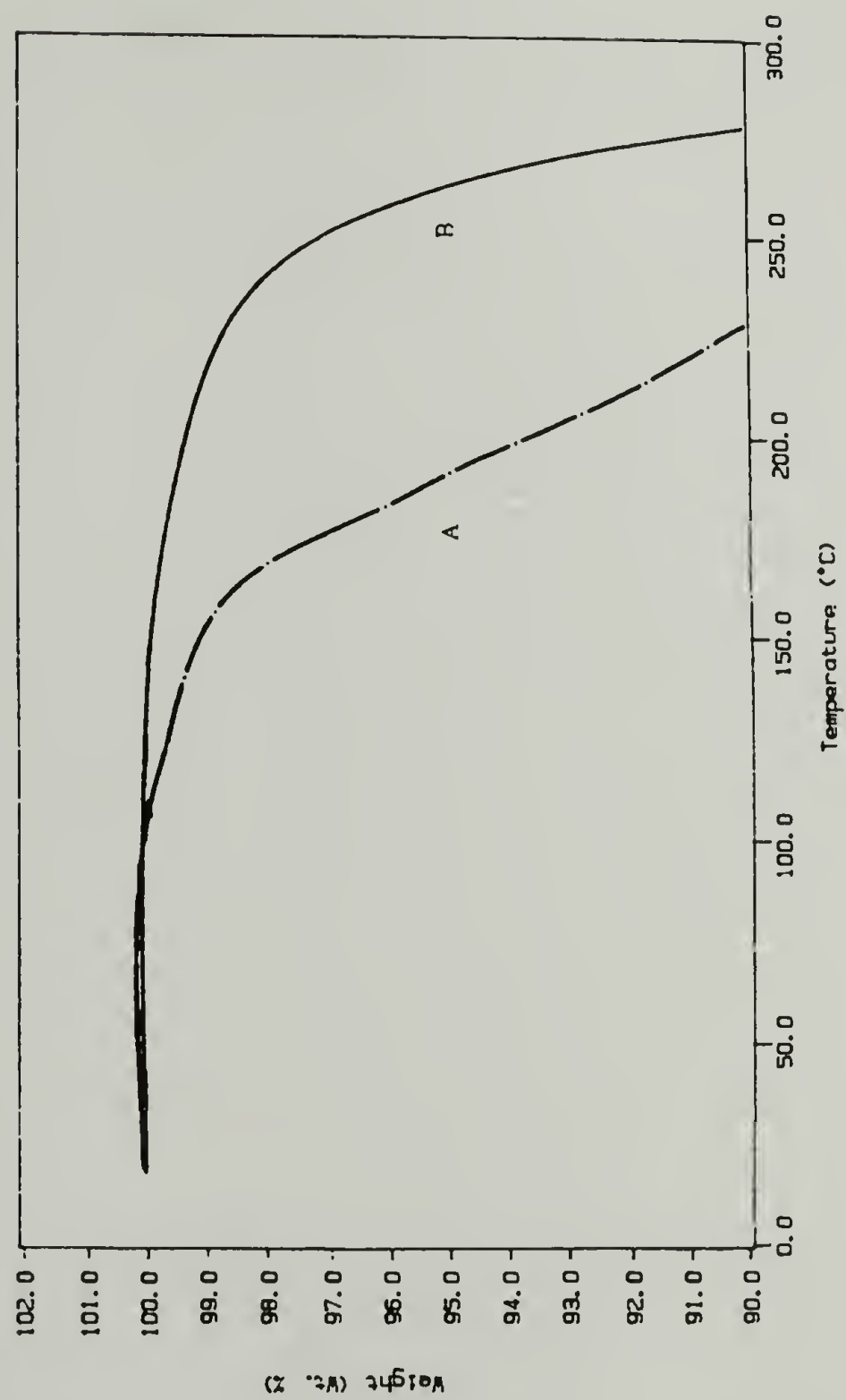


Figure 3.13 TGA curves of A: poly(RS)-TFL and B: poly(D,L-lactide) under N<sub>2</sub> at 10C° /min.

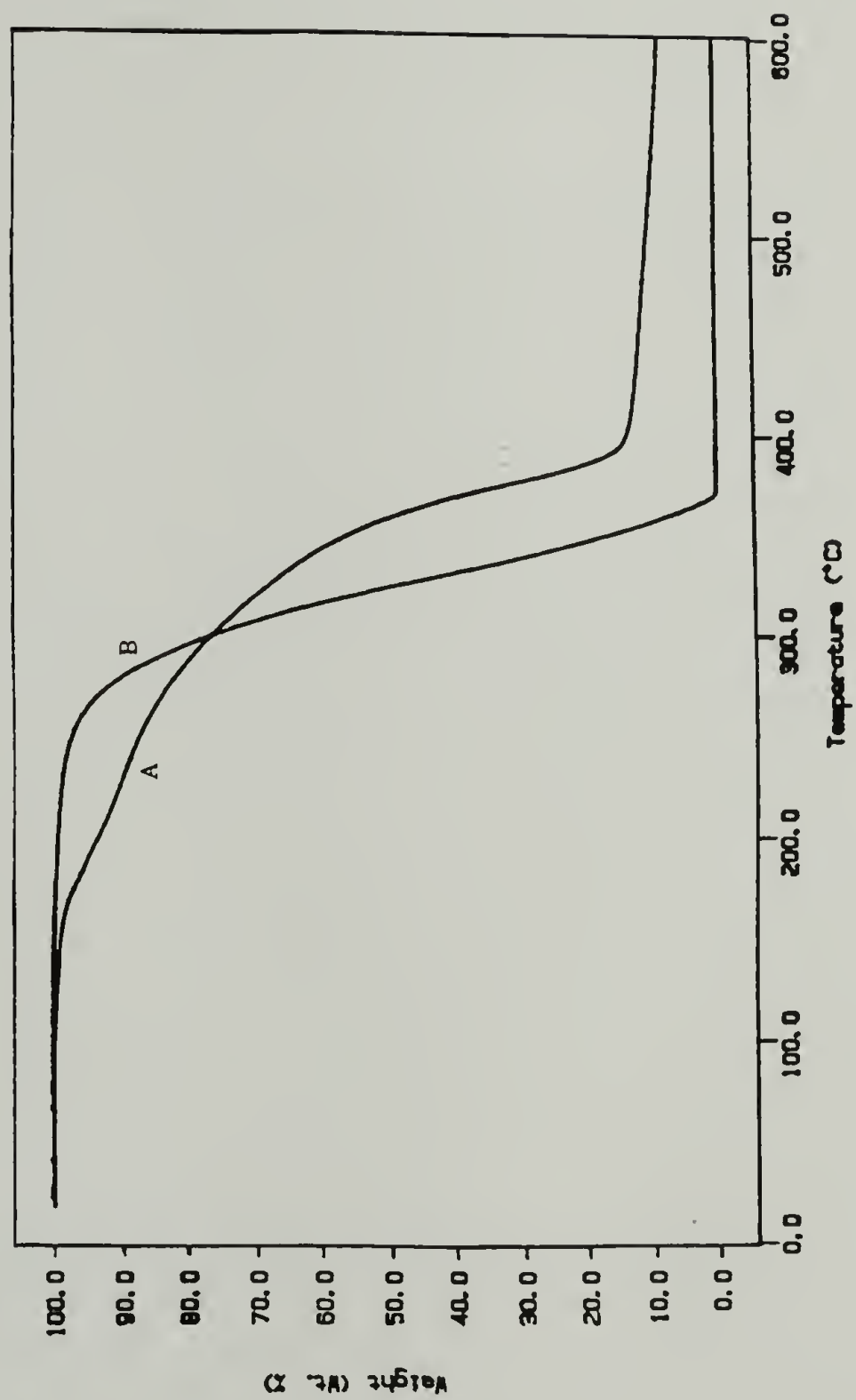


Figure 3.14 Overview of the TGA curves of A: poly(RS)-TFL and B: poly(D,L-lactide) under N<sub>2</sub> at 10C°/min.

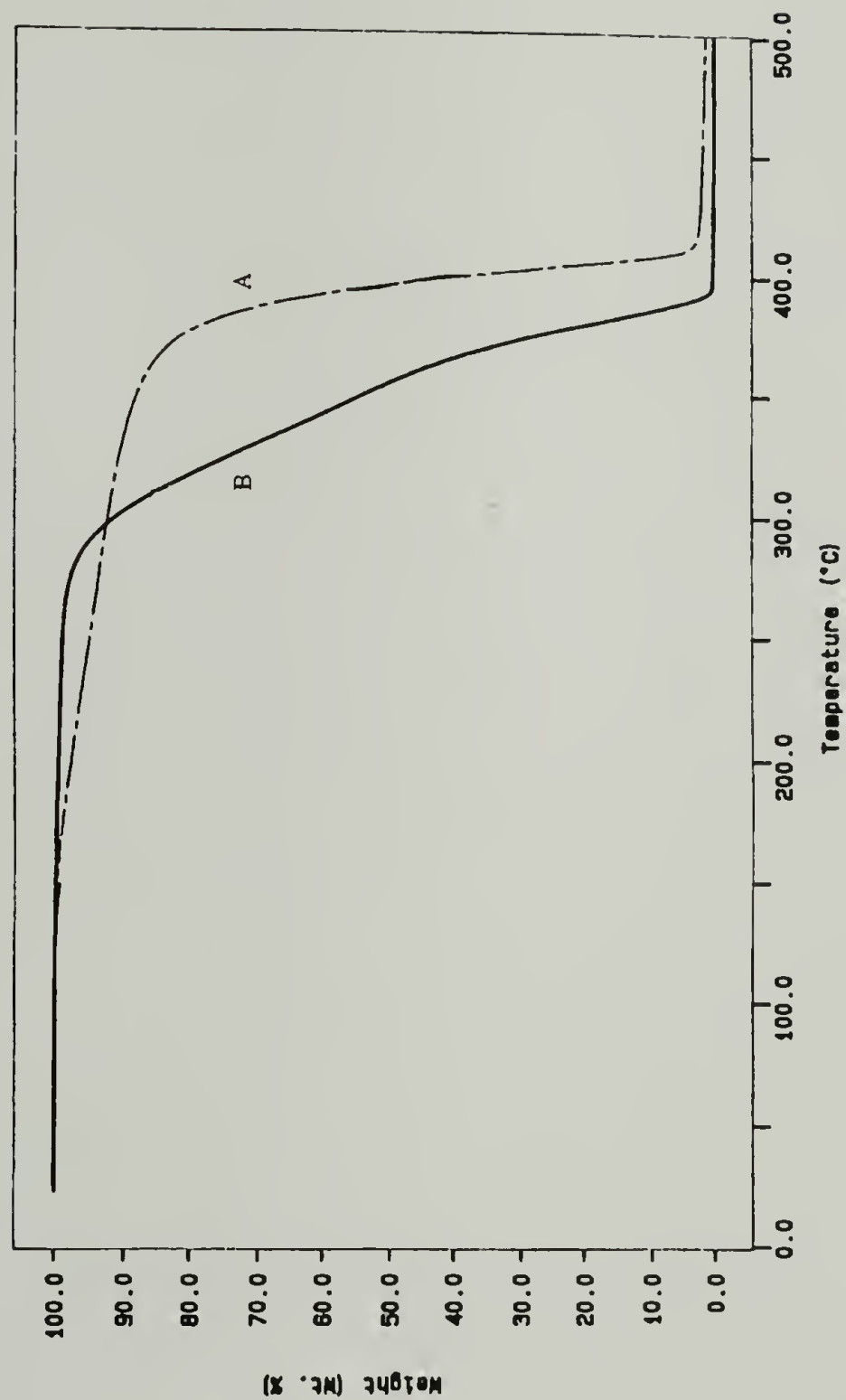


Figure 3.15 TGA curves of A: fractionated poly(RS)-TFL) and B: poly(D,L-lactide) under N<sub>2</sub> at 10C°/min.

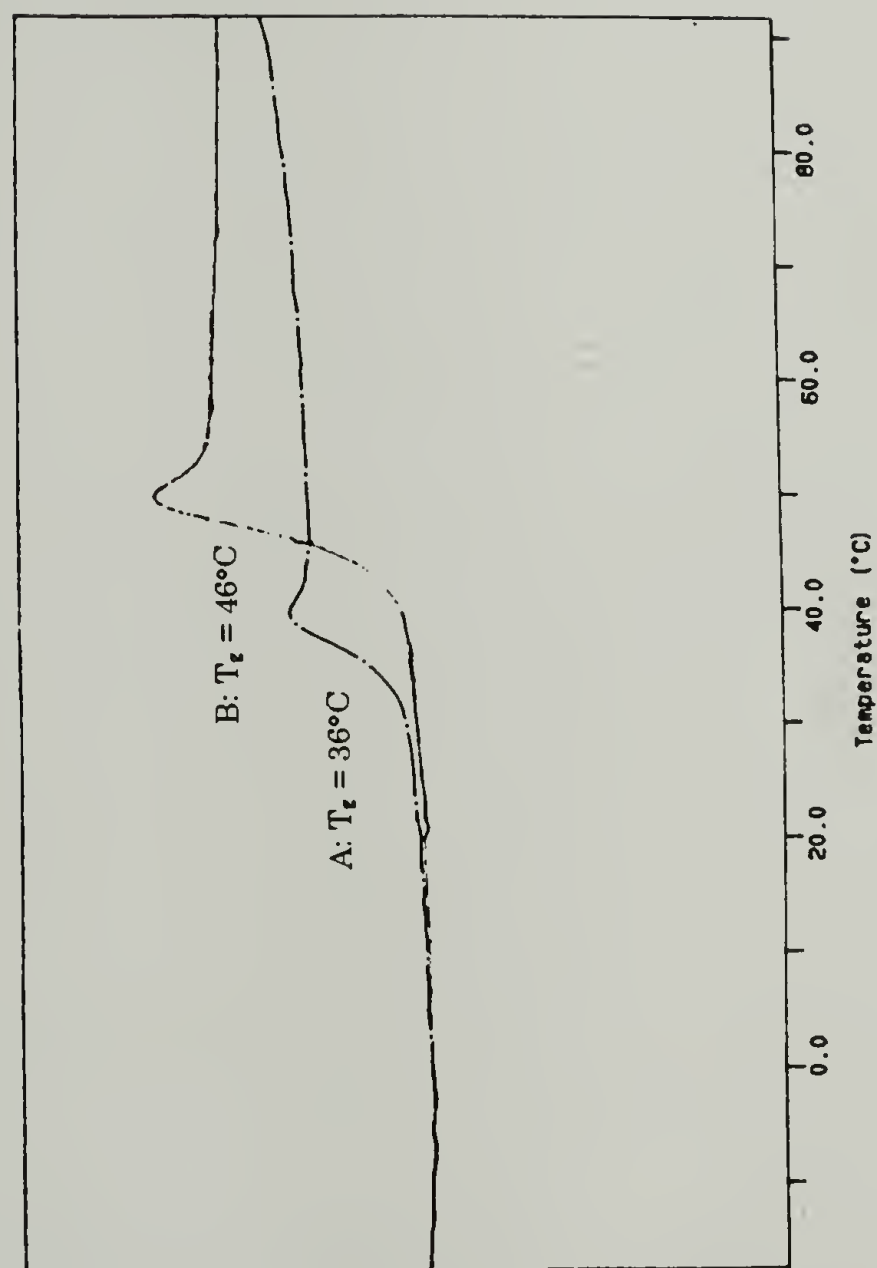


Figure 3.16 Glass transition temperatures (T<sub>g</sub>) of A: poly(RS)-TFL and B: poly(D,L-lactide) under N<sub>2</sub> at 20C°/min.

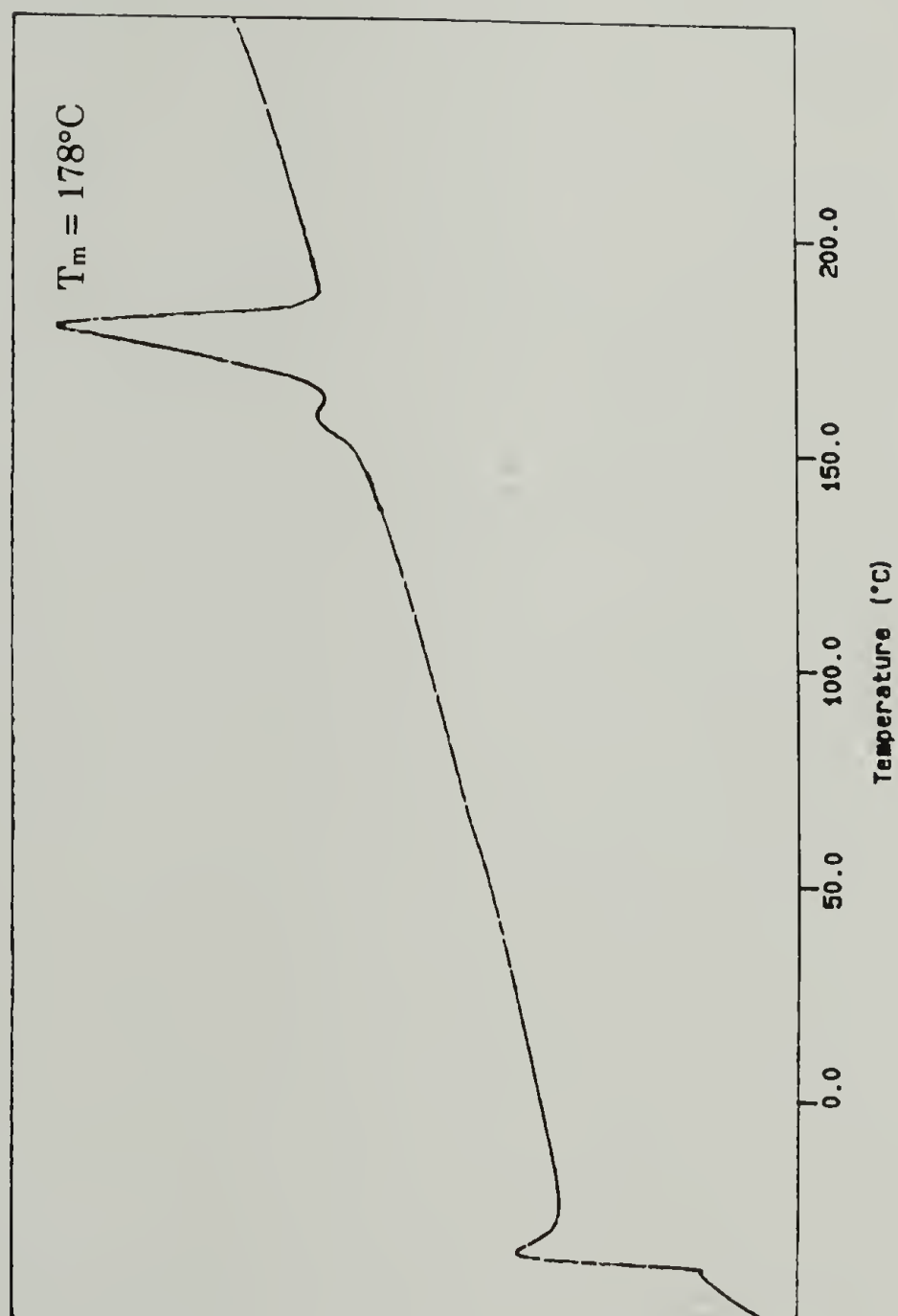


Figure 3.17 Peak melting temperature ( $T_m$ ) of poly(L-lactide) under  $\text{N}_2$  at  $10^{\circ}\text{C}/\text{min}$ .

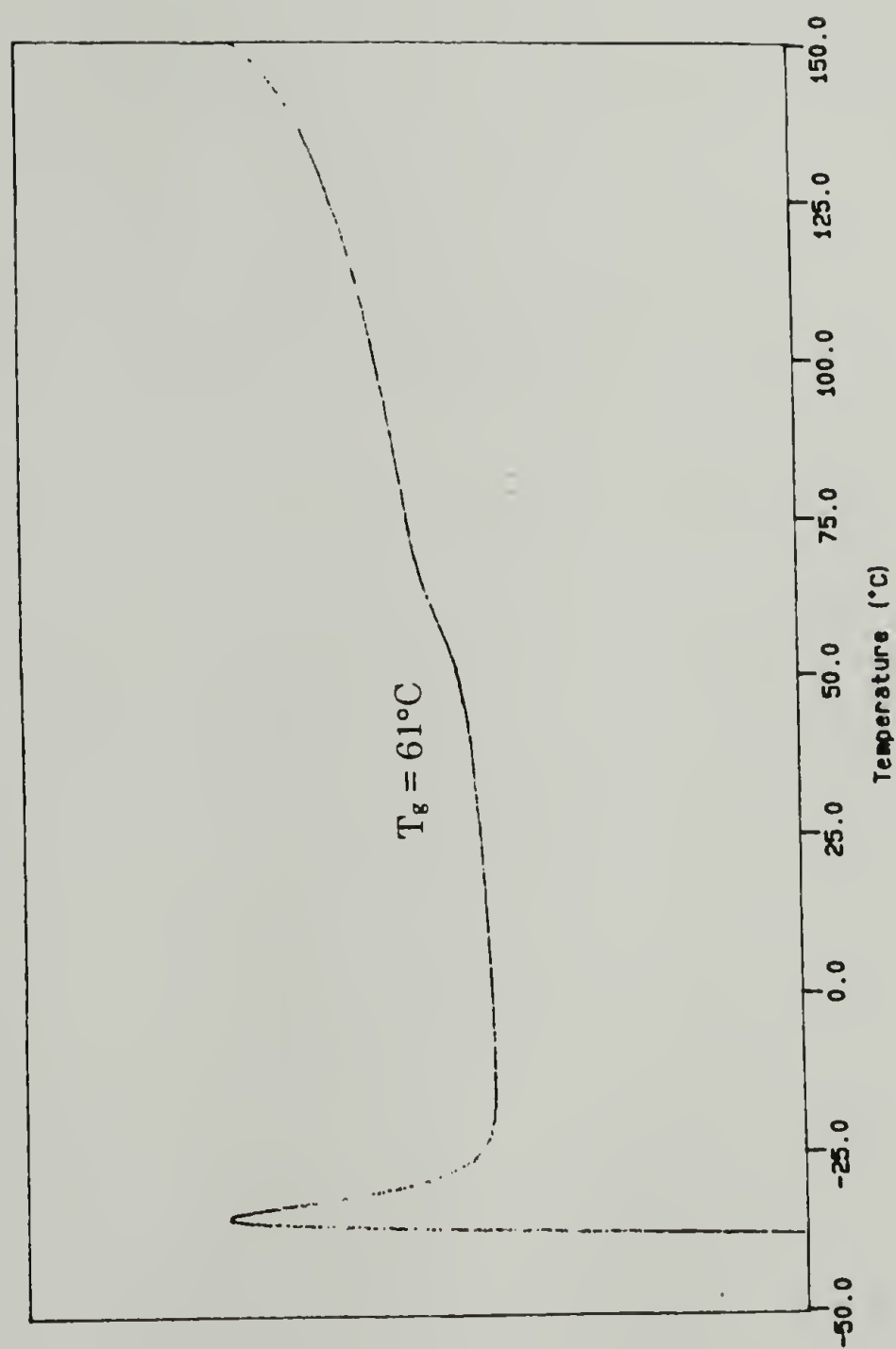
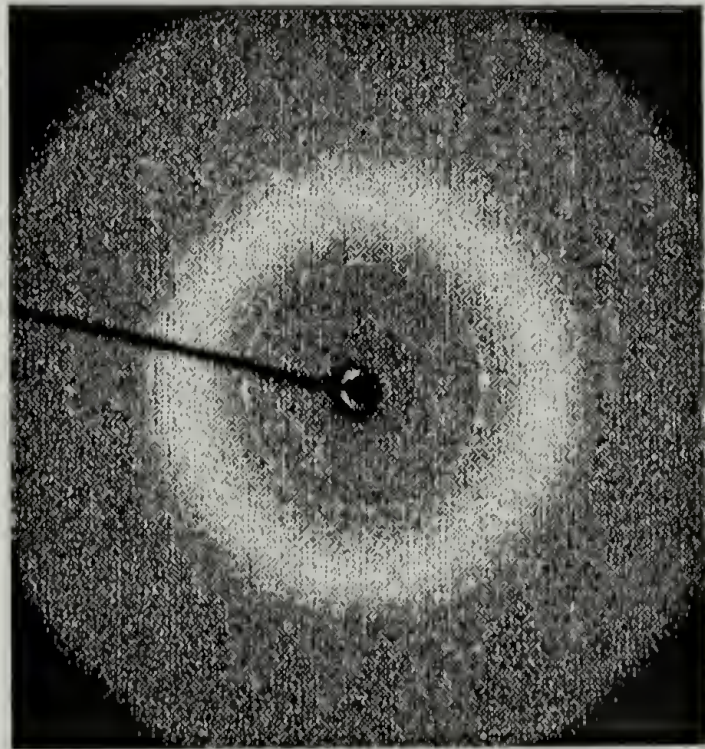
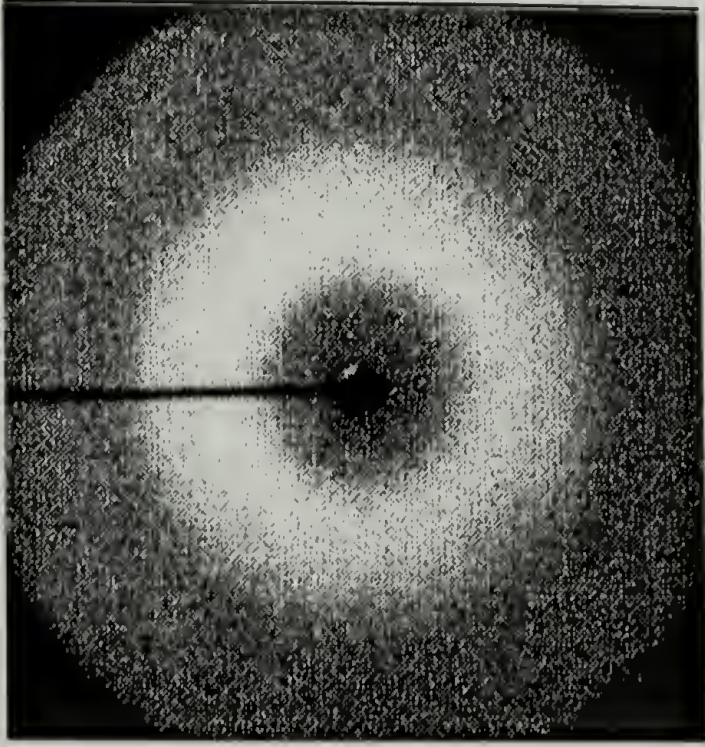


Figure 3.18 Glass transition temperature ( $T_g$ ) of poly(L-lactide) under  $\text{N}_2$  at  $10^\circ\text{C}/\text{min}$ .



A



B

Figure 3.19 Wide angle X-ray scattering patterns of A: poly((RS)-TFL) and B: poly(D,L-lactide). Neat polymer is fixed to the X-ray sample mount with a small amount of silicone grease.

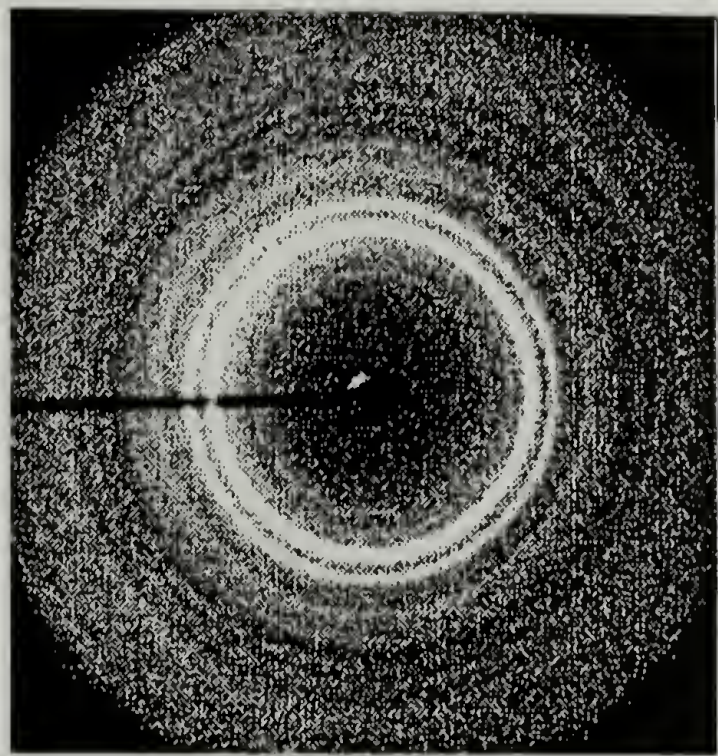
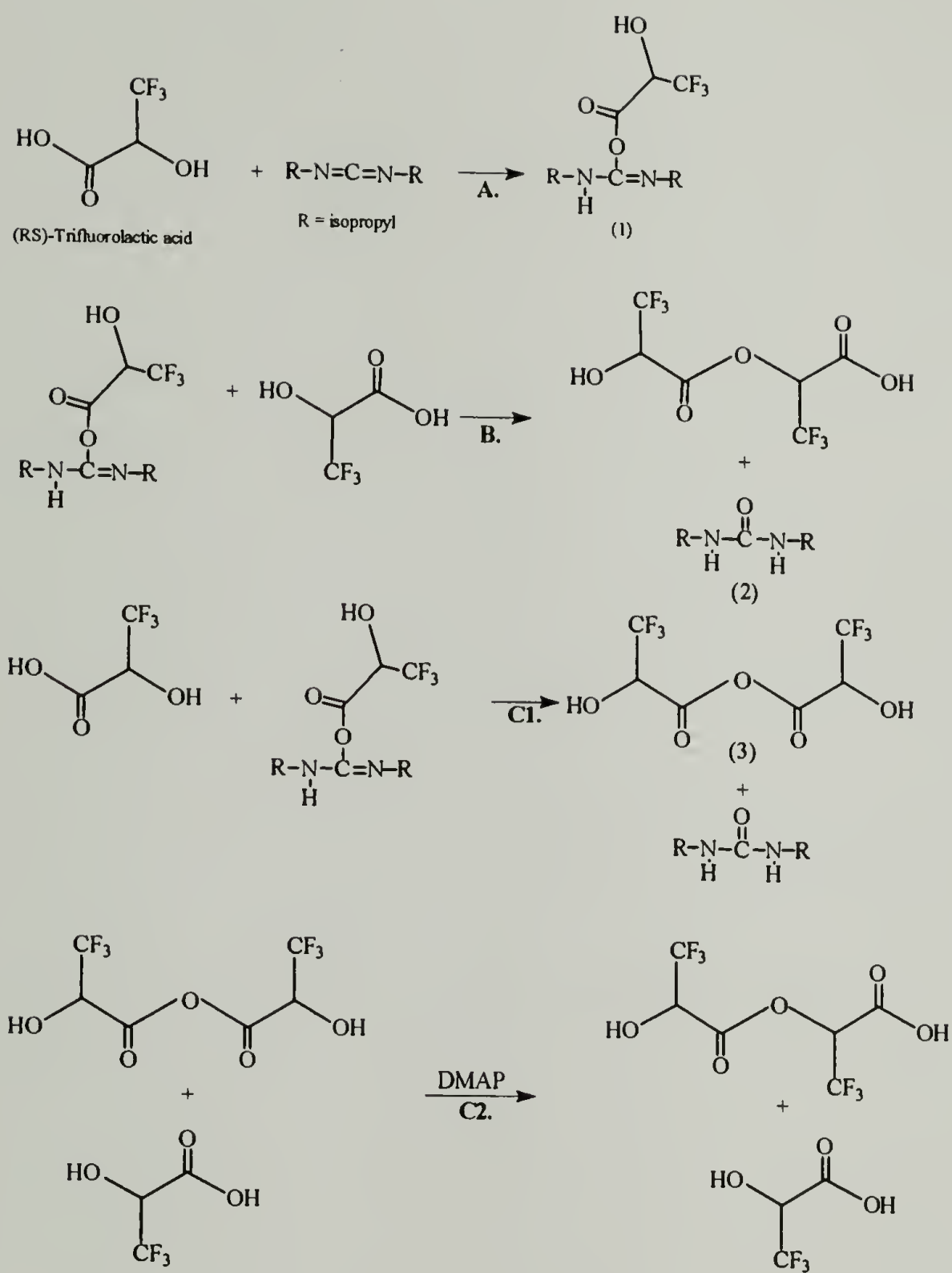
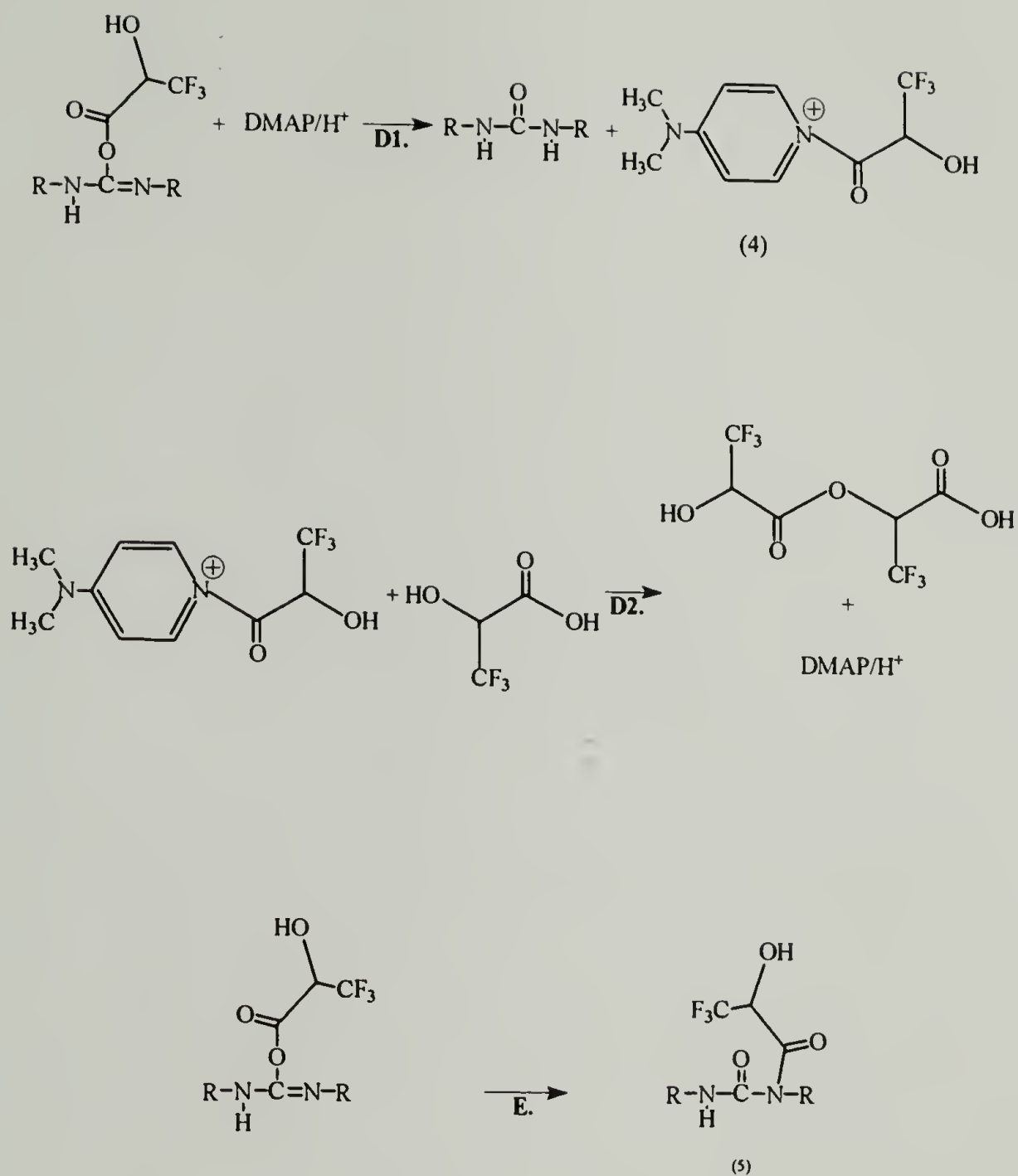


Figure 3.20 Wide angle X-ray scattering pattern of poly(L-lactide). Neat polymer is fixed to the X-ray sample mount with a small amount of silicone grease.



Scheme 3.1 Reaction pathways in the polymerization of (RS)-3,3,3-trifluorolactic acid).



Scheme 3.1 (Continued) Reaction pathways in the polymerization of (RS)-3,3,3-trifluorolactic acid).

## CHAPTER 4

### STATISTICAL OPTIMIZATION TECHNIQUES IN THE SYNTHESIS OF POLY((RS)-3,3,3-TRIFLUOROLACTIC ACID)

#### 4.1 Introduction

Lactic acid is the  $\alpha$ -hydroxyacid that is an analog of the  $\alpha$ -amino acid alanine. It is considered that if the methyl group of lactic acid is converted to a trifluoromethyl group it is reasonable to anticipate that the acidity of the  $\alpha$ -hydrogen would be significantly increased, with a concomitant enhancement of attractive intra- and intermolecular electronic interactions. Poly((RS)-3,3,3-trifluorolactic acid) (poly((RS)-TFL) is the fluoropolyester analog of the polypeptide polyalanine. As a fluoropolymer, this material is expected to have reduced surface energy. Also, the presence of fluorine can increase thermal stability and improve low temperature flexibility.<sup>1-3</sup> Poly((RS)-TFL) has the potential to form polymer blends with polyglycolide and polylactides for use as drug delivery matrices or as bioerodible materials. Moreover, the strong permanent dipole induced by the trifluoromethyl group provides potential for this polymer to form piezoelectric materials.

In this work, poly((RS)-TFL) was prepared with carbodiimide condensing agents and catalysts in solution, as shown in Scheme 4.1. Literature data on related esterification chemistry indicate that temperature,

solvent, and catalyst can affect the polymerization chemistry.<sup>4-8</sup>

Optimization of polymer product yield was important to the control of the reaction, as well as producing high molecular weight polymer in sufficient quantity for subsequent characterization. The goals of this study were to enhance the polymer yield and the molecular weight by the use of statistically designed polymerization experiments. Initial experiments were carried out to identify solvent candidates and a reasonable range of synthesis temperatures. A statistically designed set of experiments would be also beneficial for an improved understanding of the behavior of the parameters involved in the investigation, and possible correlations and/or interactions among them.

In addition to temperature and solvent, catalyst was also included as a parameter (factor) in the investigation. Two different solvents and catalysts were investigated. Also, the level of catalyst was varied. The objective of the first designed set of experiments was to improve the synthesis process and to identify the most important factors in this polymerization reaction. The results from the first set of experiments were used to develop additional experiments through statistical techniques to optimize the process.

## 4.2 Experimental Section

### 4.2.1 Materials

Anhydrous methylene chloride, chloroform and THF were obtained from Aldrich Chemical Co. and used without further purification. Methylene bromide was dried over molecular sieves to <0.01 wt.% water as determined by Karl Fischer titration. All other reagents were also obtained from Aldrich Chemical Co. and used without further purification

### 4.2.2 Methods

All glassware used for synthesis and characterization techniques was oven dried at 125°C for at least two hours and were assembled in an argon atmosphere glove box where solid reagents were weighed out and introduced into the assembly. The assembled apparatus was then placed in a fume hood for subsequent synthesis activities.

Inherent viscosity of the polymers was measured with Cannon-Ubbelohde size 50 viscometers in a constant temperature bath at 29.95°C  $\pm 0.01^\circ$ . THF was used as solvent. Solution concentration was 0.2 g/dL. The solutions were filtered (0.25  $\mu$  glass membrane) prior to measurement.

Polymer yield was based on the ratio of the weight of purified polymer to equivalent weight of monomer units introduced to the reaction vessel.

### 4.2.3 Preparations

The catalyst salt 4-(dimethylamino)pyridinium 4-toluenesulfonate (DPTS) was prepared as described by Moore and Stupp.<sup>6</sup> The other catalyst salt, 4-(dimethylamino)pyridinium triflate, (DPTL), was prepared as described previously.<sup>9</sup>

The synthesis of poly((RS)-3,3,3-trifluorolactic acid) (poly((RS)-TFL) was carried out by applying the procedure described by Moore and Stupp<sup>6</sup> with some modifications. The transformation of the  $\alpha$ -hydroxyacid to polymer was carried out with a carbodiimide condensing agent in the presence of a catalytic salt, (DPTS or DPTL) as shown in Scheme 4.1. Details of the preparation and chemistry are described in the previous chapter.

### 4.2.4 Statistically Designed Experiments

The singular objective of the initial designed set of experiments was to evaluate the importance of the factors that determine polymer yield and molecular weight as indicated by the inherent viscosity. The factors (also known as the reaction variables) that were studied are: polymerization temperature, solvent, catalyst, and level of catalyst. The temperature range chosen for the designed set of experiments was based on observations of polymer product formation at temperatures varied from 5°C to 25°. Two different solvents, methylene chloride and methylene bromide, were used in the solution polyesterification. In each, the maximum level of (RS)-TFL

monomer (limited by solubility) was introduced. Thus the monomer concentration was kept constant for all experiments in a particular solvent (0.23 mol/L in methylene chloride and 0.06 mol/L in methylene bromide).

Each catalyst salt was based on a different protic acid. The acid of DPTL (triflic acid) is stronger than *p*-toluenesulfonic acid (DPTS).<sup>10,11</sup> The comparative effect of these protic acids on the polymer product was obtained in this study. DPTL and DPTS were added in a range from catalytic to stoichiometric quantities; i.e., from 0.2 to 2.0 molar equivalents (or monomer to catalyst ratios from 5/1 to 0.5/1).

Statistically designed experiments were developed with Mr. S. Lepeniotis of the Materials, Models and Characterization Department of Hoechst Corporate Research and Technology. The design consisted of a total of 15 experiments including 2 center points to check for reproducibility. The experiments were designed with the MODDE v 3.0 software package.<sup>12</sup>

Table 4.1 lists the experimental runs, the factors at varying levels and the responses; yield and solution viscosity. Runs number 9 and 10 represent the 2 center points.

## 4.3 Results and Discussion

### 4.3.1 Statistical Data Analysis

Data from 15 experiments were analyzed using multiple linear regression (MLR) to build models that show the trends in yield and inherent viscosity as the temperature and catalyst are varied.

The general model that was fit for each response under investigation is as follows:

$$\begin{aligned} Y_m = & c + a_1x_1 + a_2x_2 + a_3x_3 + a_4x_4 \\ & + a_5x_1x_2 + a_6x_1x_3 + \dots + a_{10}x_3x_4 \\ & + a_{11}x_1^2 + a_{12}x_4^2 + e \end{aligned} \quad (1)$$

where:

$c$  = constant and  $a_i$  are the coefficients,  $e$  is unexplained error

$Y_m$  = dependent variable

$X_k$  = independent variables as follows:

$x_1$  = temperature (tmp)

$x_2$  = catalyst (-1 for DPTS and +1 for DPTL) (pra)

$x_3$  = solvent (-1 for  $\text{CH}_2\text{Cl}_2$  and +1 for  $\text{CH}_2\text{Br}_2$ ) (slv)

$x_4$  = catalyst level (cl)

MLR analysis allowed us to model the responses independent of each other. The final models were derived based on the same terms for both responses. In this manner, the two responses were compared by contrasting the coefficients and therefore identifying the relative effect that each common term had on the respective response.

The final refined model for percent yield ( $Y_i$ ) is given below:

$$Y_i = -1.063 - 0.11(\text{tmp}) + 0.485(\text{pra}) + 0.157(\text{slv}) - 0.233(\text{cl}) \\ + 0.147(\text{tmp})^2 + 0.192(\text{tmp} \cdot \text{cl}) + 0.355(\text{pra} \cdot \text{cl}) \quad (2)$$

These coefficients are graphically depicted in Figure 4.1 for the Yield. The interaction of catalyst with the catalyst level have the largest effect on the yield. DPTS has a strong positive effect while DPTL has a negative effect.

A general model was also fitted for the solution viscosity data. The model was refined based on the final model for yield. Some unimportant terms were not eliminated from the model because it is desirable to have the same terms in both models for comparison and any further experimentation. Even though some coefficients are very small they are left in the model. The final refined model for solution viscosity (SolVisco), with scaled and centered coefficients, is as follows:

$$\text{SolVisco} = -1.085 - 0.05(\text{tmp}) + 0.054(\text{pra}) + 0.367(\text{slv}) + 0.007(\text{cl}) \\ + 0.063(\text{tmp})^2 - 0.0042(\text{tmp} \cdot \text{cl}) - 0.0011(\text{pra} \cdot \text{cl}) \quad (3)$$

In Figure 4.2, the scaled and centered coefficients for the solution viscosity are compared. It is clear that the factor with the largest effect on solution viscosity is the type of solvent.

Three dimensional plots of the response surfaces were constructed for the yield and solution viscosity with selected factors. The three-dimensional

plots (Figures 4.3-4.6) provide visualization of the optimum operating conditions for this synthesis. The temperature and catalyst level are used as the x and y axes for the three-dimensional plots since these are the continuous factors for both responses (shown on z axis).

Figure 4.3 is a response surface of the yield with catalyst DPTS and solvent methylene chloride. The catalyst level axis ranges from the minimum to maximum levels used in the experiments. A maximum yield can be achieved at low temperature (5-7°C) with low catalyst level (0.2 - 0.4 equivalents). High yield can also be achieved at relatively high temperature (16-18 °C) and high catalyst level (1.0 - 1.2 molar equivalents).

Figure 4.4 also presents a 3-D plot of the yield when DPTL is used. A maximum yield can be achieved at low temperature (5-7 °C) with low catalyst level (0.2 - 0.4 equivalents), with solvent methylene chloride. By examining these two plots we see that we have more flexibility when using DPTS instead of DPTL, because our region of optimum performance is greater. The yield that we can achieve with DPTS is higher than with DPTL.

Figure 4.5 displays a 3-D plot of solution viscosity with catalyst DPTS and solvent methylene chloride. High solution viscosity can be achieved at low temperature 5-7 °C; the catalyst level does not affect the results of this response; i.e., the surface is approximately parallel to the catalyst (DPTS) level axis.

A solution viscosity surface with DPTL is shown in Figure 4.6. High solution viscosity can be achieved again at low temperature (5-7 °C); the catalyst level does not affect the results of this response and we see that the surface is approximately parallel to the catalyst level axis. The solvent is methylene chloride.

Three dimensional plots were also constructed with methylene bromide as the solvent. The results for yield and inherent viscosity were much lower than they are for methylene chloride.

#### 4.4 Conclusions

The analysis of this experimental design study provides direction for further synthetic investigations with this polymerization chemistry. Relatively low temperature for the reaction and low DPTS level are preferred not only for the optimum synthesis productivity but also for the polymer product workup. Yield and solution viscosity are not a function of these two factors only but also depend on the type of catalyst and solvent as well. Since the objective is to achieve high yield and solution viscosity we show that the solvent of choice is methylene chloride with the DPTS catalyst.

DPTL can produce polymer with good solution viscosity but the yield is not as high as with DPTS. The region of operability is also smaller with DPTL than when DPTS is used. In summary, the best results can be achieved under the following conditions:

solvent: methylene chloride

catalyst: DPTS

temperature: 5°C - 7°C

catalyst level: 0.2 - 0.4 molar equivalents with respect to (RS)-TFL.

#### 4.5 References and Notes

- (1) Johncock, P.; Barnett, S. P.; Rickard, P. A. *J Polym Sci Part A: Polym Chem* **1986**, *24*, 2033.
- (2) Knight, G. J.; Wright, W. W. *J Appl Polym Sci* **1972**, *16*, 683.
- (3) Koo, G. P. In *Fluoropolymers*; L. A. Wall, Ed.; Wiley-Interscience: New York, 1972, p 515.
- (4) Balcom, B. J.; Petersen, N. O. *J. Org. Chem.* **1988**, *54*, 1922.
- (5) Boden, E. P.; Keck, G. E. *J. Org. Chem.* **1985**, *50*, 2394.
- (6) Moore, J. S.; Stupp, S. I. *Macromolecules* **1990**, *23*, 65.
- (7) Neises, B.; Steglich, W. *Angew Chem Int Ed* **1978**, *17*, 522.
- (8) Wagener, K. B.; Linert, J. G.; O'Gara, J. E. *J Macromol. Sci. - Pure Appl. Chem.* **1994**, *A31*, 775.
- (9) McKie, D. B.; Tirrell, D. A.; Lillya, C. P.; Muthukumar, M.; Jaffe, M. , manuscript in preparation.
- (10) March, J. *Advanced Organic Chemistry*; Wiley Interscience: New York, 1992, p 250.
- (11) Olah, G. A.; Prakash, G. K. S.; Sommer, J. *Superacids*; Wiley Interscience: New York, 1985, p 33.
- (12) *MODDE Software manual, UMETRI AB* Umea, Sweden, 1996

Table 4.1 Experimental design worksheet with response results.

Exp.No.	Run Order	Temperature [°C]	Catalyst	Solvent	Catalyst Level [molar equiv.] (with respect to monomer)	Yield [wt.%]	Solution viscosity (conc. = 0.2 g/dL) at 29.95°C in THF [dL/g]
1	11	25	DPTS	MethBr	0.2	10.2	0.07
2	9	25	DPTS	MethBr	0.4	18.4	0.04
3	6	5	DPTL	MethBr	0.2	17.6	0.04
4	12	5	DPTL	MethBr	0.4	11.6	0.05
5	4	5	DPTS	MethCl	0.2	41.3	0.33
6	15	5	DPTS	MethCl	2	31.4	0.3
7	13	25	DPTL	MethCl	0.2	16.5	0.32
8	7	25	DPTL	MethCl	2	3.4	0.26
9	10	15	DPTS	MethCl	1.1	32.4	0.19
10	1	15	DPTS	MethCl	1.1	38.5	0.3
11	8	5	DPTS	MethCl	1.2	36.2	0.25
12	5	9.3	DPTS	MethCl	0.2	35.4	0.22
13	2	18	DPTL	MethCl	1.2	1.5	0.16
14	14	5	DPTL	MethCl	0.2	26.5	0.16
15	3	9.3	DPTL	MethCl	0.2	15.1	0.15

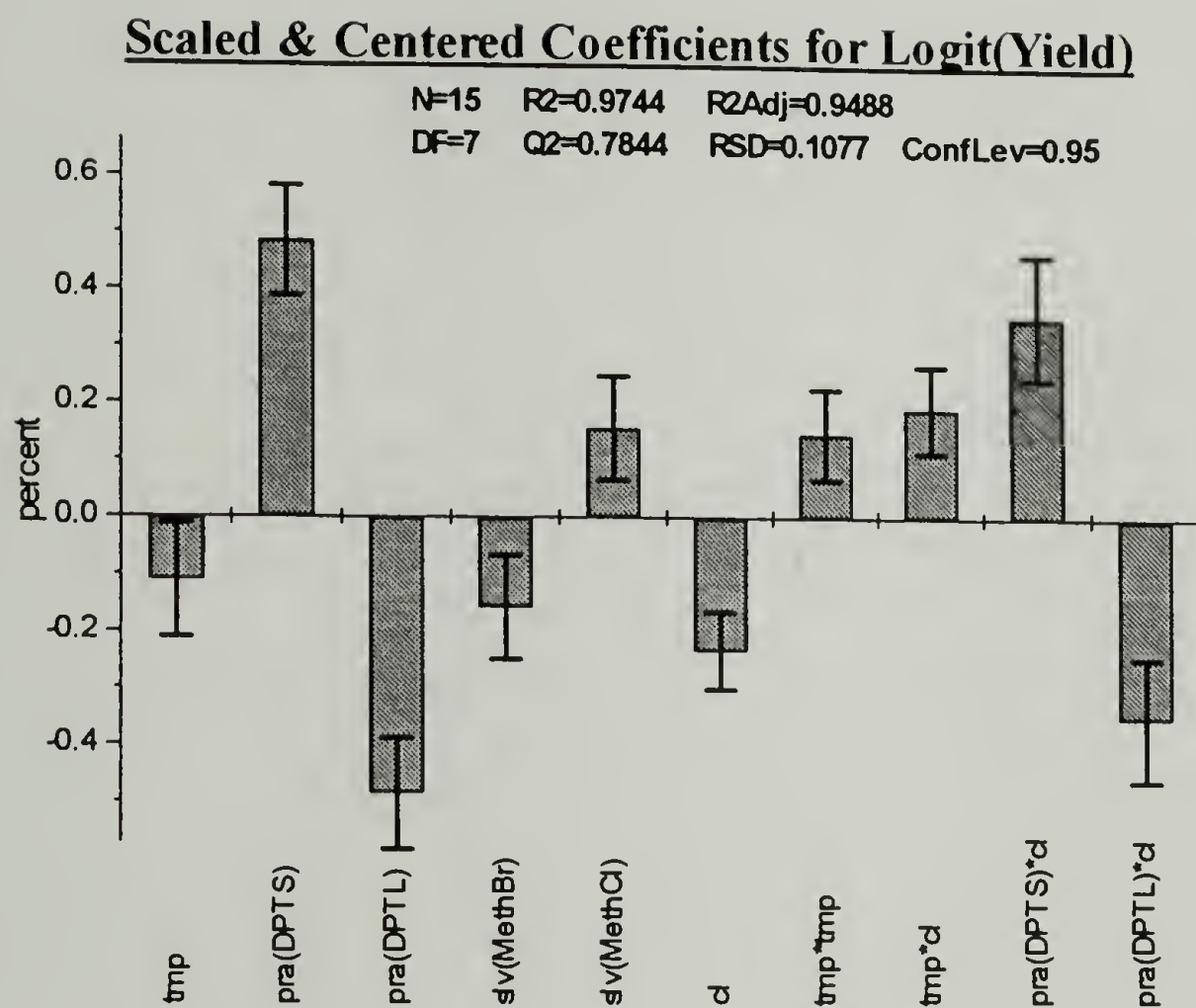


Figure 4.1 Comparison of yield model coefficients.

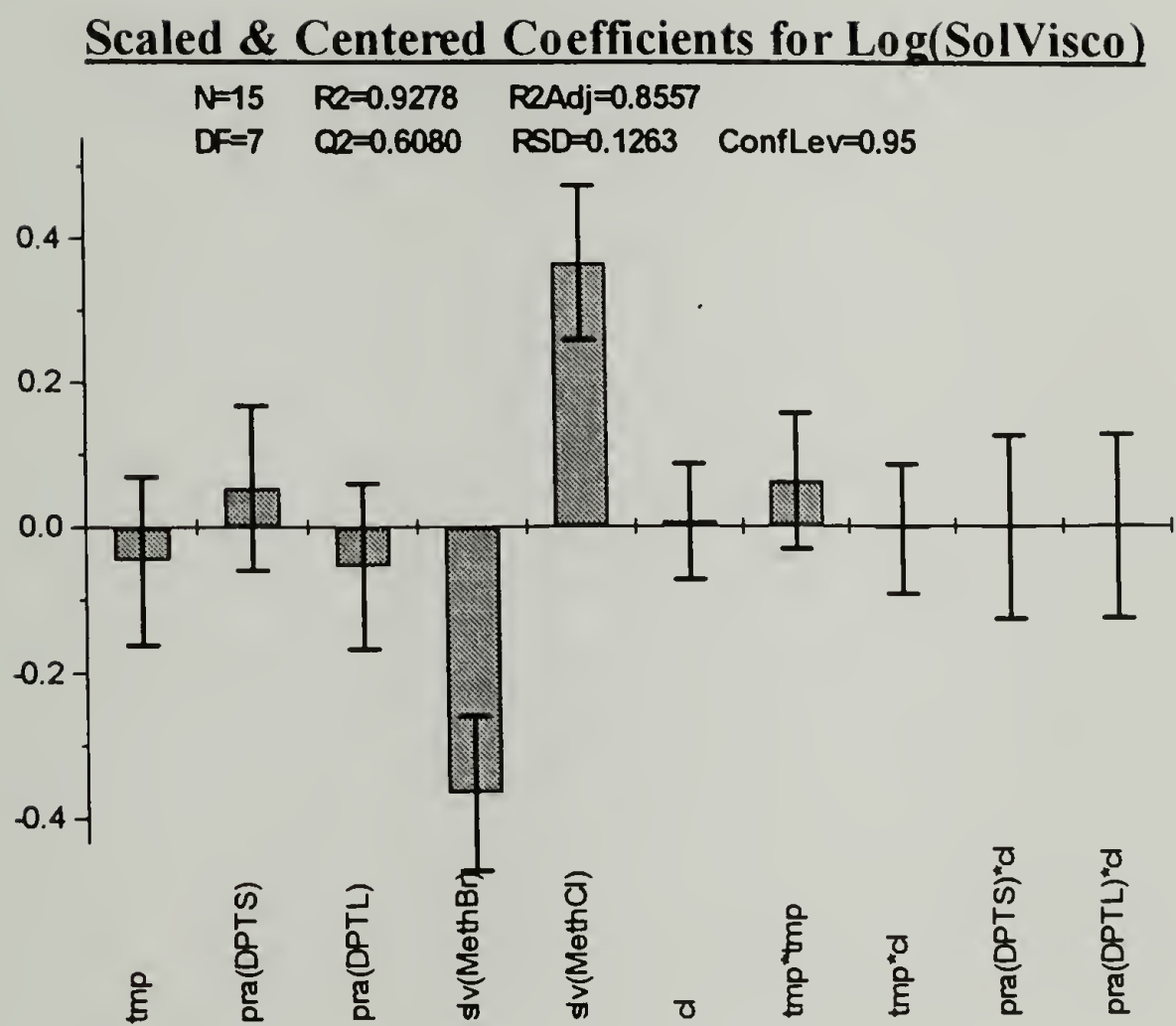


Figure 4.2 Comparison of solution viscosity model coefficients.

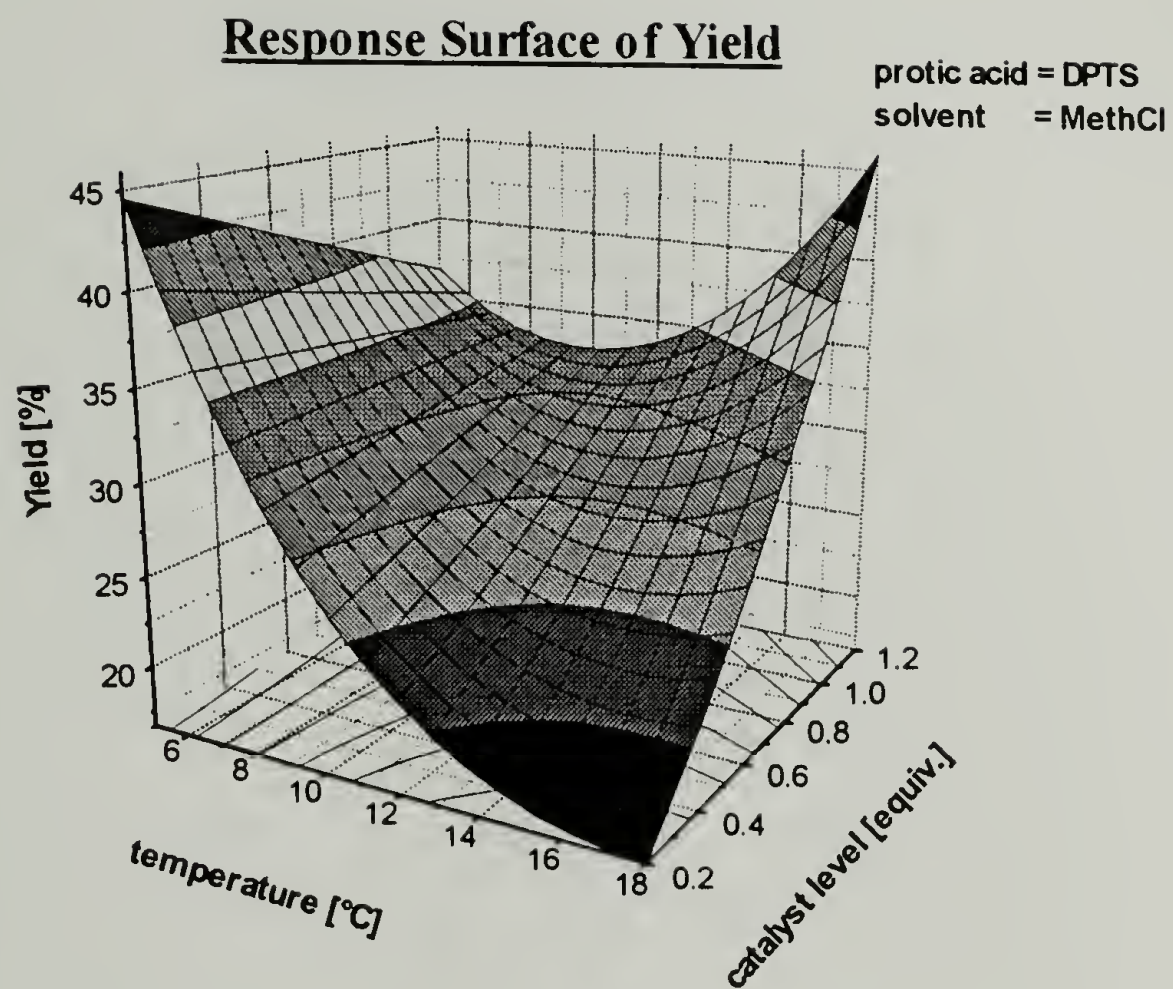


Figure 4.3 Optimization surface of the yield with DPTS.

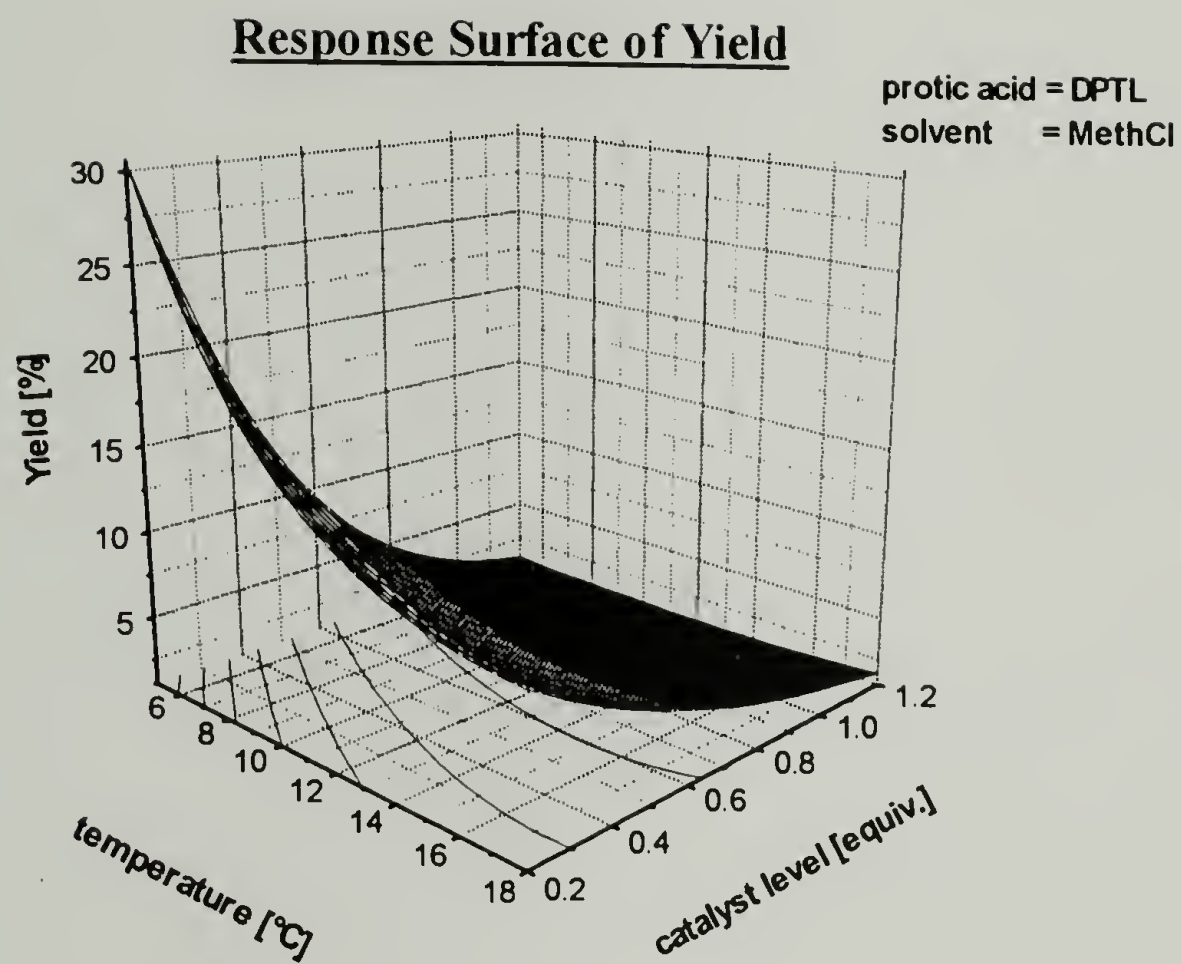


Figure 4.4 Optimization surface of the yield with DPTL.

### Response Surface of Solution Viscosity

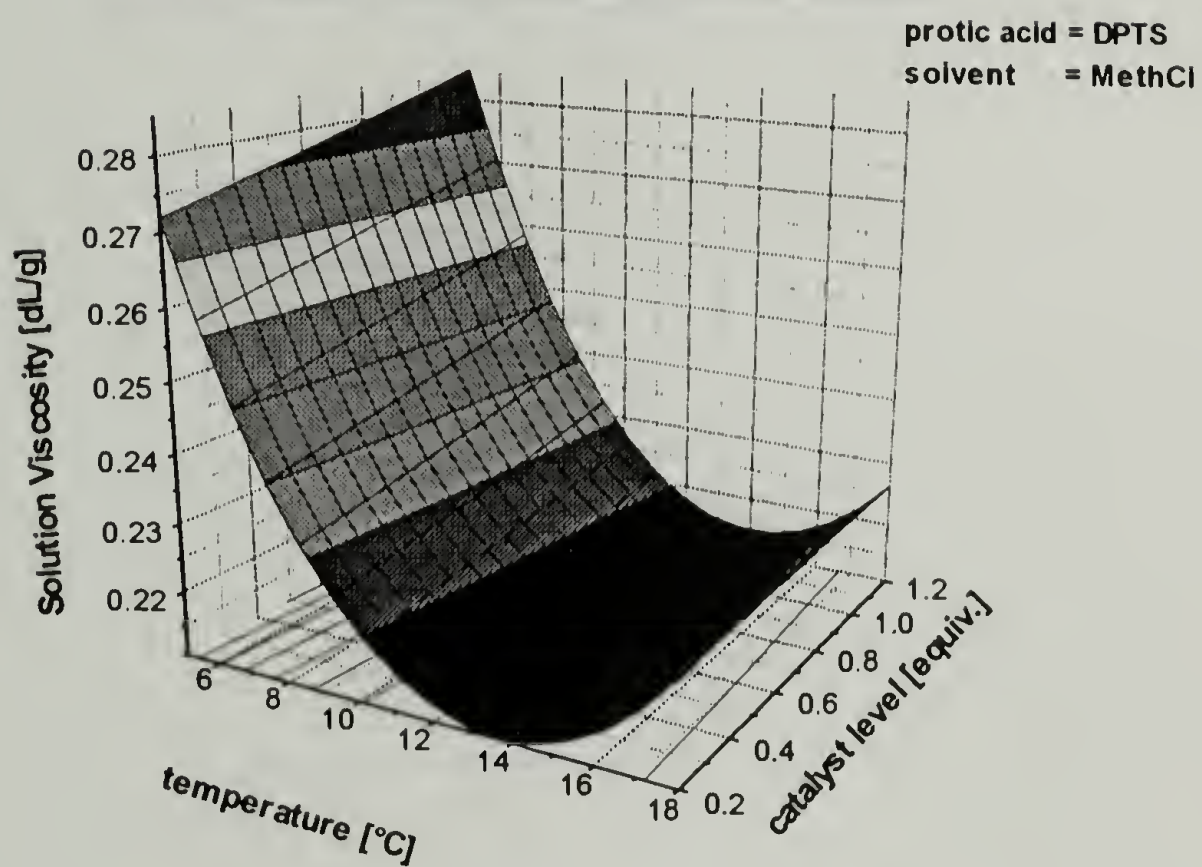


Figure 4.5 Optimization surface of the solution viscosity with DPTS.

### Response Surface of Solution Viscosity

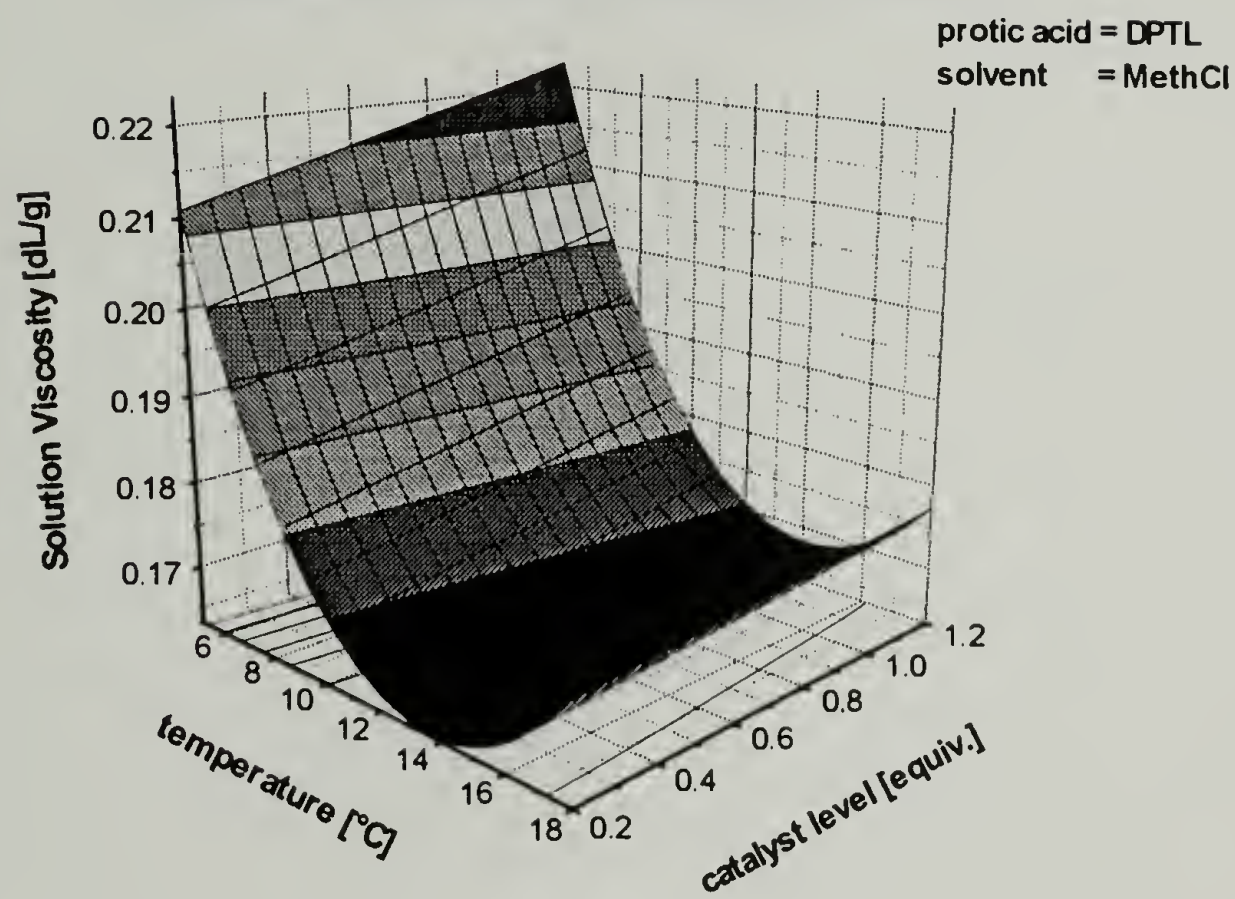
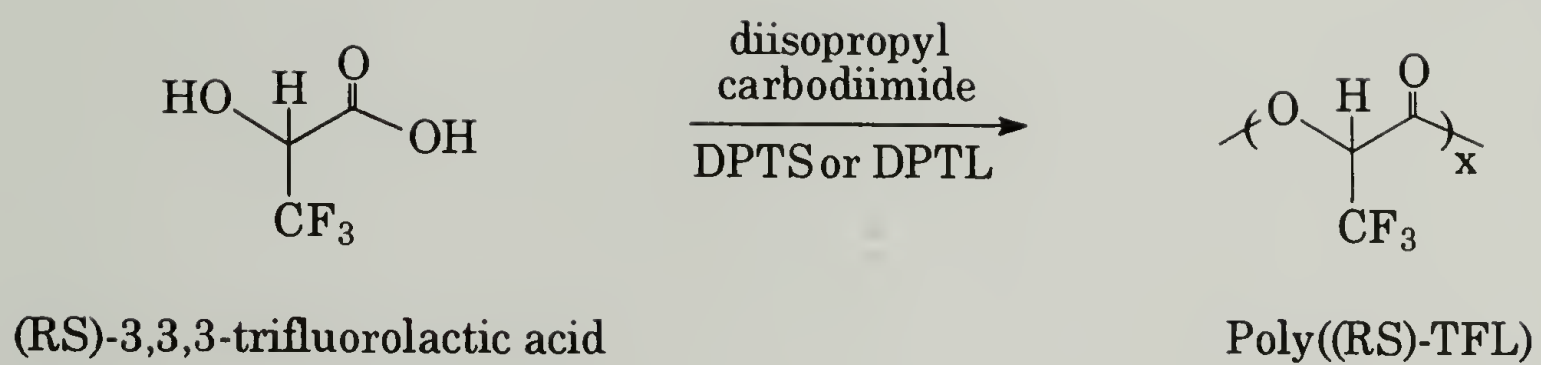


Figure 4.6 Optimization surface of the solution viscosity with DPTL.



Scheme 4.1 Synthesis of Poly((RS)-3,3,3-trifluorolactic acid).

## CHARACTERIZATION OF POLY((RS)-3,3,3-TRIFLUOROLACTIC ACID)

### 5.1 Introduction

Poly((RS)-3,3,3-trifluorolactic acid) (poly(RS)-TFL) as an analog of poly(D,L-lactide), has the potential utility in industrial, pharmaceutical<sup>1</sup> and medical applications. With an acidic methine hydrogen, this polymer may form compatible polymer blends with reduced surface energy. The presence of fluorine can increase thermal stability and improve low temperature flexibility. Potential for blends with polyglycolide and polylactides as drug delivery matrices or as bioerodible materials is enormous.<sup>2-4</sup>

In this effort, the effect of polymerization time on polymer yield and molecular weight was studied. It has been shown that carboxylic acids can be successfully esterified at room temperature in 3 h. by a carbodiimide condensing agent and 4-(dimethylamino)pyridine (DMAP),<sup>5</sup> and hydroxyacids have been polymerized under similar conditions in 12 h..<sup>6</sup> Thus it may be possible to reduce the 24 h reaction used in the previous chapter to prepare poly((RS)-TFL). Poly((RS)-3,3,3-trifluorolactic acid) was also fractionated to study physical properties without the presence of a significant

low molecular weight component. Finally, blends of lactide and trifluorolactic acid polyesters were subjected to preliminary studies of surface properties.

The experimental design described in the previous chapter informed the optimal conditions for preparing poly(RS-TFL); i.e., polymerization at 5°C in methylene chloride with 4-(dimethylamino)pyridinium 4-toluenesulfonate (DPTS) catalyst. With the exception of some polymers prepared in the polymerization time study, these conditions were used to prepare the polymer described in this chapter.

## 5.2 Experimental Section

### 5.2.1 Materials

Methylene chloride, chloroform and THF, all anhydrous, were obtained from Aldrich Chemical Co. and used without further purification.

1,1,1,3,3,3-Hexafluoro-2-propanol (HFIP) and acetone were also obtained from Aldrich Chemical Co.. Fluorinert<sup>®</sup> FC-72 was obtained from 3M Company. All reagents were used without further purification.

Medisorb<sup>®</sup> 100DL (poly(D,L-lactide)) low IV was obtained from Medisorb Technologies International L.P..

### 5.2.2 Methods

All glassware was oven dried at 125°C for at least two hours.  $^1\text{H}$  and  $^{13}\text{C}$  NMR spectra were recorded on a Varian XL-200 (200 MHz  $^1\text{H}$ ) spectrometer. Deuterated DMSO, THF, chloroform and HFIP were used as solvents. Elemental analyses were performed at Galbraith Laboratories, Knoxville, Tennessee. Inherent solution viscosity was measured as described in Chapter 3. Gel permeation chromatography (GPC) data were obtained at ambient temperature in a Waters 210 GPC with a WISP 712 sample autoinjector and a Waters 410 visible LED differential refractometer. A Wyatt DAWN-FH 1992 flow through instrument with 18 simultaneously scattering angles of detection was used to obtain light scattering data. The incremental indices of the refraction ( $dn/dc$ ) for the polymer solutions were measured in a Wyatt optilab DSP interferometric refractometer. Solutions at 3 different concentrations were prepared for each type of polymer. Shot size was 200  $\mu\text{L}$  at a concentration of 12 mg/mL. Columns were from American Polymer Standards PL-Gel, 10  $\mu\text{m}$  particles, mixed-B (bed with nominal 500,  $10^3$ ,  $10^4$ ,  $10^5$ , and  $10^6$  nominal Å particle porosity). THF solvent was degassed and passed through a 5  $\mu\text{m}$  filter.

Polymer was fractionated by dissolving in HFIP followed by addition of the nonsolvent fluorocarbon/perfluorinated ether mixture Fluorinert<sup>®</sup> FC-72. Precipitated polymer was separated from the supernatant in a Fisher Scientific Marathon 21K centrifuge. Glass tubes (25 mL) were spun at 5000

RPM for 15 min under ambient conditions. The recovered precipitate was washed with a mixture of the solvent and nonsolvent in the ratio that formed the precipitate. The complete procedure was repeated and then the polymer was dried in a vacuum oven at 35°C for 48 h.

DSC and TGA data were obtained in a Perkin-Elmer series 7 thermal analysis system. Thermal responses were measured with samples in a nitrogen atmosphere at a 10° C/min rate of temperature rise. Data from second heating traces are reported.

Wide angle X-ray scattering (WAXS) data were obtained with a Siemens instrument in a helium atmosphere with monochromatic CuK $\alpha$  (1.542 Å) radiation produced by a Rigaku Ru-200 rotating anode generator. Data were processed by Siemens HI-STAR software. Diffraction spacings were calculated from the Bragg equation ( $d = n\lambda / 2\sin\theta$ , where  $d$  is the spacing,  $n$  is an integral number,  $\lambda$  is X-ray wavelength, and  $\theta$  is  $\frac{1}{2}$  the angle between the incident and diffracted beams.<sup>7</sup>

Polymer blends were prepared by solution casting. Appropriate quantities of poly(D,L-lactide) and poly((RS)-TFL) were placed in 15 mL Erlenmeyer flask, and solvent (~10 mL, either HFIP or acetone) was added to prepare the solutions. Thin glass cover slips were dipped into the solutions and clipped on a support for solvent evaporation in the vacuum oven at ambient temperature for 4 days. Solvent was evaporated from the remaining solutions and the polymer mixture recovered for elemental analysis. These

dip coated cover slips were used for contact angle measurements and X-ray photoelectron spectroscopy.

Dynamic contact angle measurements were obtained in an ATI Cahn DCA 315 Wilhelmy plate apparatus. Test specimens (18 x 18 x 0.1mm) suspended on a balance were lowered into deionized distilled water at 80  $\mu$ /s. The specimen was then raised out of the water at the same rate. Force measurements as a function of immersion depth were converted to advancing and receding contact angle with a correction for the buoyancy of the test specimen.<sup>8</sup>

$$\gamma_L p \cos\theta = F - xAdg$$

where:

$\gamma_L$  = surface tension of water

$p$  = perimeter of the test

specimen parallel to the test fluid

$\theta$  = contact angle

$F$  = force measurement

$x$  = immersion depth of the test specimen

$A$  = cross-sectional area of the test

specimen parallel to the test fluid

$d$  = density of water

$g$  = acceleration of gravity

X-ray photoelectron spectroscopy (XPS) was done with a Physical Electronics model 5701 LSci with a monochromatic aluminum X-ray source. Data were obtained with the electron analyzer at 85° and 15° to the sample

plane. Dynamic secondary ion mass spectrometry (SIMS) was carried out with a Perkin Elmer/PHI model 6300 quadrupole SIMS system. Experiments were conducted with  $O_2^+$  primary ion bombardment with 3 keV impact energy at an angle of  $60^\circ$  and negative secondary ion detection. XPS and SIMS experiments were conducted at Evans East Analytical Services in Plainsboro, NJ.

### 5.3 Results and Discussion

#### 5.3.1 Polymer Molecular Weight as a Function of Polymerization Time

The poly((RS)-TFL) were prepared with DPTS catalyst in methylene chloride at  $5^\circ\text{C}$  and worked up as described in Chapter 4. Polymerization time was varied from 8 to 48 h. Polymer inherent viscosity, absolute  $M_w$ , polydispersity, and yield for the various polymerization times are displayed in Table 5.1. The data indicate that there was no significant increase in molecular weight with increased polymerization time after 8 hours as indicated by inherent viscosity or weight average molecular weight. Judging by the typical variation in yield described in Chapter 4 only a modest increase in yield is achieved by increasing polymerization time to 48 h. Also remarkable here is that the observation that despite low yields high polymer was produced. According to the well known Carothers' theory, high polymer results from step growth processes only at very high conversions ( $>99\%$ ).<sup>9</sup>

Chain growth mechanisms (such as radical and ionic) typically produce high polymer very quickly dependent upon the relative rates of the addition steps and termination steps.<sup>10</sup> Also interesting is that the molecular polydispersity approaches the Flory most probable distribution ( $M_w/M_n = 2$ ). This is typical for a step growth polymerization at very high conversions. The most probable distribution also arises in polymerization systems where interchange reactions or random chain cleavage pathways are available.<sup>11</sup> That is, the polymer system can be driven to the distribution characterized by maximum entropy. One or both of these pathways may be available in the solution polyesterification of trifluorolactic acid.

### 5.3.2 Fractionation of Poly((RS)-trifluorolactic acid)

The GPC refractive index chromatogram trace (Figure 5.1B) of the poly((RS)-TFL) control (without fractionation) clearly shows the presence of a low molecular weight tail on the major peak and also a small low molecular weight peak centered near a retention volume of 26 mL. All the peaks at retention volumes greater than 26 mL are solvent peak artifacts. A portion (500 mg) of the control polymer was doubly fractionated (145 mg were recovered; a yield of 29 %). The fractionated poly((RS)-TFL) (Figure 5.1A) is quite a contrast to the control. The peak is clearly shifted to a higher molecular weight and narrower molecular weight distribution than the control and the low molecular weight peak is eliminated. Indeed, the

distribution is similar to that of the commercial poly(D,L-lactide), shown in Figure 5.1C, for comparison. This is quite evident in the plot of differential weight fraction versus molecular weight in Figure 5.2. The cumulative molecular weight curves in Figure 5.3 also show how a significant quantity of the low molecular weight component of the control polymer was removed by the fractionation process.

The proton NMR spectra of the control and fractionated polymer are displayed in Figures 5.4A and B, respectively. They are contrasted by the elimination of the methyl peak signal at 0.9 PPM. This band can be associated with urea contamination of the polymer (see Figure 3.1). A comparison of the integration of the isopropyl methine octet and the amide hydrogen doublet suggests this. In diisopropylurea, in principle, the ratio of these two peaks is 1:1. In the case of *N*-3,3,3-trifluorolactoylurea or the presence of this as an end group of polymer chains, the ratio is 2:1. The ratio of these peaks is 1:1 as shown in Figure 5.5. The fractionation process not only eliminates the low molecular weight polymer, it also removes residual diisopropylurea.

The absolute molecular weight measurements obtained by light scattering are consistent with the GPC results as shown in Table 5.2. Inherent viscosity was also measured and the data are also reported in Table 5.2. The unexpectedly high value of solution viscosity of the control relative to the fractionated polymer may be a confounding effect of residual

diisopropylurea (DIPU). The DIPU may form a complex with the polymer resulting in increased viscosity. The inherent viscosity of poly(D,L-lactide) is greater than that of the fractionated poly((RS)-TFL) yet the  $M_w$  values is significantly less. This is explained by the significant difference between the molar masses of the two repeat units. Poly(D,L-lactide) repeat unit mass is 72 g/mol whereas the poly((RS)-TFL) unit is much more massive at 126 g/mol.

The GPC instrument separates polymer fractions in solution by hydrodynamic volume. The overlap of the GPC traces of fractionated poly((RS)-TFL) and poly(D,L-lactide) (Figure 5.1A and C, respectively) is apparent. The product of the molar mass and the intrinsic viscosity is proportional to the hydrodynamic volume.<sup>12</sup> The inherent viscosity is an approximation of the intrinsic viscosity. It is also shown in Table 5.2 that the products of the inherent viscosity times the weight average molecular weight for these two samples are essentially equivalent.

The TGA data of the fractionated polymer and control compare as expected. In Figure 5.6A, the control polymer shows a significant weight loss below 300°C. This is evidence of the removal of a volatile or degrading component in poly(RS-TFL). Fractionated poly((RS)-TFL) (Figure 5.6B) does not show major weight loss until well above 300°. Also interesting is that the fractionated fluoropolyester compares quite favorably with poly(D,L-lactide) in terms of thermal stability (Figure 5.7).

The DSC traces (Figure 5.8) indicate that both the control and fractionated polymer have the same  $T_g$ . The measured  $T_g$  of the fractionated poly((RS)-TFL) shown in Figure 5.9 is 38°C.

The wide angle X-ray scattering patterns for the two samples are quite different. Shown in Figure 5.10A is the control fluoropolyester, with a broad amorphous halo and discrete spots indicative of polycrystallinity, probably due to diisopropylurea, displayed throughout. A different pattern emerges in the purified poly((RS)-TFL); in Figure 5.10B, a sharper band appears at smaller angles than the broad halo. The X-ray scattering curves for the control and fractionated poly((RS)-TFL) are compared in Figure 5.11A and B, respectively. The broad dominant peak centered near  $2\theta$  of 22° corresponds to an equivalent Bragg spacing of  $\sim 4$  Å and is associated with the average van der Waals distance of closest atomic approach in the polymer sample. The intensity maximum near  $2\theta$  of 14° corresponds to an equivalent Bragg spacing of  $\sim 6$  Å. This indicates the emergence of weak interchain correlation in this amorphous polymer.<sup>13</sup> The analogous poly(D,L-lactide) shows no such correlation (Chapter 3, Figure 3.19B). Perhaps the strong permanent dipole of the trifluoromethyl group and the associated acidity of the methine hydrogen impose some interchain order on the system despite the lack of chain stereoregularity.<sup>14</sup>

### 5.3.3 Blends of Poly((RS)-3,3,3-trifluorolactic acid) with poly(D,L-lactide)

Solution cast films from blends of amorphous poly(D,L-lactide) and poly((RS)-TFL) were prepared from HFIP or acetone on glass cover slip substrates. Film formation was quite rapid with these rather volatile solvents. The samples were loaded into a vacuum oven at ambient temperature with a steady flow of dry nitrogen passing through for 24 h. Full vacuum was then applied and kept for several days to maximize solvent removal from the test specimens. Multiple force measurements used to calculate the advancing contact angle were obtained by the data acquisition system upon lowering test specimens into the water at a specified rate. Force data collected with removal at the same rate were used to calculate the receding contact angle. This is the Wilhelmy plate technique that is described by Garbassi et al..<sup>8</sup> Contact angle measurement provides useful information about surface energetics but is affected by surface roughness and inhomogeneity as well as contamination.<sup>15</sup>

The contact angle data are shown in Table 5.3 (with XPS data) and Table 5.4 (with bulk elemental analysis data) for films cast from HFIP and in Tables 5.5 for films cast from acetone.

In films prepared from HFIP, as the level of poly((RS)-TFL) is increased in the blends only a slight increase in advancing contact angle is indicated. Only the film made from the pure fluoropolyester shows a

significant increase in contact angle at 102°. Higher contact angle is associated with the very low surface energy of the hydrophobic trifluoromethyl group.<sup>16</sup> It is surprising to observe no notable increase in advancing contact angle with such large increases in fluoropolymer content in the blend where fluorine containing groups are expected to dominate the surface. The receding contact angle behavior too is quite interesting. Receding contact angle value is dominated by hydrophilic interactions and advancing contact angle is dominated by hydrophobic interactions.<sup>17</sup> Upon introduction of the fluoropolyester to poly (D,L-lactide), the receding contact angle decreases. The pure fluoropolyester has a relatively low receding contact angle. This level of hysteresis is quite high and is dramatic for poly((RS)-TFL) (sample #6).

The advancing contact angle data are consistent with the relative atom % data obtained by XPS (Table 5.3). They suggest that fluorine is underrepresented near the surface as compared to the calculated bulk values. In Table 5.4, elemental analysis data show bulk values of fluorine that are higher than those reported (by XPS) to be near the surface.

Dynamic secondary ion mass spectrometry (SIMS) was used for further analysis of selected films cast from HFIP. It is a technique used to develop a depth profile of the specimen based on the secondary ions ejected (sputtered) from the surface by an ion beam.<sup>18</sup> The dynamic SIMS profiles of film samples from 100 % poly((RS)-TFL) (sample #6) and 25 wt.% poly((RS)-

TFL) with poly(D,L-lactide) (sample #3) are shown in Figures 5.12 and 5.13, respectively. Approximate sputtering depth was calculated by measuring the depth of a “crater” with a stylus profilometer after the experiment.

Sputtering rate was then determined with the total depth and total time of experiment. The sputtering rate for these experiments was determined to be 1.8 Å/s. This factor can be used to convert the time scale to a depth scale.

Sputtering depth was ~240 Å in the blend sample #3. The carbon and fluorine ion intensity parallel each other in the pure fluoropolymer as expected from the surface into the sample. However, in the blend specimen, fluorine level relative to carbon increases from the surface into the sample. This result corresponds to the XPS and bulk elemental analysis data presented (*vide supra*).

Surface characterization of blend films prepared from acetone behave differently (Table 5.5); the advancing contact angle increases significantly with increasing level of fluoropolyester in the blend. Indeed, the XPS data indicate the surface region enriched with fluorine when compared to the calculated bulk values. The receding contact angles increase with increasing fluoropolyester but they are half the value obtained for polytetrafluoroethylene. Bulk elemental analysis on a selected (sample #3, Table 5.5) specimen shows a bulk value of fluorine that is lower than what is measured near the surface.

The analogous films (25 wt.% poly((RS)-TFL) cast from HFIP and acetone were annealed in a vacuum oven at 80°C (above the  $T_g$  of both polymers) for 3 days. The XPS data are shown in Table 5.6. The film prepared from HFIP after annealing now clearly has a surface enriched with fluorine as shown by XPS measurement at 15° (which probes about 20 Å in the film).<sup>19</sup> Moreover, the 85° XPS measurement, which is approximately 80 Å into the film,<sup>19</sup> corresponds to the bulk elemental analysis (see Table 5.4, sample #3). XPS data at 85° from an annealed film cast from acetone also corresponds to the bulk elemental analysis (see Table 5.5, sample #3). The surface of this film is now shown (15° XPS) to be depleted in fluorine compared to the sample prior to annealing. Different surface properties after annealing suggest that the initial films were kinetic products that were driven toward the equilibrium state with annealing.

It would be worthwhile to repeat these experiments using the very pure fractionated poly((RS)-TFL) and compare results.

## 5.4 Conclusions

(RS)-3,3,3-Trifluorolactic acid forms high polymer scattering in several hours as indicated by inherent viscosity and light scattering measurements. Poly((RS)-TFL) was fractionated to remove low molecular weight polymer and urea by-products. Weight loss below 300°C as measured by TGA was minimal; behavior that was quite different from that of polymer that had not

been fractionated. DSC thermal traces of the fractionated polymer and the control were indistinguishable. The WAXS patterns of the two polymer samples however, were strikingly different. The appearance of an additional broad reflection at  $2\theta = 14^\circ$  in the fractionated poly((RS)-TFL) suggested weak correlations that can be associated with intermediate order in this substantially amorphous polymer. Blends of the aliphatic fluoropolyester with poly (D,L-lactide) showed fluorine concentration on the surface was dependent upon the solvent used to cast the film. Contact angle, XPS and dynamic SIMS data confirmed that in some cases, fluorine was underrepresented on the surface compared to the bulk of the film. However, upon annealing the film, the surface became enriched with fluorine.

## 5.5 References and Notes

- (1) Haydock, D. B.; Mulholland, T. P. C.; Telford, B.; Thorp, J. M.; Wain, J. *S. Eur J Med Chem- Chim Ther* **1984**, *19*, 205.
- (2) Shalaby, S. W.; Johnson, R. A. In *Biomedical Polymers*; S. W. Shalaby, Ed.; Hanser: Munich Ger, 1994, p 1.
- (3) Domb, A. J.; Amselem, S.; Langer, R.; Maniar, M. In *Biomedical Polymers*; S. W. Shalaby, Ed.; Hanser: Munich, 1994, p 69.
- (4) Kohn, J.; Langer, R. In *Biomaterials Science*; B. D. Ratner, A. S. Hoffman, F. J. Shoen, and J. E. Lemons, Eds.; Academic Press: San Diego, 1996, p 64.
- (5) Neises, B.; Steglich, W. *Angew Chem Int Engl* **1978**, *17*, 522.
- (6) Moore, J. S.; Stupp, S. I. *Macromolecules* **1990**, *23*, 65.
- (7) Sperling, L. H. *Introduction to Physical Polymer Science*; Wiley Interscience: New York, 1986, p 150.
- (8) Garbassi, F.; Morra, M.; Occhiello, E. *Polymer Surfaces*; J Wiley & Sons: Chichester, 1994, p 168.
- (9) Young, R. J.; Lovell, P. A. *Introduction to Polymers*; 2nd ed.; Chapman & Hall: London, 1991, p 23.
- (10) Hiemenz, P. C. *Polymer Chemistry*; Marcel Dekker: New York, 1984, p 346.
- (11) Odian, G. *Principles of Polymerization*; 3rd ed.; J. Wiley & Sons: New York, 1991, p 86.
- (12) Young, R. J.; Lovell, P. A. *Introduction to Polymers*; 2nd ed.; Chapman & Hall: London, 1991, p 165 214.

- (13) Miller, R. L. In *Order in the Amorphous State of Polymers*; S. E. Keinath, R. L. Miller, and J. K. Rieke, Eds.; Plenum Press: New York, 1985, p 35.
- (14) Rodriguez, F. *Principles of Polymer Systems*; 3rd ed.; Hemisphere: New York, 1989, p 58.
- (15) Johnson, R. E., Jr; Dettre, R. H. In *Surface and Colloid Science*; E. Matijevic, Ed.; Wiley Interscience: New York, 1969; Vol. 2, p 86.
- (16) Johnson, R. E., Jr; Dettre, R. H. In *Surface and Colloid Science*; E. Matijevic, Ed.; Wiley Interscience: New York, 1969; Vol. 2, p 132.
- (17) Johnson, R. E., Jr; Dettre, R. H. In *Surface and Colloid Science*; E. Matijevic, Ed.; Wiley Interscience: New York, 1969; Vol. 2, p 108.
- (18) Russell, T. P.; Deline, V. R.; Wakharkar, V. S.; Coulon, G. *MRS Bulletin* **1989**, 33.
- (19) Garbassi, F.; Morra, M.; Occhiello, E. *Polymer Surfaces*; J Wiley & Sons: Chichester, 1994, p 94.

Table 5.1 The effect of polymerization time on poly((RS)-TFL) molecular weight and yield.\*

Polymerization time [h]	$\eta_{inh}$ (0.2 g/dL) at 29.95°C in THF [dL/g]	$M_w$ [g/mol]	Polydispersity [ $M_w/M_n$ ]	Yield [%]
8	0.36	18,400	1.9	32.4
24	0.34	20,600	2.2	38.8
48	0.32	19,200	2.2	43.0

\*solvent:  $CH_2Cl_2$ , catalyst: DPTS, [DPTS] = 0.05 mol/L, [(RS)-TFL] = 0.23 mol/L, 1,3-diisopropylcarbodiimide, [DIPC] = 0.35 mol/L.

Table 5.2 A comparison of the molecular weight of the fractionated polymer, control and poly(D,L-lactide).

Polymer	$\eta_{inh}$ (0.2 g/dL) at 29.95°C in THF [dL/g]	$M_w$ [g/mol]	$\eta_{inh} M_w$ [dL/mol]	Polydispersity [ $M_w/M_n$ ]
Poly((RS)-TFL (control)	0.35	29,600	10,360	3.1
Poly((RS)-TFL) (fractionated)	0.36	69,400	24,984	1.6
Poly(D,L-lactide)	0.53	41,300	21,889	1.4

Table 5.3 XPS and contact angle measurements of poly(D,L-lactide) / poly((RS)-TFL) blend films cast from HFIP.

Blend #	poly(D,L-lactide) / poly((RS)-TFL) [wt. %]	Composition		Contact angles	
		Calculated (Bulk) / Measured (XPS at 85°)		Advancing [°]	Receding [°]
		Carbon [atom %]	Fluorine [atom %]		
1	100 / 0	100 / 99.4	0 / 0.6	88±1	60±1
2	90 / 10	91 / 97.5	9 / 2.6	90±1	59±1
3	75 / 25	80 / 95.7	20 / 4.4	92±1	57±1
4	50 / 50	67 / 92.7	33 / 7.3	85±1	18±2
5	25 / 75	57 / 81.7	43 / 18.3	91±2	32±2
6	0 / 100	50 / 50.6	50 / 49.5	102±3	25±2
glass without film	----	----	----	17±1	18±1
glass dipped in HFIP and dried	----	----	----	34±1	14±2

Table 5.4 Elemental analysis of poly(D,L-lactide) / poly((RS)-TFL) blend films cast from HFIP.

Blend #	poly(D,L-lactide) / poly((RS)-TFL) [wt. %]	Composition	
		Calculated (Bulk) / Measured (Elemental Analysis)	
		Carbon [atom %]	Fluorine [atom %]
1	100/0	100 / 90.3	0 / 9.7
2	90/10	91 / 86.0	9 / 14.0
3	75/25	80 / 82.8	20 / 17.2
4	50/50	67 / 75.7	33 / 24.3
5	25/75	57 / 62.0	43 / 38.0
6	0/100	50 / 67.0	50 / 33.0

Table 5.5 XPS and contact angle measurements of poly(D,L-lactide) / poly((RS)-TFL) blend films cast from acetone.

Blend #	poly(D,L-lactide) / poly((RS)-TFL) [wt. %]	Composition		Contact angles	
		Calculated (Bulk) / Measured (XPS at 85°) / Measured (XPS at 15°)		Advancing [°]	Receding [°]
		Carbon [atom %]	Fluorine [atom %]		
1	100 / 0	100 / 95.6 / 95.8	0 / 4.4 / 4.6	32±1	16±1
2	90 / 10	91 / 54.6 / 52.3	9 / 45.4 / 47.7	103±1	50±2
3	75 / 25	80 / 52.0 (89.0)* / 51.6	20 / 48.0 (11.0)* / 48.4	116±1	40±1
4	0 / 100	50 / 49.9 / 49.5	50 / 50.1 / 50.5	106±1	55±2
poly(tetrafluoroethylene)	----	33 / 56.5 / 54.0	67 / 43.5 / 46.0	126±1	104±1

\* elemental analysis

Table 5.6 XPS data of annealed\* test specimens cast from HFIP and acetone.

Blend #	poly(D,L-lactide) / poly((RS)-TFL) [wt. %]	Composition	
		Calculated (Bulk) / Measured (XPS at 85°) / Measured (XPS at 15°)	
		Carbon [atom %]	Fluorine [atom %]
3 (cast from HFIP)	75 / 25	80 / 83.1 / 72.3	20 / 16.9 / 27.7
3 (cast from acetone)	75 / 25	80 / 89.4 / 87.2	20 / 10.6 / 12.8

\*annealed in a vacuum oven 80°C (above the T<sub>g</sub> of both polymers) for 3 days.

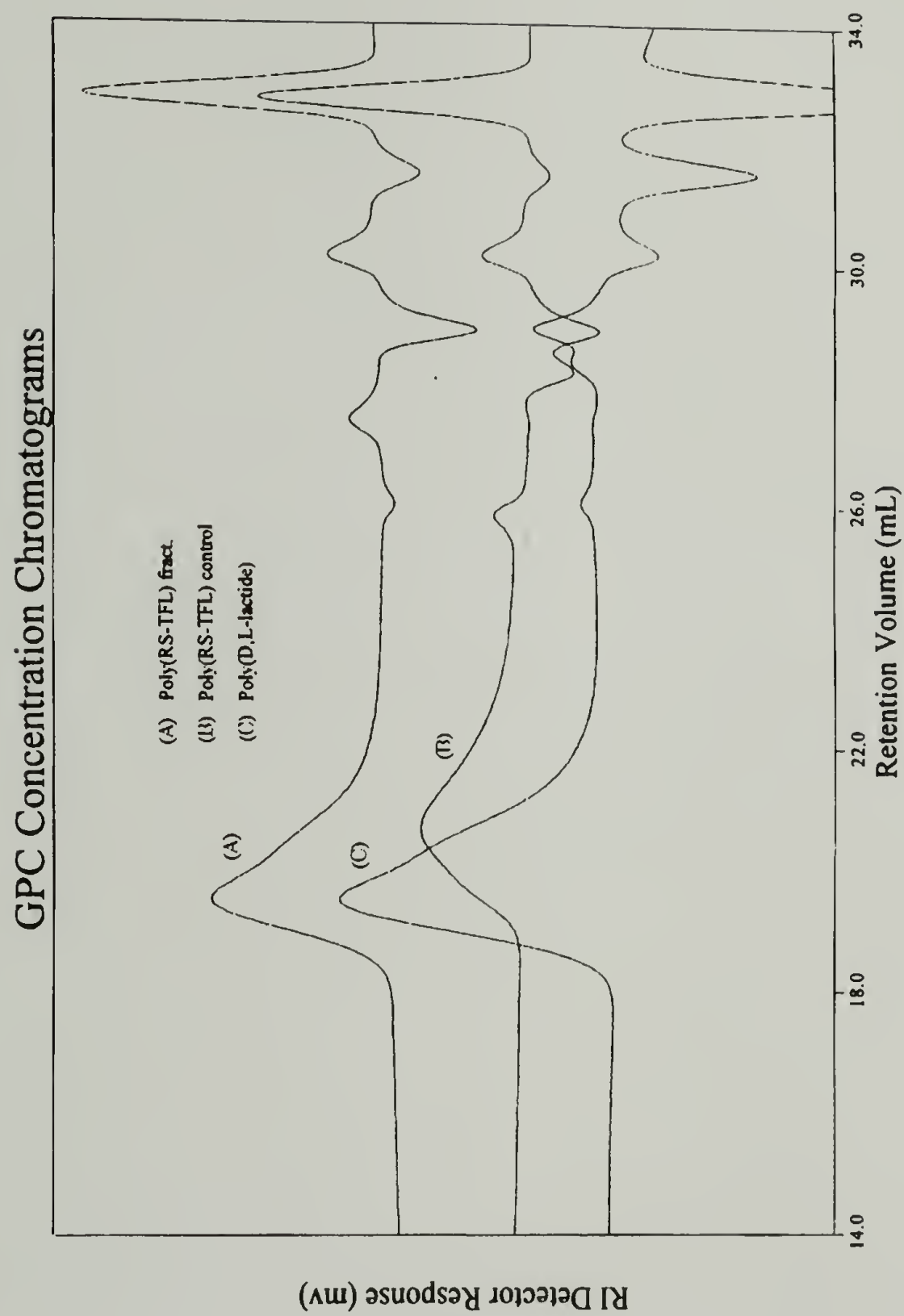


Figure 5.1 GPC of A: poly((RS)-TFL) fractionated, B: poly((RS)-TFL) control and C: poly(D,L-lactide).

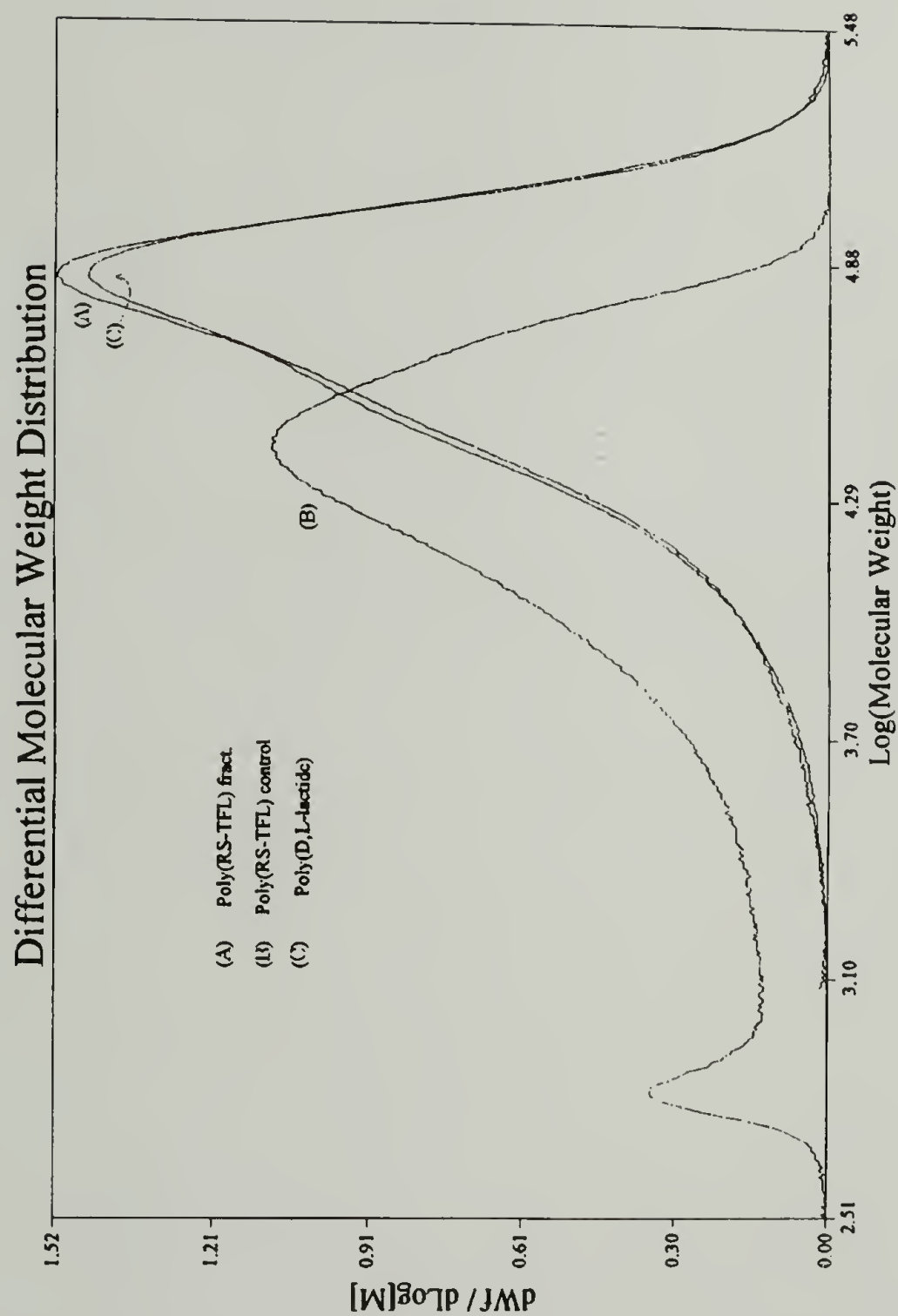


Figure 5.2 Differential weight fraction vs. molecular weight of A: poly((RS)-TFL) fractionated, B: poly((RS)-TFL) control and C: poly(D,L-lactide).

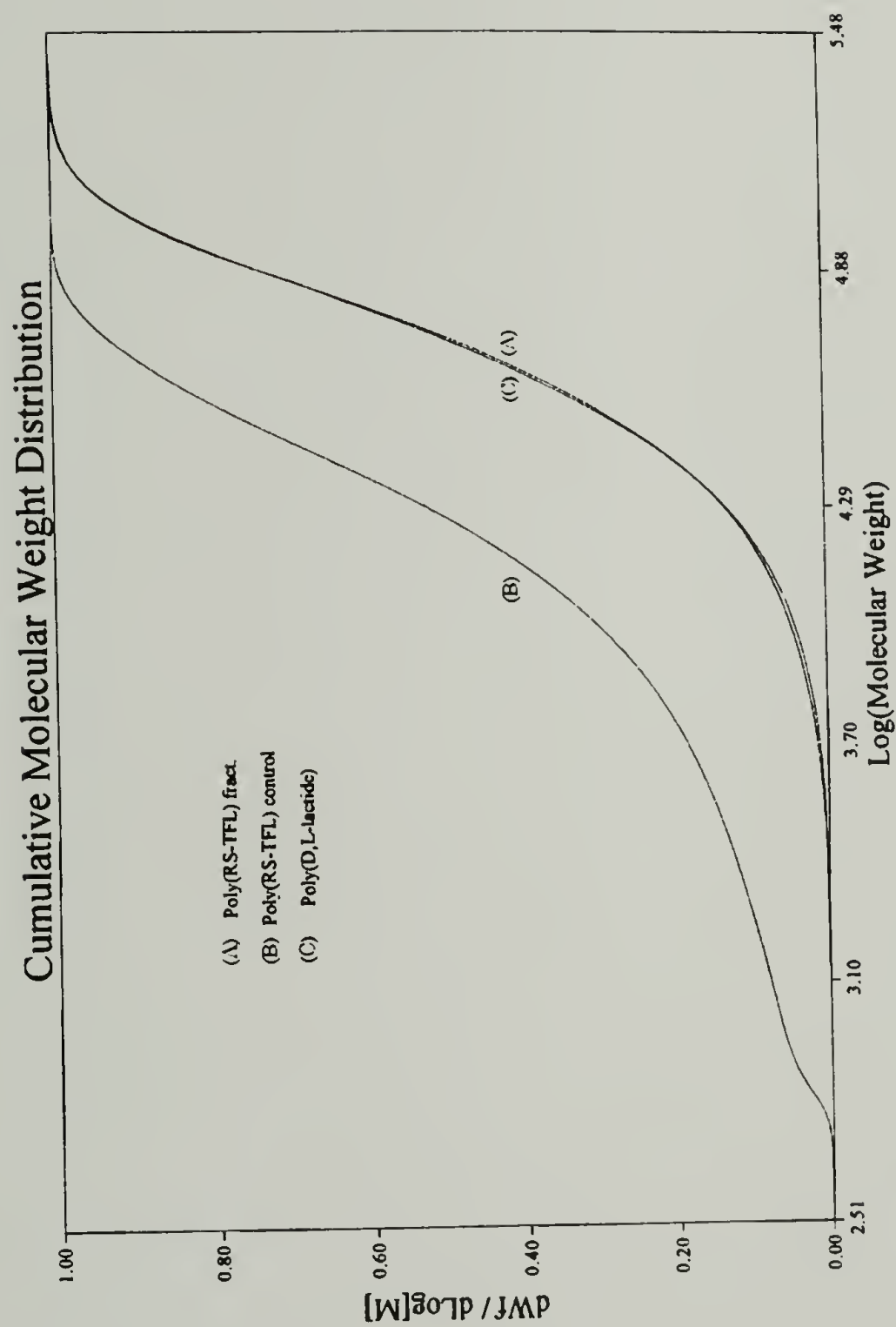


Figure 5.3 Cumulative weight fraction curves of A: poly((RS)-TFL) fractionated, B: poly((RS)-TFL) control and C: poly(D,L-lactide).

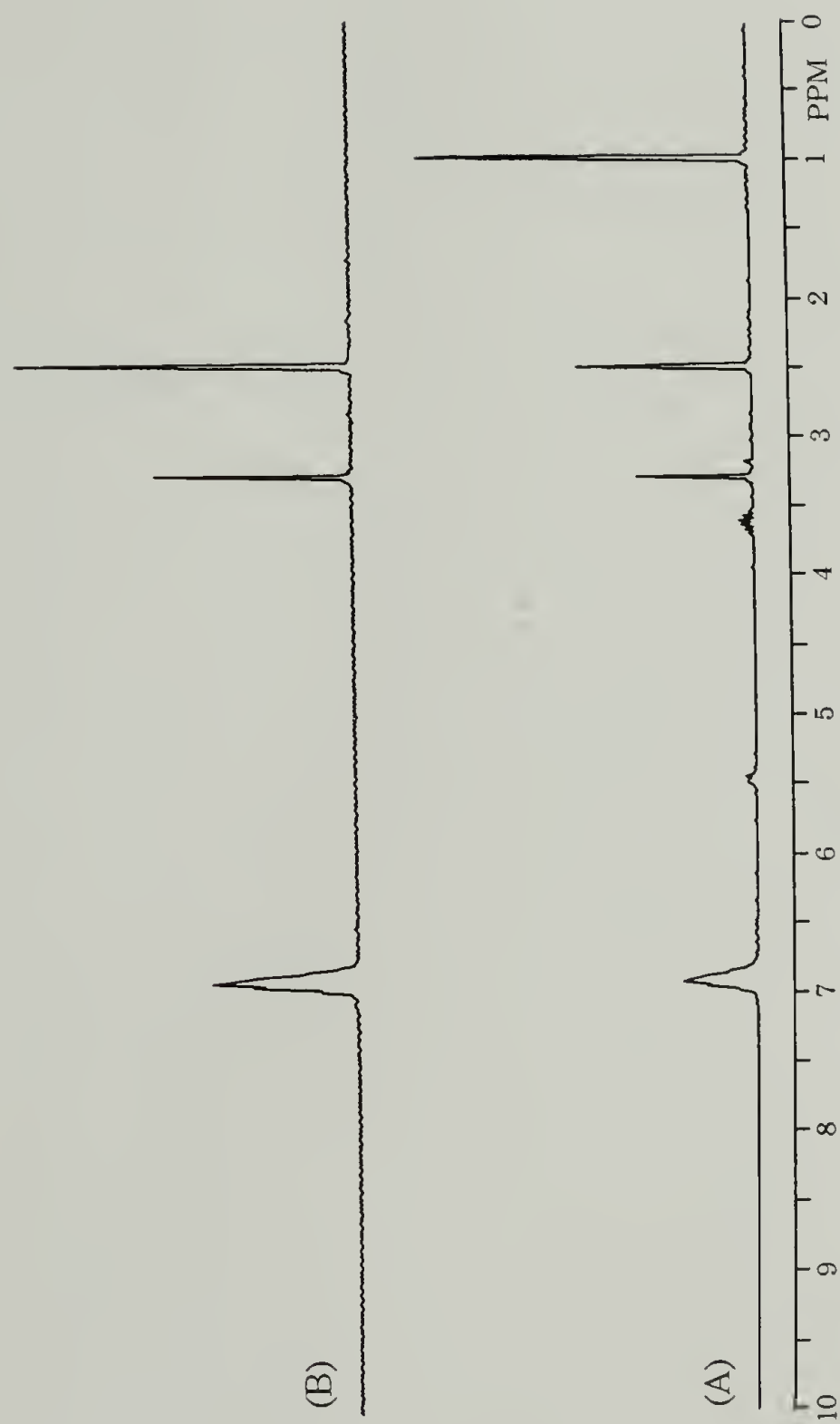


Figure 5.4 200-MHz proton NMR spectra of A: control poly((RS)-TFL) and B: fractionated poly((RS)-TFL) in DMSO- $d_6$ .

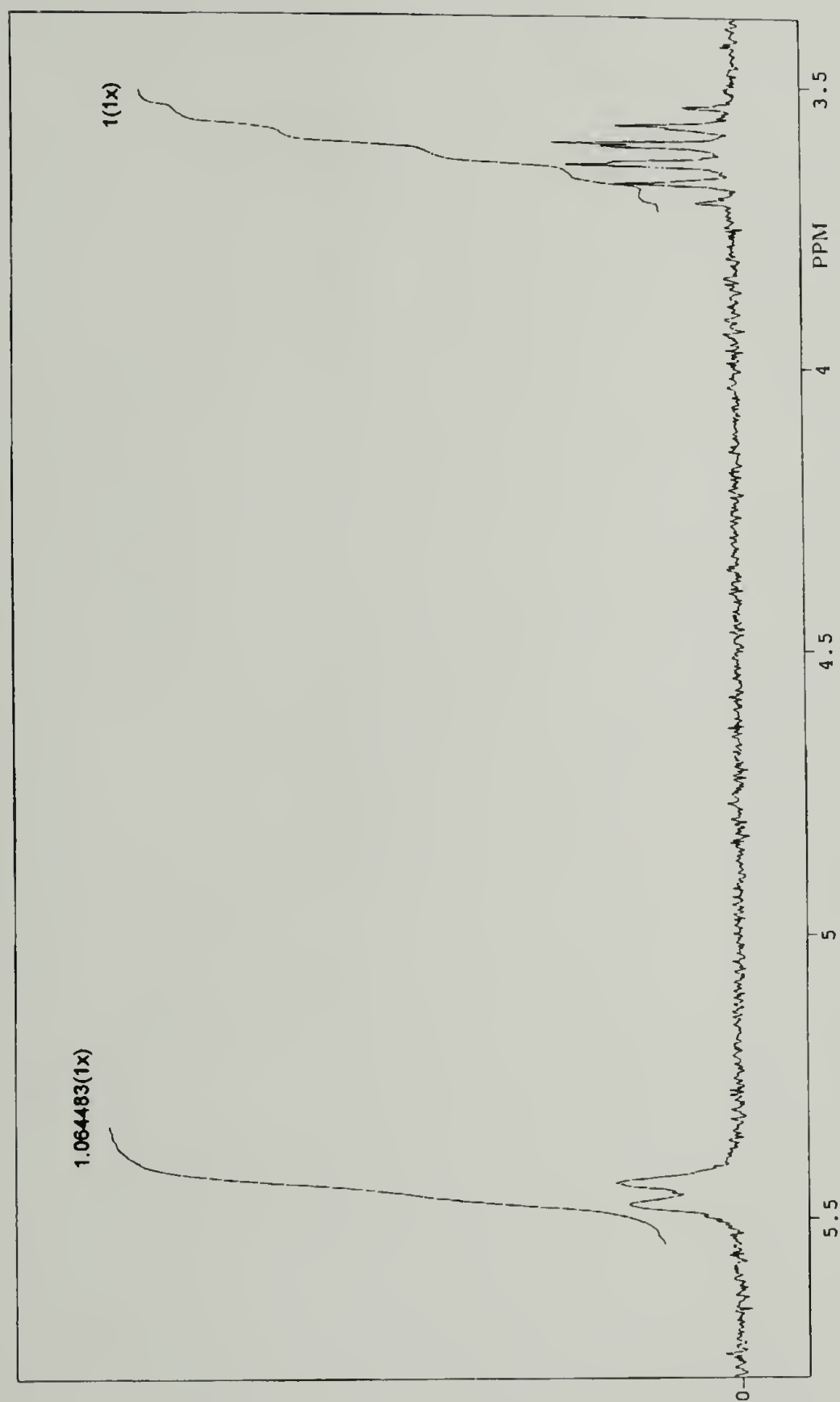


Figure 5.5 Integration of the isopropyl methine hydrogen and the amide hydrogen of Figure 5.4A.

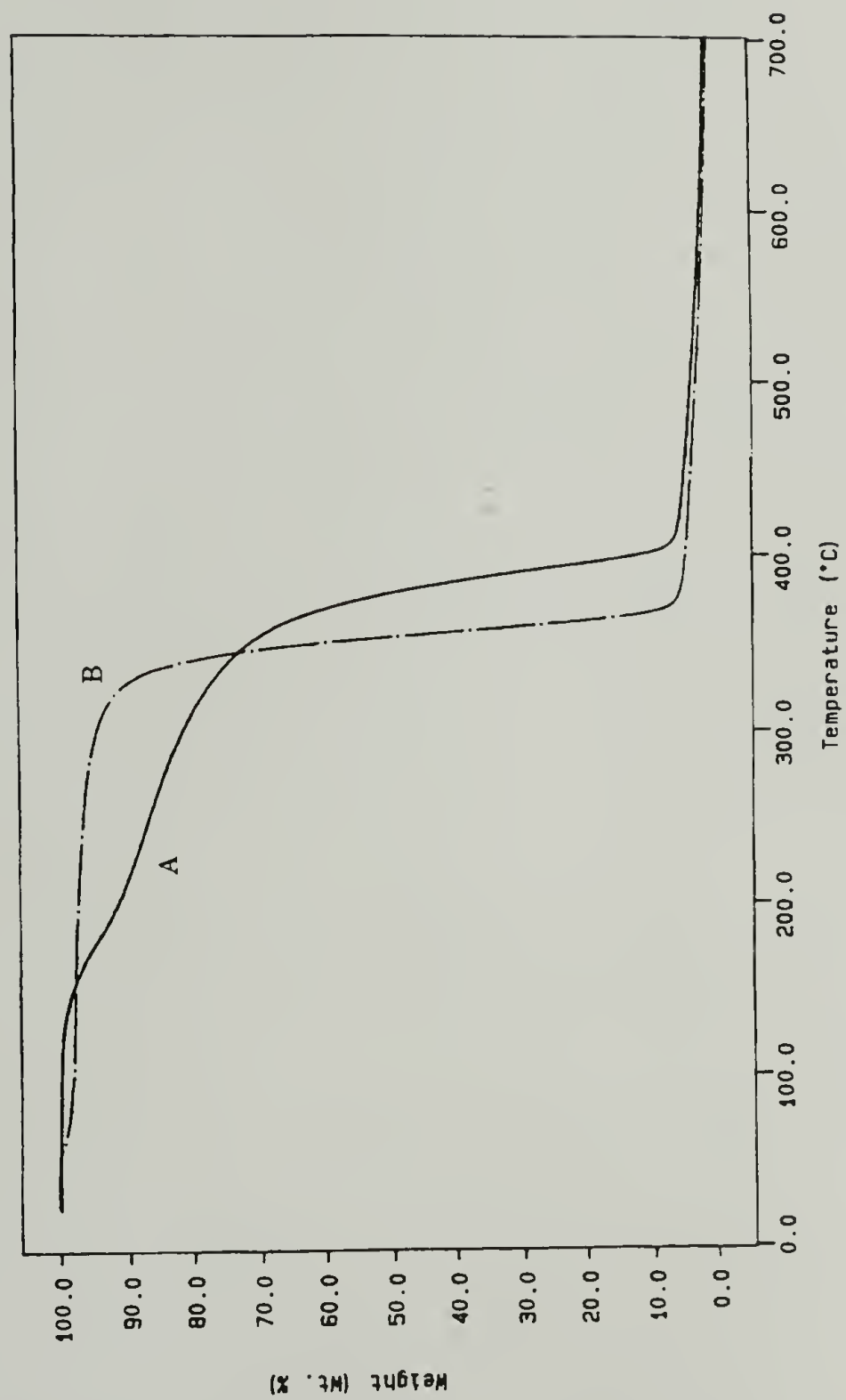


Figure 5.6 TGA curves of A: control and B: fractionated poly((RS)-TFL) under N<sub>2</sub> at 10C°/min.

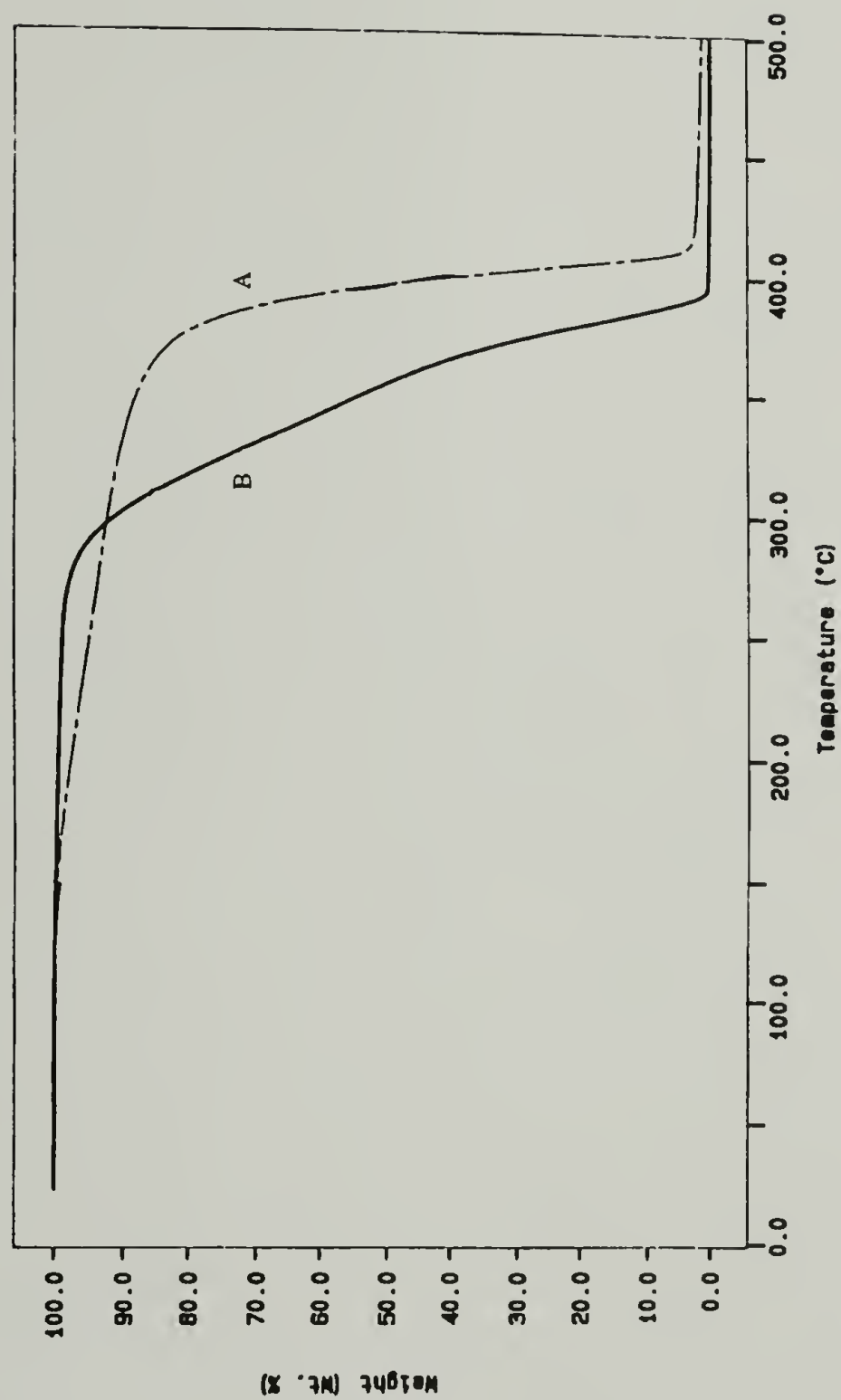


Figure 5.7 TGA curves of A: fractionated poly((RS)-TFL) and B: poly(D,L-lactide) under N<sub>2</sub> at 10C°/min.

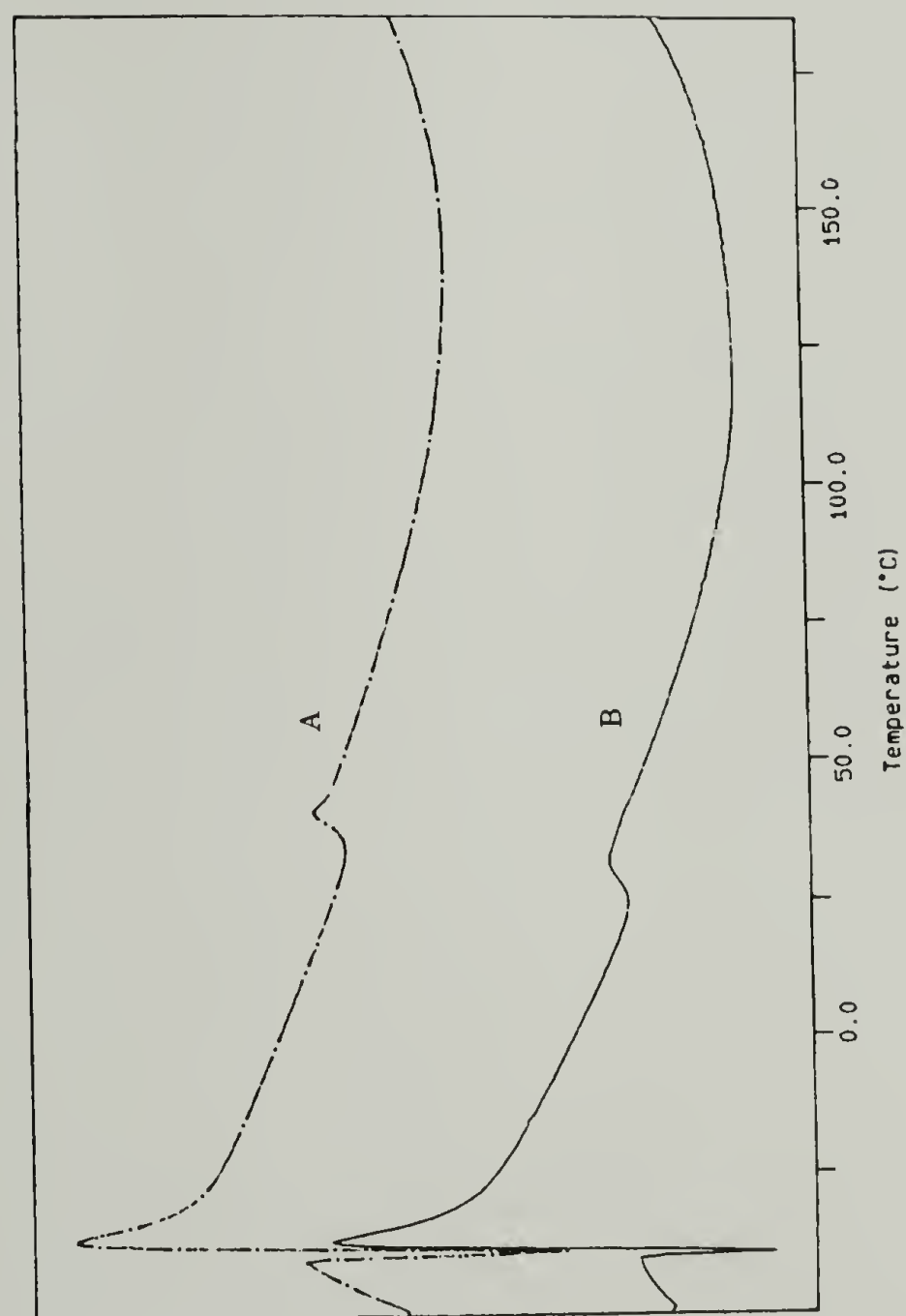


Figure 5.8 DSC thermal traces of A: fractionated poly((RS)-TFL) and B: the control under N<sub>2</sub> at 10C°/min.

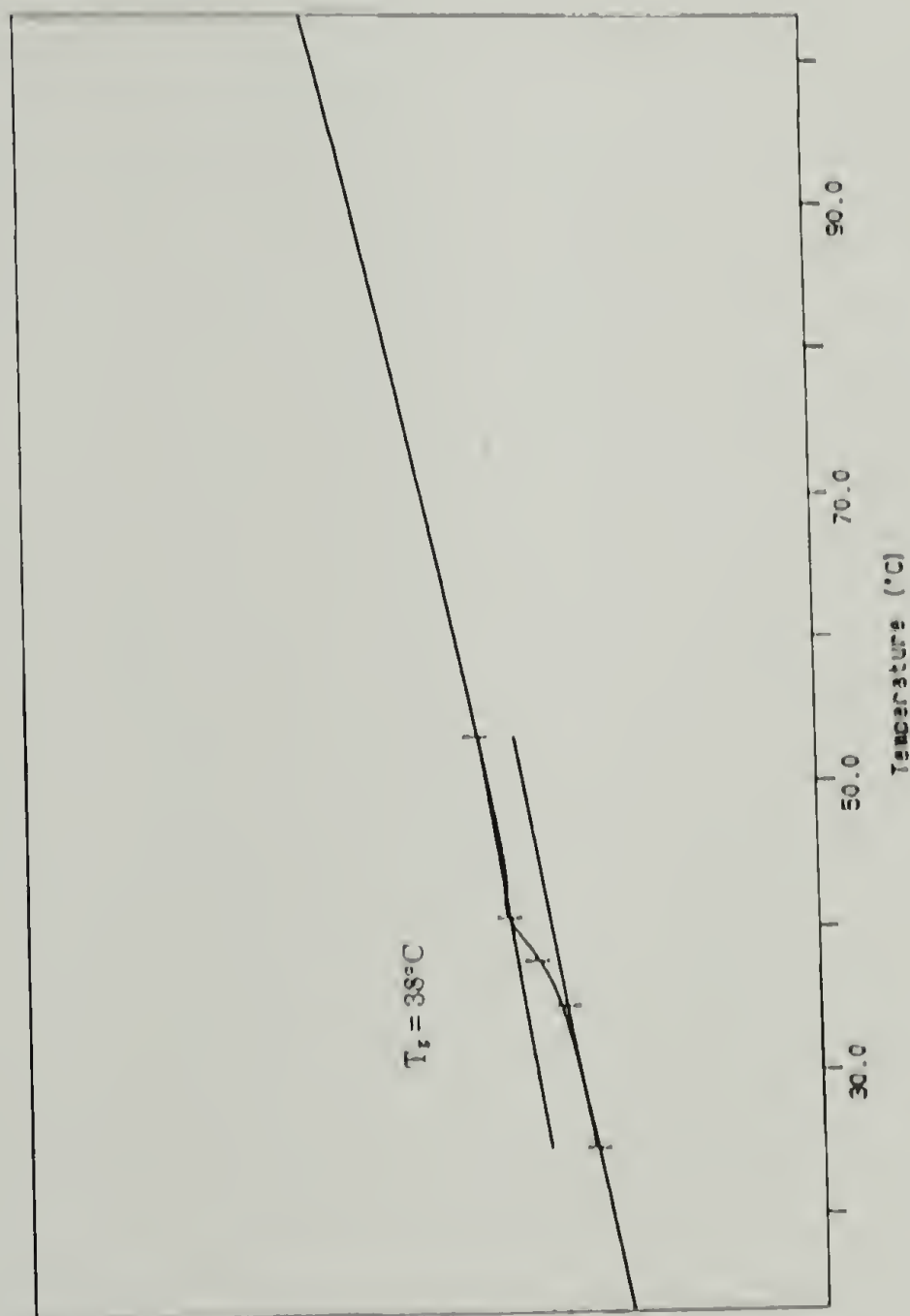
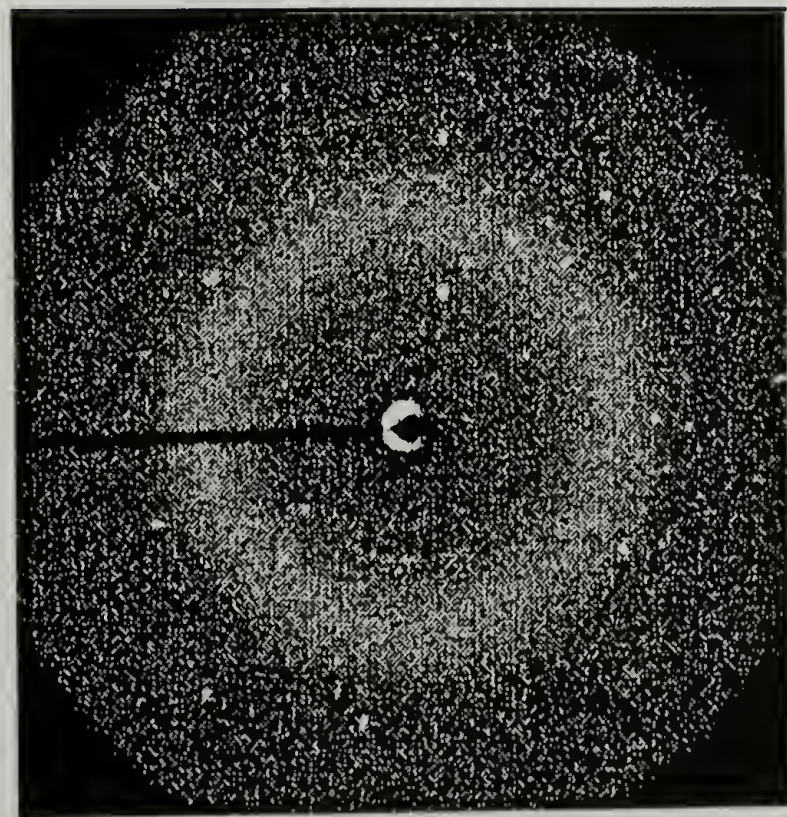
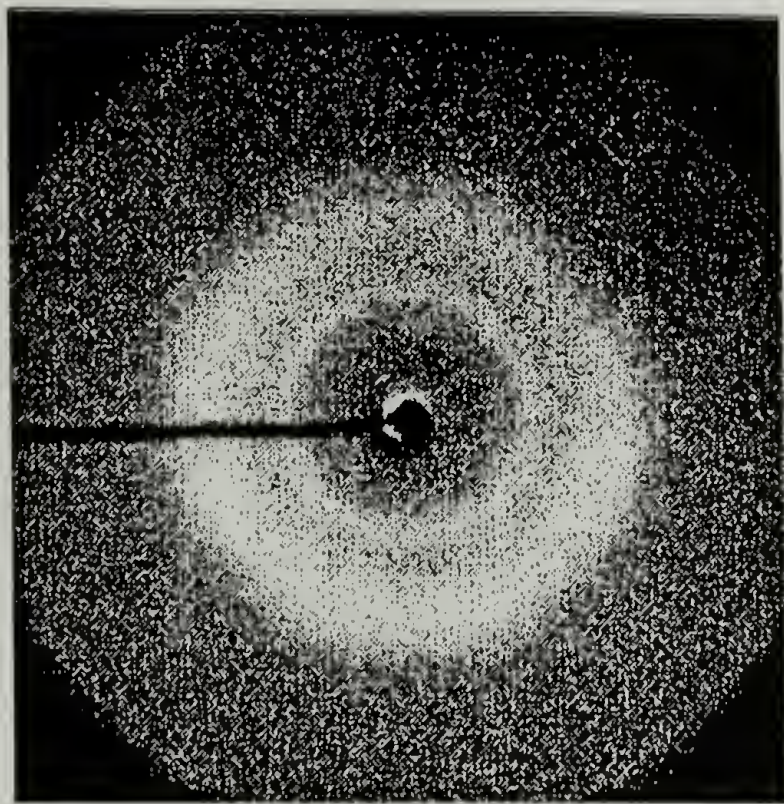


Figure 5.9 DSC of fractionated poly((RS)-TFL) under  $\text{N}_2$  at  $10^\circ\text{C}/\text{min}$ .



A



B

Figure 5.10 WAXS of the A: control poly((RS)-TFL) and B: fractionated poly((RS)-TFL).

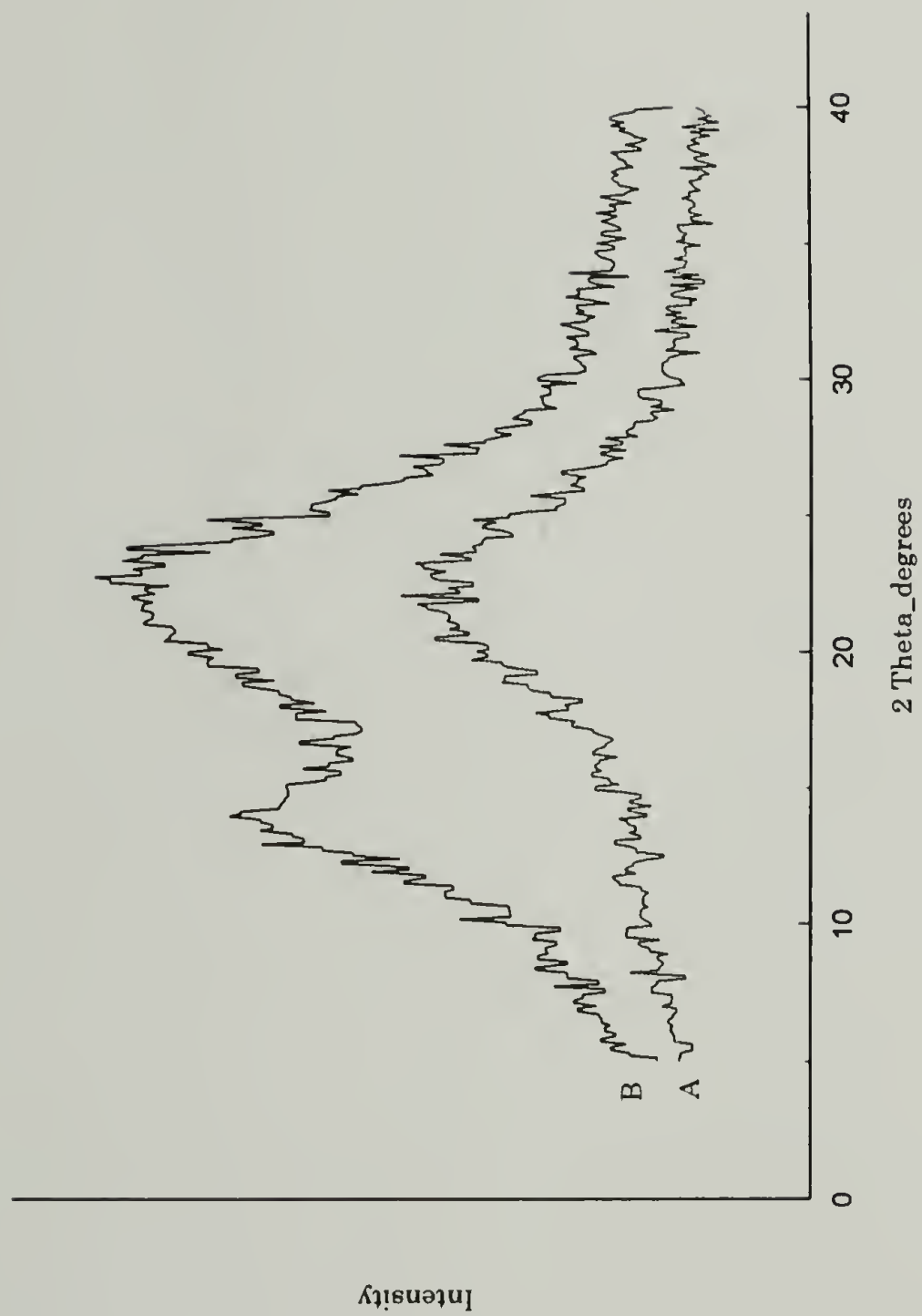


Figure 5.11 2 $\theta$  vs. intensity of the A: the control and B: fractionated poly((RS)-TFL).

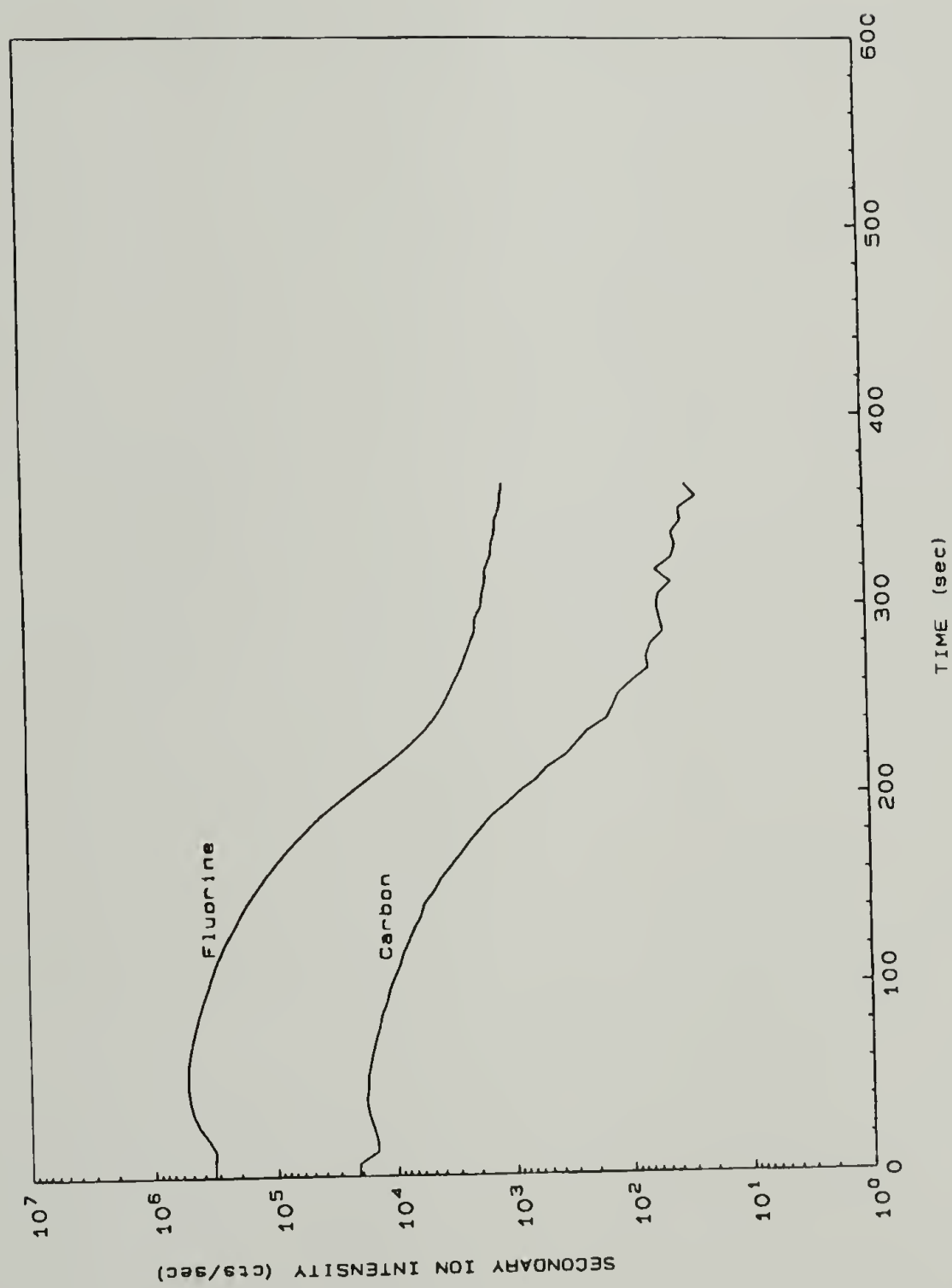


Figure 5.12 Dynamic SIMS of poly((RS)-TFL) cast from HFIP.

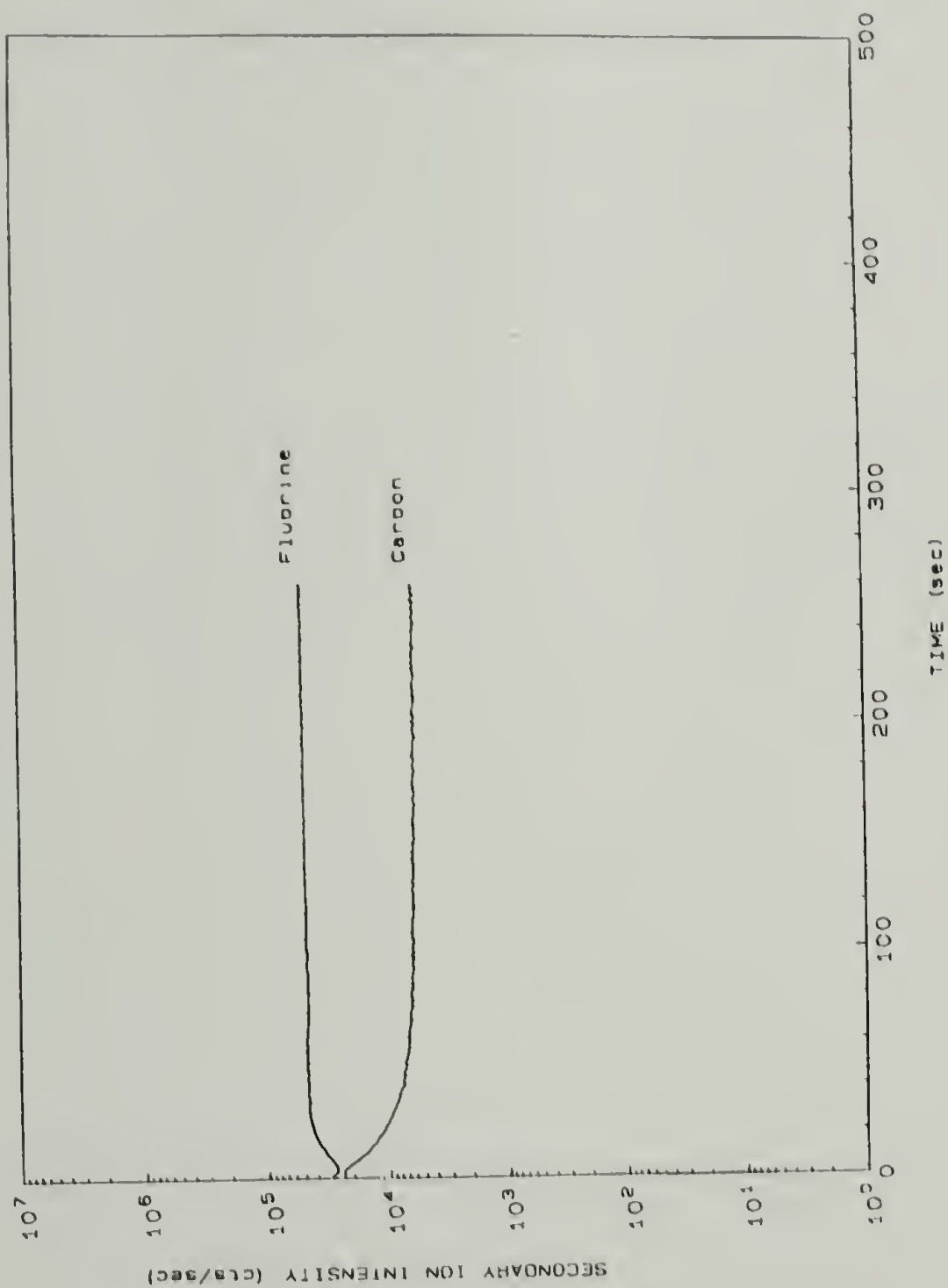


Figure 5.13 Dynamic SIMS of sample #3 (75/25, wt., poly(D,L-lactide) / poly((RS)-TFL) cast from HFIP

## BIBLIOGRAPHY

- Balcom, B. J.; Petersen, N. O. *J. Org. Chem.* **1988**, *54*, 1922.
- Benoiton, L. N.; Chen, F. M. F. *J. Chem. Soc. Chem. Commun.* **1981**, *11*, 543.
- Boden, E. P.; Keck, G. E. *J. Org. Chem.* **1985**, *50*, 2394.
- Bovey, F. A.; Jelinski, L.; Mirau, P. A. *Nuclear Magnetic Resonance Spectroscopy*; 2nd ed.; Academic Press: San Diego, 1988, p 457.
- Bravo, P.; Frigerio, M.; Resnati, G. *J Org Chem* **1990**, *55*, 4216.
- Brochu, S. Ph.D. Dissertation, Laval University, 1993.
- Burstein, S. H.; Ringold, H. J. *Can J Chem* **1961**, *39*, 1848.
- Cappello, J.; Crissman, J.; Dorman, M.; Mikolajczak, M.; Textor, G.; Marquet, M.; Ferrari, F. *Biotechnol Prog* **1990**, *6*, 198.
- Carey, F. A. *Organic Chemistry*; 2nd ed.; McGraw-Hill: New York, 1992, p 258.
- Chambers, R. D. *Fluorine in Organic Chemistry*; R D Chambers: Durham UK, p 65.
- Colthup, N. B.; Daly, L. H.; Wiberley, S. E. *Introduction to Infrared and Raman Spectroscopy*; 3rd ed.; Academic Press Inc: Boston, 1990, p 16, 290.
- Dessipri, E. Ph.D. Dissertation, University of Massachusetts Amherst, 1995.
- Domb, A. J.; Amselem, S.; Langer, R.; Maniar, M. In *Biomedical Polymers*; S. W. Shalaby, Ed.; Hanser: Munich, 1994, p 69.

E.I. DuPont Co. *U.K. Pat.* 1,007,347 **1965**.

Eliel, E. L. *Stereochemistry of Carbon Compounds*; McGraw-Hill: New York, 1962, p 88.

Ellman, J. A.; Mendel, D.; Schultz, P. G. *Science* **1992**, 255, 197.

Garbassi, F.; Morra, M.; Occhiello, E. *Polymer Surfaces*; J Wiley & Sons: Chichester, 1994, p 94, 168.

Hauptschein, M.; Oesterling, R. E. *J Org Chem* **1963**, 28, 1279.

Hauptschein, M.; Oesterling, R. E. *U.S. Pat.* (assigned to Pennsalt Chem Corp) 3,202,706 **1965**.

Hauptschein, M.; Oesterling, R. E.; Braid, M.; Tyczkowski, E. A.; Gardener, D. M. *J Org Chem* **1963**, 28, 1281.

Hauptschien, M.; O'Brien, J. F.; Stokes, C. S.; Filler, R. *J Am Chem Soc* **1953**, 75, 87.

Haydock, D. B. *France Pat.* (assigned to Imp Chem Ind) 2,293,196 **1976**.

Haydock, D. B.; Mulholland, T. P. C.; Telford, B.; Thorp, J. M.; Wain, J. S. *Eur J Med Chem- Chim Ther* **1984**, 19, 205.

Hendrickson, J. B.; Cram, D. J.; Hammond, G. S. *Organic Chemistry*; 3rd edition; McGraw-Hill: New York, 1970, p 306.

Henne, A. L.; Pelley, R. L. *J Am Chem Soc* **1952**, 74, 1426.

Hiemenz, P. C. *Polymer Chemistry*; Marcel Dekker: New York, 1984, p 346.

Hinman, M. B.; Stauffer, S. L.; Lewis, R. V. In *Silk Polymers*; D. Kaplan, W. W. Adams, B. Farmer and C. Viney, Eds.; American Chemical Society: Washington DC, 1994, p 226.

Holten, C. H. *Lactic Acid*; Verlag Chemie: Weinheim Germany, 1971, p 3, 20, 53, 192, 518.

Iannace, S.; Ambrosio, L.; Huang, S. J.; Nicolais, L. *J. Appl. Polym. Sci.* **1994**, *54*, 1525.

Imperiali, B. *Biotechnol Processes* **1988**, *10*, 97.

Jacobson, H. W. *U.S. Pat.* (assigned to Ethicon Inc) 3,498,957 **1970**.

Johncock, P.; Barnett, S. P.; Rickard, P. A. *J Polym Sci Part A: Polym Chem* **1986**, *24*, 2033.

Johnson, R. E., Jr; Dettre, R. H. In *Surface and Colloid Science*; E. Matijevic, Ed.; Wiley Interscience: New York, 1969; Vol. 2, p 86, 108, 132.

Juaristi, E. *Introduction to Stereochemistry and Conformational Analysis*; Wiley-Interscience: New York, 1991, p 23, 36.

Kalb, B.; Pennings, A. J. *Polymer* **1980**, *21*, 607.

Katagiri, T.; Obara, F.; Toda, S.; Furuhashi, K. *Synlett Letters* **1994**, 507.

Katagiri, Y. *Japan Pat.* (assigned to Nikko Kyoseki Co Ltd) Public Patent Disclosure Bulletin no 5-78278 **1993**.

Katagiri, Y.; Sata, I.; Ohara, I. *Japan Pat.* (assigned to Nikko Kyoseki Co Ltd) Public Patent Disclosure Bulletin no 5-70406 **1993**.

Knight, G. J.; Wright, W. W. *J Appl Polym Sci* **1972**, *16*, 683.

Knunyants, I. L.; et al. *Izv Akad Nauk SSSR Otdele Khim* **1961**, 808.

Kohn, J.; Langer, R. In *Biomaterials Science*; B. D. Ratner, A. S. Hoffman, F. J. Shoen and J. E. Lemons, Eds.; Academic Press: San Diego, 1996, p 64.

- Koo, G. P. In *Fluoropolymers*; L. A. Wall, Ed.; Wiley-Interscience: New York, 1972, p 515.
- Kortum, G.; Vogel, W.; Andrussow, K. *Dissociation Constants of Organic Acids in Aqueous Solution*; Butterworths: London, 1961
- Kricheldorf, H. R.; Boettcher, C.; Tonnes, K. *Polymer* **1992**, 33, 2817.
- Kricheldorf, H. R.; Sumbel, M. *Eur Polym J* **1989**, 25, 585.
- Kubota, T. *Japan Pat.* (assigned to Nikko Kyoseki Co Ltd) Public Patent Disclosure Bulletin no 3-148249 **1991**.
- Lavallée, C.; Leborgne, A.; Spassky, N.; Prudhomme, R. E. *J Polym Sci Polym Chem* **1987**, 25, 1315.
- Letinski, J. "Analytical Services Report ref. no. R95-679-680", Hoechst Celanese Advanced Technology Group, 1995.
- March, J. *Advanced Organic Chemistry*; Wiley Interscience: New York, 1992, p 250.
- McKie, D. B.; Lepeniotis, S., manuscript in preparation.
- McKie, D. B.; Tirrell, D. A.; Lillya, C. P.; Muthukumar, M.; Jaffe, M. , manuscript in preparation.
- Miller, R. L. In *Order in the Amorphous State of Polymers*; S. E. Keinath, R. L. Miller and J. K. Rieke, Eds.; Plenum Press: New York, 1985, p 35.
- Moore, J. S.; Stupp, S. I. *Macromolecules* **1990**, 23, 65.
- Murdoch, J. R.; Loomis, G. L. *U.S. Pat.* (assigned to E I Du Pont de Nemours Inc) 4,766,182 **1988**.
- Neises, B.; Steglich, W. *Angew Chem Int Ed* **1978**, 17, 522.

Nijenhuis, A. J. Ph.D. Dissertation, University of Groningen, 1995.

Nikko Kyoseki Co. Ltd *Japan Pat.* Public Patent Disclosure Bulletin no.:  
5-78277 **1993**.

O' Neal, C. C., Jr. Ph.D. Dissertation, University of Arizona, 1980.

Odian, G. *Principles of Polymerization*; 3rd ed.; J. Wiley & Sons: New York, 1991, p 86.

Olah, G. A.; Prakash, G. K. S.; Sommer, J. *Superacids*; Wiley Interscience: New York, 1985, p 33.

Pattison, F. L. M. *Toxic Aliphatic Fluorine Compounds*; Elsevier: Amsterdam, 1959, p 90, 100.

Pogolotti, A., Jr.; Rupley, J. A. *Biochem Biophys Res Comm* **1973**, 55, 1214.

Rodriguez, F. *Principles of Polymer Systems*; 3rd ed.; Hemisphere: New York, 1989, p 58.

Russell, T. P.; Deline, V. R.; Wakharkar, V. S.; Coulon, G. *MRS Bulletin* **1989**, 33.

Schweiker, G. C.; Robitschek, P. *J Polym Sci* **1957**, XXIV, 33.

Shalaby, S. W.; Johnson, R. A. In *Biomedical Polymers*; S. W. Shalaby, Ed.; Hanser: Munich Ger, 1994, p 1.

Sheppard, W. A.; Sharts, C. M. *Organic Fluorine Chemistry*; W.A. Benjamin: New York, 1969, p 27, 462.

Silverstein, R. M.; Bassier, G. C.; Morrill, T. C. *Spectrometric Identification of Organic Compounds*; 5th ed.; J Wiley & Sons: New York, 1991, p 103, 162.

Sinclair, R. G.; Gynn, G. M. "U.S. Tech Inform Serv report no. AD748411", 1972.

Smart, B. E. In *Organofluorine Chemistry*; R. E. Banks, B. E. Smart and J. C. Tatlow, Eds.; Plenum Press: New York, 1994, p 66.

Sperling, L. H. *Introduction to Physical Polymer Science*; Wiley Interscience: New York, 1986, p 150.

Stryer, L. *Biochemistry*; 3rd ed.; W. H. Freeman: New York, 1988, p 28.

Swarts, F. *Bull. Soc. Chim. Belg.* **1934**, *43*, 476.

Tirrell, D. A.; Fournier, M. J.; Mason, T. L. *Curr Opin Struct Biol* **1991**, *1*, 638.

von dem Bussche-Hunnefeld, C.; Cescato, C.; Seebach, D. *Chem Ber* **1992**, *125*, 2795.

Wagener, K. B.; Linert, J. G.; O'Gara, J. E. *J Macromol. Sci. - Pure Appl. Chem.* **1994**, *A31*, 775.

Young, R. J.; Lovell, P. A. *Introduction to Polymers*; 2nd ed.; Chapman & Hall: London, 1991, p 23, 165, 214.



